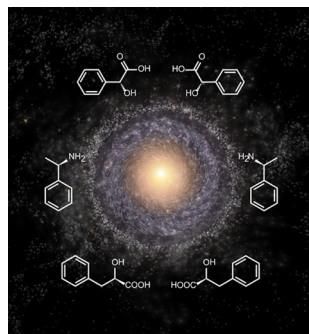


Recent Advances in Development of Chiral Fluorescent and Colorimetric Sensors

Xin Zhang,[†] Jun Yin,^{†,‡} and Juyoung Yoon*,[†]

[†]Department of Chemistry and Nano Science and Department of Bioinspired Science (WCU), Ewha Womans University, Seoul 120-750, Korea

[‡]Key Laboratory of Pesticide and Chemical Biology, Ministry of Education, College of Chemistry, Central China Normal University, Wuhan 430079, P. R. China



CONTENTS

1. Introduction	4918
2. General Design Principles	4919
3. Small Organic Molecule-Based Chiral Chemosensors	4920
3.1. Inherently Chiral Fluorophore-Based Chemosensors	4920
3.1.1. Binaphthyl-Based Chemosensors	4920
3.1.2. 1,8-Diheteroaryl naphthalene-Derived Chemosensors	4920
3.1.3. Other Inherently Chiral Fluorophore-Based Chemosensors	4929
3.2. Chiral Probes with Particular Binding Units	4930
3.2.1. Crown or Azacrown Ether-Based Chemosensors	4931
3.2.2. Thiourea- or Urea-Based Chemosensors	4933
3.2.3. Schiff-base-derivatized chemosensors	4937
3.2.4. Amino Acid- or Peptide-Based Sensors	4937
3.2.5. Imidazolium-Based Chemosensors	4938
3.2.6. Phenylboronic Acid-Based Chemosensors	4940
3.3. α -Aromatic Cinnamylnitrile-Derivatized Chemosensors	4944
4. Chiral Probes with Macroyclic Non-Fluorescent Rigid Scaffolds	4945
4.1. Calixarene-Based Chemosensors	4945
4.2. Calixpyrrole-Based Chemosensors	4946
4.3. Cyclodextrin-Based Chemosensors	4946
5. Metal Complex-Based Chiral Probes	4948
6. Polymer-Based Chiral Probes	4952
7. Nanomaterial-Based Chiral Probes	4953
8. Conclusions and Future Perspectives	4954
Author Information	4955
Corresponding Author	4955

Notes	4955
Biographies	4955
Acknowledgments	4956
List of Abbreviations	4956
References	4956

1. INTRODUCTION

Chirality is a universal phenomenon throughout nature. Most biologically important molecules are chiral and many key biological processes involve specific interactions between chiral substances, which govern the distribution as well as diffusion of biological molecules across natural membranes.^{1,2} Additionally, most modern drugs and those under development are single enantiomers of chiral compounds, which often display higher potencies and lower toxicities than do their counterparts.^{3,4} For example, L-dopamine has been found to be a Parkinson's disease agent but its D-enantiomer elicits neurotoxic side effects, such as granulocytopenia. As a result, the D-dopamine content of the commercial drug must be accurately determined and limited.⁵ Considering its practical importance, the development of powerful techniques for analysis of the enantiomeric purities of substances has become a focus of large numbers of research efforts over the past few decades. Currently, the approaches that are typically employed for the determination of the enantiomeric contents of chiral compounds rely on high-performance liquid chromatography (HPLC), capillary electrophoresis (CE), and gas chromatography (GC).^{6–11}

However, these methods are usually time-consuming and quite expensive as a result of requirement for sophisticated instrumentation. As a consequence, simple, inexpensive, and convenient techniques for this purpose are still in demand. Optical methodologies, especially those that are based on fluorescence/UV spectroscopic techniques, have drawn substantial interests of researchers owing to their advantageous features including simplicity, low cost, high sensitivity, adaptation to automation and real-time analysis, and diverse signal output modes.^{12–16} Not only do fluorometric methods enable fast in situ determinations of the enantiomeric compositions of chiral analytes but also they are useful in the high-throughput screening (HTS) of chiral catalysts or drugs that arise using combinatorial chemistry.¹⁷ In addition, colorimetric assays based on UV/vis spectral changes provide a visible means for determining

Received: October 10, 2013

Published: February 5, 2014



enantiomeric compositions without the need for advanced instrumentation.

The key requirement of UV and fluorescence approaches to evaluate enantiomeric compositions are chiral sensors that have the ability to differentially interact with different enantiomers of a chiral target in a manner that gives rise to different optical signal outputs. As a consequence of the major developments that have resulted from molecular sensing and supramolecular chemistry investigations, a large number of enantioselective chemosensors have been developed over the past decades. The intensity of these advancements is highlighted by the more than 180 papers, which have been published regarding fluorescence and colorimetric chiral sensors since 2000. Several reviews have been published recently that cover different perspectives of some of these contributions. For example, Pu summarized the results of efforts carried out in his group focusing on 1,1'-binaphthyls based chiral sensors.¹⁸ Enantioselective sensing by using luminescence methods along with a description of diverse sensing methods and mechanisms for enantioselective luminescent recognition have been reviewed by Corradini et al.¹⁹ In addition, Sirlin and Dieng reviewed the area of artificial receptors developed for recognition of chiral carboxylic anions,²⁰ and Anslyn et al. reviewed methods for the rapid determination of enantiomeric excesses (ee) using fluorescence and colorimetric approaches.²¹ Recently, new strategies, such as those involving bionics technologies, nanotechnologies, and real-time monitoring, have been developed for fluorescence sensing and detection of chiral guests. Owing to the existence of the reviews summarized above, the discussion presented below focuses only on developments that have arisen from research studies of novel fluorescence and colorimetric chiral sensors carried out over the past ten years. In this review, the results of these efforts are organized based on the constitutional components and structural features of the sensors including small organic molecule based chiral chemosensors, metal complex based chiral probes, polymer based chiral probes, and nanomaterial based chiral sensors. Attention is also given to the chemical mechanisms involved in the chiral recognition and binding interactions involved in each sensing process.

2. GENERAL DESIGN PRINCIPLES

Chiral fluorescent and colorimetric chemosensors are the molecules or materials that can interact with the chiral targets and convert the enantioselective recognition events into observably optical signal outputs, such as fluorescence quenching/enhancement, ratiometric changes, or UV-vis spectral changes, etc. Therefore, design of such optical sensors relates to the chiral host–guest chemistry in combination with the spectroscopy. In the process of the design of chemosensors, there are two predetermined considerations involving sensing mechanisms and interaction modes for the hosts/receptors with analytes. In terms of the selected sensing and recognition mechanisms, proper constitutional components, such as fluorophores, linkers and binding units must be chosen to construct the objective chemosensors.^{22–25} The sensing mechanisms frequently emerging in chiral sensing systems include photoinduced electron transfer (PET), aggregation-induced emission enhancement (AIEE), and formation of excimer/exciplex species, etc.¹⁹ The sensing mechanisms may be determined by properties of the chosen fluorophores, as well as the linking approaches between the fluorophores and the binding units. On the other hand, with different binding units fitted onto the fluorescent sensors, varied interaction or binding

manners occur, such as hydrogen bond interaction, covalent interaction and charge–charge ionic electrostatic interaction, etc. Another critical ingredient should be emphasized concerning the chiral sensing systems: the introduced chiral sources. These have a vital role to play in ensuring that the resulting sensors have the capability of enantioselective recognition of chiral organic molecules.

In most cases, two building approaches are involved in the construction of chiral chemosensors with the components mentioned above. One approach is about the direct combination of the receptors/binding units with the signaling reporters (fluorophore or chromophore) without any linkers, in other words, the receptor is the integrated part of the π -conjugation system of a reporter. In this case, the interaction of analytes with receptors may induce fluorescence quenching due to the intermolecular PET effect between them, or cause UV-vis absorption changes because of the ICT (intramolecular charge transfer) mechanism. The other method lies on the covalent linkage between the reporters and the receptors with short aliphatic spacers that can avoid the ground-state variation. Intramolecular PET is the major sensing mechanism for such “reporter–spacer–receptor” sensing systems, which can only give rise to changes in the fluorescence intensity upon the receptor-guest interaction. In either of these two approaches, the chiral sources are generally introduced in the vicinity of the hosts to realize the enantioselective recognition, or the fluorophore/chromophore can be the chiral unit itself. In addition, indicator displacement assay (IDA) is another alternative method for the design of a chiral sensing system, which is also called an enantioselective indicator displacement assay (eIDA).²¹ In such a strategy, the association of an indicator (fluorophore or chromophore) with a receptor containing the chiral unit can form a chiral receptor-indicator scaffold, in which the indicator can be dissociated selectively by the two enantiomers of one chiral analyte from the chiral receptor inducing the enantioselective fluorescence or UV-vis spectral responses. This approach applies to those reversible interaction system designs, such as metal complexes or boronate esters.

The ultimate aim of various chiral fluorescent and colorimetric sensors is to realize high differences in the spectroscopic responses of the sensor toward the two enantiomers of one chiral analyte. The enantioselective spectroscopic responses are reflected in the differential affinity of the sensor host for different guest enantiomers. So how to afford the high enantioselective affinity is the crucial point in the chiral sensor design. Large chiral barrier and rigid structure are deemed to be two helpful factors for the receptor to preferentially interact with one of the guest enantiomers than another one. In order to obtain these two conditions, macrocyclic structures, such as crown ethers, calixarenes, cyclodextrins, bisbinaphthyl macrocycles, etc. have been frequently used as the scaffolds of chiral sensors. These rigid macrocycles generally possess multiple interaction points that allow chiral guest enantiomers to accommodate their cavities forming lowly flexible and highly stable diastereomeric complexes, which may induce a high enantioselectivity in cooperation with the large chiral barriers. For those acyclic chiral sensors, the formation of the rigid cyclic sensor-analyte complexes or multipoint interactions may usually show good enantioselectivity due to the higher structural complementarity and spatial compatibility for one chiral guest enantiomer than for another one. For example, the bisboronic acid-based chiral sensors can display good enantioselectivity toward chiral polyols but those monoboronic acid chiral sensors can not. In the

following chapters and sections, we will indicate the designing rules that have been applied in the practical examples for gaining fluorescent or colorimetric enantioselective sensing including some specific ones.

3. SMALL ORGANIC MOLECULE-BASED CHIRAL CHEMOSENSORS

Artificial fluorescent chemosensors based on the synthesized small organic dyes have been researched in the past few decades for certain applications, including environmental and biological assays or bioimaging, owing to the advantages of high sensitivity and selectivity with various target molecules, easy synthesis and storage, low cost, low toxicity, excellent stability toward different experimental conditions, and others.^{26–34} In recent decades, a large number of excellent chiral fluorescent chemosensors with various small organic molecules as building blocks have been reported for the chiral recognition. In this review, we classify the chiral sources into two types: nonfluorophore chiral molecules and inherently chiral fluorophores. Theoretically, all of the nonfluorophore chiral analytes, e.g., chiral amines, amino alcohols, α -hydroxy acids, α -amino acids, sugars, and other polyols, can be exploited as the chiral scaffolds of the enantioselective fluorosensors. In contrast, the use of inherently chiral fluorophores for the application of chiral recognition is much more limited. Considering this point, we exploit one independent section to discuss the enantioselective fluorosensors based on inherently chiral fluorophores.

3.1. Inherently Chiral Fluorophore-Based Chemosensors

The reported chiral fluorophores that have been used in enantioselective fluorescent sensors include 1,1'-binaphthyls such as 1,1'-bi-2-naphthol (BINOL) derivatives, helicenes, 1,8-diacridylnaphthalene, and the recently reported axially chiral hydroxycarbazole biaryl (BICOL) derivatives. Among them, chiral 1,1'-binaphthyl compounds are the most frequently used chiral fluorophores for enantioselective recognition, and most of them are based on BINOLs with hydrogen bond interaction between probes and analytes as the binding mode. We will utilize one subsection to summarize this part of the content, and those based on other binding modes such as covalent interaction will be discussed in other chapters or sections.

3.1.1. Binaphthyl-Based Chemosensors. Binaphthyl compounds are versatile fluorophores and have been actively used in the development of optoelectric materials,^{35–38} catalysts for asymmetric synthesis,^{39–41} and optical sensors for molecule or ion recognition,^{42,43} due to their particularities, such as special C₂ axial chirality and rigid structure, high stability of their enantiomeric configuration, relatively high emission efficiency, and readily selective functionalization. In the field of the chiral recognition with fluorescence responses, early studies have revealed that exposure of some binaphthyl derivatives to the enantiomers of certain chiral organic analytes can induce enantioselective fluorescence quenching.^{44–48}

Two representative examples of binaphthyl compounds are 1,1'-bi-2-naphthol (**1**) and 2,2'-diamino-1,1'-binaphthyl (**2**; Figure 1).⁴⁹ Both **1** and **2** can be used to discriminate the enantiomers of α -methylbenzylamine (MBA) with slight but detectable diminishment in the fluorescence intensity caused by the PET process with the hydrogen bond formation between fluorophores and chiral analytes. Interestingly, (*R*)-**1** has been found through a fluorescence reduction signaling to be more sensitive to (*S*)-MBA than to (*R*)-MBA, whereas (*R*)-**2** is more sensitive to (*R*)-MBA than to (*S*)-MBA. Thus, these two

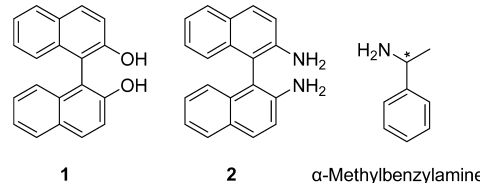


Figure 1. Structure of binaphthyl compounds **1**, **2**, and α -Methylbenzylamine (MBA).

naphthyls have the latent capacity of the enantioselective detection of the enantiomers of MBA. Subsequently, as an attempt to magnify the fluorescence signal and to further elevate the chiral recognition sensitivities of naphthyls toward chiral analytes, some BINOL derivatives with dendritic structures have been reported by Pu and co-workers. Since this topic has been summarized detailedly in extensive reviews by Pu,^{18,50} we will not go into any further detail in this review.

Recently, Wang and co-workers synthesized three binaphthyl molecules **3–5** with the respective attachment of benzoyl, ethoxy formyl, and ethyl oxalyl into the BINOL core (Figure 2).^{51,52} Moreover, compounds **6** and **7** are prepared, in which the two aryl hydroxyl groups are protected with methyl groups. It has been demonstrated by fluorimetric titration experiments that sensors **3**, **4**, and **5** display excellent performance on the enantioselective discrimination between the enantiomers of either *N*-Boc-protected alanine (Ala) anion or *N*-Boc-protected phenylalanine (Phe) anion in CHCl₃. For instance, in the presence of 11.4 equivalent of the (*S*)-Ala anion, the fluorescence intensity of sensor (*S*)-**3** is reduced by 48.4%, whereas exposure of (*S*)-**3** to the same amount level of (*S*)-Ala anion only induces 15.5% of fluorescence quenching. Thus, the enantioselectivity with the ratio of quenching efficiencies of sensor (*S*)-**3** toward the enantiomers of Ala anion is 3.12. The similar enantioselective performances of (*S*)-**4** and (*S*)-**5** on the chiral recognition of Ala or Phe anions have been also observed. In terms of the association constants, these three sensors also exhibit excellent enantiodiscrimination ability between the enantiomers of either the Ala or Phe anion. For example, the association constant of (*S*)-**3** with (*S*)-Ala anion has been found to be $(3.90 \pm 0.12) \times 10^4 \text{ M}^{-1}$ and that of (*S*)-**3** with (*R*)-Ala anion is $(5.43 \pm 0.03) \times 10^3 \text{ M}^{-1}$. Thus, with the 1:1 binding form of receptor-Ala complex, the enantioselectivity of (*S*)-**3** toward Ala anions, defined as K_S over K_R, is obtained as 7.18:1, which indicates that (*S*)-**3** binds to the (*S*)-Ala anion more stably than to the (*R*)-Ala anion. Moreover, with an opposite enantioselectivity of (*R*)-**3** toward the Ala anions, the ratio of association constants (K_S/K_R) is calculated as 1:7.04, which shows that the stability of the complex of (*R*)-**3** with (*R*)-Ala anion is much stronger than that of the complex (*R*)-**3** with the (*S*)-Ala anion. In order to investigate the chiral recognition mechanism, ¹H NMR experiments have been carried out to demonstrate that the main interaction mode between these sensors and the chiral anionic analytes is multiple hydrogen bonding. Moreover, the fact that exposure of either compound **6** or **7** to anionic substrates is not able to produce any changes in the fluorescence intensity suggests the critical role that hydroxyl protons play in the multiple hydrogen bonds formation.

It is well-known that, compared with fluorescence quenching, the off-on fluorescence response mode is more reliable and efficient for reporting fluorescence recognition events.⁵³ Therefore, in order to realize off-on fluorescence responses for chiral recognition, the BINOL derivatives containing nonconjugated

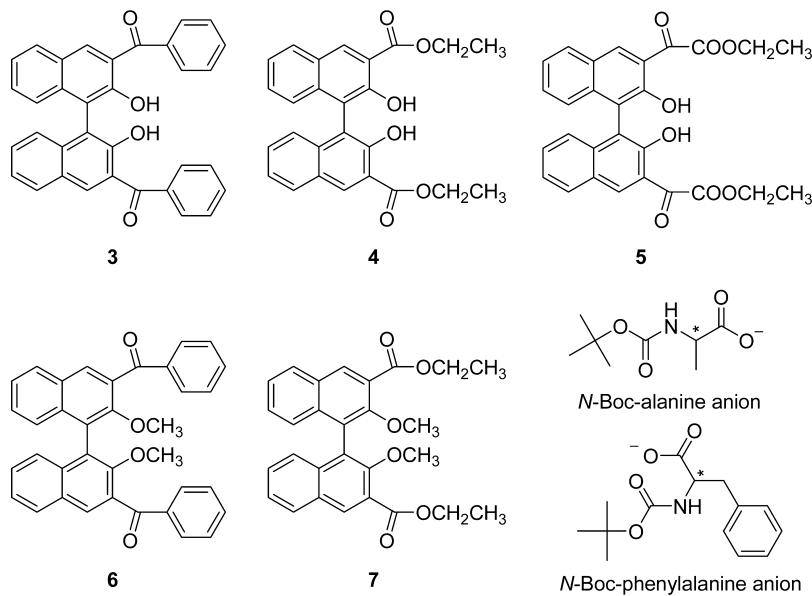


Figure 2. Structure of binaphthyl compounds 3–7 and two Boc-protected amino acid anions.

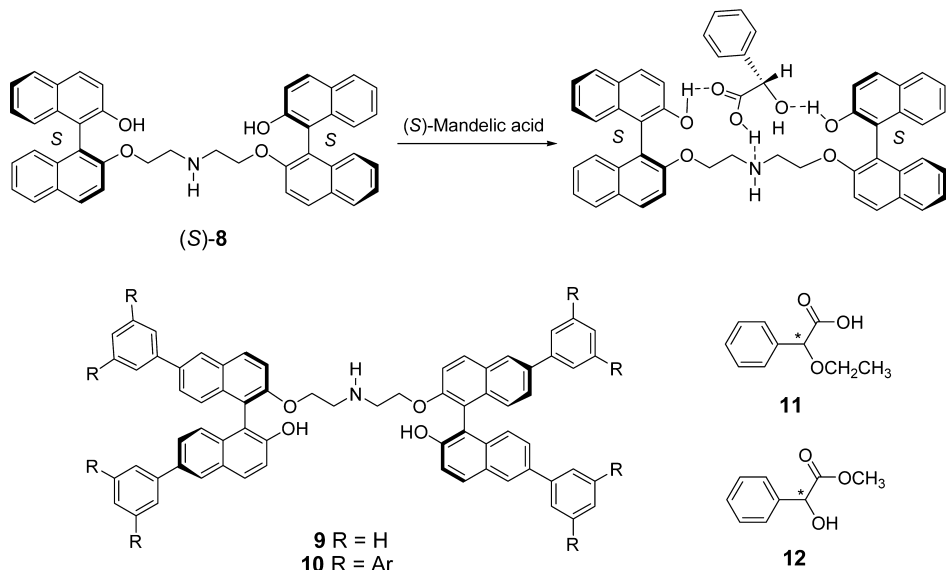


Figure 3. Proposed interaction mode between (S)-8 and (S)-MA and the structures of sensors 9 and 10 and MA derivatives 11 and 12.

amine groups, which serve as the quenchers of the BINOL fluorophores by the PET effect, have been developed. The group, led by professor Pu, has been active in developing this kind of chiral chemosensors for many years, and recently, much impressive progress has been made. In 2002, Pu and co-workers synthesized a bisbinaphthyl compound 8 bearing a secondary amine group for the chiral recognition of mandelic acid (MA).^{54,55}

As shown in Figure 3, sensor 8 can interact with MA by the multiple hydrogen bondings, which can induce an increase in the fluorescence intensity of sensor 8 through the suppression of the PET process. Due to the formation of two different diastereomeric complexes between sensor 8 and the two enantiomers of MA, the enantiodiscrimination can be observed through the different enhancement degrees of the fluorescence. In practice, (S)-8 displays a distinct enantioselectivity toward (S)- and (R)-MA, as shown by $\Delta I_S/\Delta I_R = 2.49$ [$\Delta I_S = I_S - I_0$ and $\Delta I_R = I_R - I_0$, where I_S and I_R represent the fluorescence

intensities of the sensor in the presence of (S)- and (R)-MA, respectively, and I_0 is the background fluorescence intensity of the sensor], and the enantioselectivity in terms of association constant ratio is shown to be 2.13:1 (K_S/K_R). On the other hand, sensor (R)-8 exhibits a reversed enantioselective effect toward MAs; that is, (R)-MA binds to sensor (R)-8 much stronger than (S)-MA does, which further testifies to the existence of enantioselectivity. In order to investigate the interaction mode between sensor 8 and MA, two derivatives of MA, α -hydroxyl group-protected 11 and carboxylic acid-protected 12, have been employed to interact with 8. The fact that both (S)- and (R)-11 can intensify the fluorescence of 8 without any observed difference and exposure of 8 to substrate 12 is not capable of inducing any fluorescence enhancement demonstrates that both alpha and carboxylic hydroxyls are fundamental to the formation of multiple hydrogen bonds, which is in accordance with the proposed binding mode between 8 and MA. With molecule 8 as the template, two dendritic bisbinaphthyl compounds 9 and 10

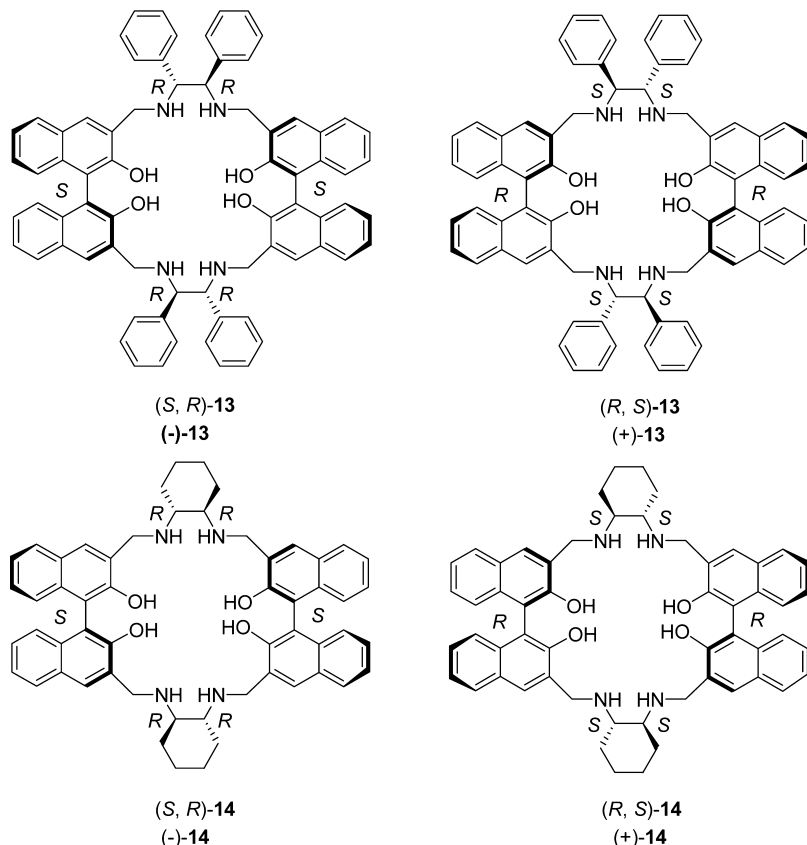


Figure 4. Enantiomeric compositions of bisbinaphthyl macrocycles (*S,R*)-13, (*R,S*)-13, (*S,R*)-14, and (*R,S*)-14, in which the first letter represents the chirality of the BINOL units and the second letter represents the chirogenic center of the chiral diamines.

have been also prepared.⁵⁵ The fluorescent emissions of both of these two compounds have been found to be much stronger than that of **8** due to the intramolecular energy transfer from the dendritic branch units to the binaphthyl cores. In spite of the enhanced fluorescence, compounds **9** and **10** show better sensitivities in detecting MA. Compared with the fluorescence enhancement of **8** on exposure to MA, the improvements of **9** and **10** are ~14 and ~22 times greater, respectively. Moreover, good enantioselectivities ($\Delta I_R / \Delta I_S$) of (*R*)-**9** and (*R*)-**10** toward (*R*)- and (*S*)-MA are also observed respectively as 2.05 and 1.49.

In order to further improve the sensitive and enantioselective behaviors of binaphthyl-based sensors to chiral analytes, chiral diamines have been introduced into BINOL molecules. Pu and co-workers have developed a series of bisbinaphthyl macrocyclic compounds, among which, compounds **13** and **14** are two classical compounds with the respective attachment of chiral 1,2-diphenylenediamine and cyclohexane-1,2-diamine onto the BINOL scaffolds (Figure 4). It is noteworthy that the molecular frameworks of both **13** and **14** contain four secondary amine groups that are capable of quenching the fluorescence of the BINOL fluorophores more efficiently through the PET effect, and four hydroxyl groups that can bind chiral analytes more tightly via multiple hydrogen bondings. Moreover, the four extra chiral centers introduced by the chiral diamines in cooperation with the axial chirality of BINOL units are capable of increasing the enantioselective interaction of the macrocycles with chiral substrates. Experimentally, two emission peaks from both the monomer and excimer have been observed in the fluorescence spectra of macrocycles **13** and **14**. Interestingly, in the benzene solution with some proportion of dimethoxyethylene (DME) which is used to increase the solubility of acid substrates, the

enantioselective fluorescence responses of **13** toward MA concentrate mainly at the excimer fluorescence signal, while the enantioselective enhancement chiefly in the emission from the monomer of macrocycle **14** has been observed in response to the enantiomers of MA.

When (*S*)-MA was added to the solution of (*S,R*)-**13** (1.0×10^{-4} M) in benzene with 2% DME, the intensity of the excimer emission (424 nm) of (*S,R*)-**13** was increased significantly, whereas the addition of (*R*)-MA only induced slight changes.⁵⁶ The enantioselectivity of (*S,R*)-**13** toward the two enantiomers of MA exhibited a $\Delta I_S / \Delta I_R$ as high as 12 with the concentration of MA up to 2.0×10^{-2} M. (*S,R*)-**13** displayed a similar enantioselective response toward hexahydromandelic acid (HMA), that is, the excimer emission intensity of (*S,R*)-**13** can be increased by (*S*)-HMA much more significantly than by (*R*)-HMA.⁵⁷

In addition, α -amino acid derivatives can be also enantioselectively discriminated with fluorescence responses by macrocycle **13**. For instance, the enantioselectivity of (*R,S*)-**13** toward the two enantiomers of *N*-benzyloxycarbonylphenylglycine (BPG) is able to be measured as $\Delta I_D / \Delta I_L = 5.7$ [$\Delta I_D = I_D - I_0$ and $\Delta I_L = I_L - I_0$, where I_D and I_L represent the fluorescence intensities of sensor **13** in the presence of *D*- and *L*-BPG, respectively, and I_0 indicates the background fluorescence intensity of sensor **13**] in benzene with 2% DME at the excimer emission (430 nm). This indicates that the association of (*R,S*)-**13** with *D*-BPG is much stronger than with (*L*)-BPG, and vice versa. ^1H NMR titration experiments of (*S,R*)-**13** with (*L*)-BPG have demonstrated that all of the four amine groups of (*S,R*)-**13** are protonated by four carboxylic groups of *L*-BPG through the formation of a **13**-BPG complex with 1:4 form, which leads to the

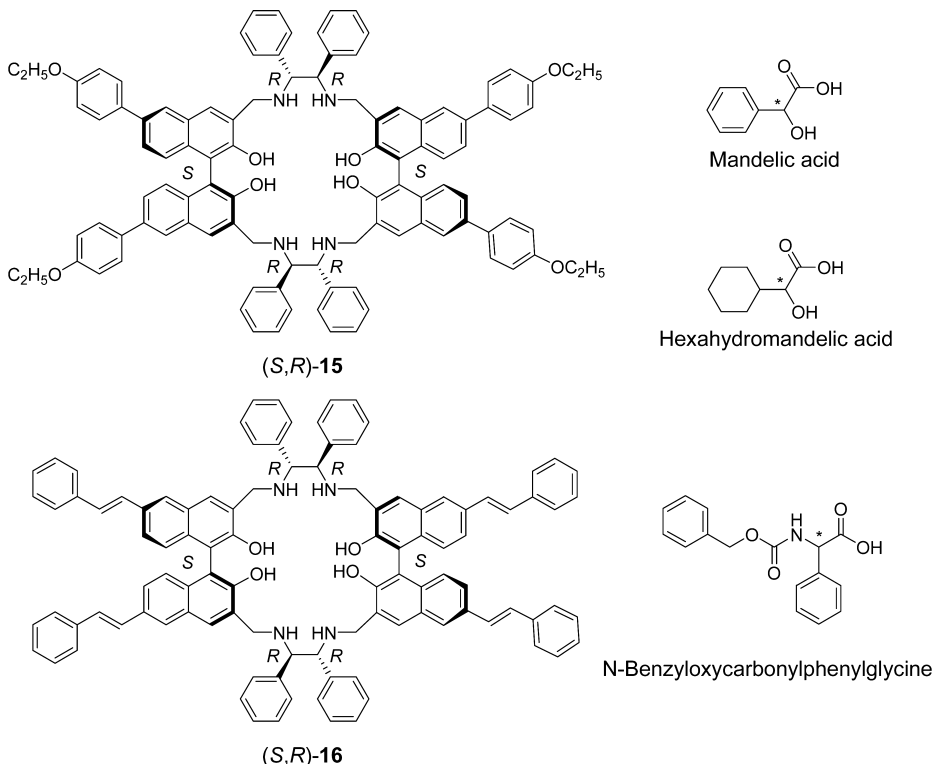


Figure 5. Structures of bisbinaphthyl macrocycles **(S,R)-15**, **(S,R)-16**, MA, HMA, and BPG.

significant fluorescence enhancement by the inhibition of the PET process.⁵⁸

For the sake of improving the spectral properties, Li et al. have decorated **(R,S)-13** with two conjugated groups, *p*-ethoxyphenyl and styryl, on the 6,6'-positions of the binaphthyl scaffolds, which created bisbinaphthyl macrocyclic compounds **(S,R)-15** and **(S,R)-16** (Figure 5).⁵⁷ As expected, in contrast with **13**, macrocycles **15** and **16** have longer wavelength absorptions and emissions from either monomers or excimers and the background fluorescence is more intense, which is beneficial for these two macrocyclic sensors in order to recognize chiral substrates with relatively low probe concentrations. The studies on chiral fluorescence recognition of MA and BPG have been implemented in dichloromethane (DCM) solutions of **13**, **15**, and **16**. Different from the cases in benzene solution, the enantioselective fluorescence responses are mainly dominated by the monomer emissions of these three sensors. For example, the monomer emission intensity of **(R,S)-13** (1.0×10^{-4} M) can be enantioselectively increased by the two enantiomers of MA with the enantioselectivity defined as $\Delta I_R / \Delta I_S$ of 3.2 in DCM (2% DME). The enantioselective fluorescence responses of **(S,R)-15** and **(S,R)-16** (2.0×10^{-6} M) in the emissions of monomers at 380 and 403 nm, respectively, are similar to the enantiomers of MA in DCM (0.4% DME) with the same enantioselectivity of 2 ($\Delta I_S / \Delta I_R$). In particular, both **(S,R)-15** and **(S,R)-16** can be used for the enantioselective detection of L- and D-BPG with good enantioselectivities of more than 3.5 ($\Delta I_L / \Delta I_D$).

As for bisbinaphthyl macrocycle **14**, much higher enantioselective fluorescence behaviors have been found to perform upon chiral recognition of MA at the monomer fluorescence signal in benzene solution.⁵⁹ When 5.0×10^{-4} M of **(R)-MA** is added into the benzene solution (0.05% DME) of **(S,R)-14** (1.0×10^{-5} M), almost no changes in the monomer fluorescence signal are observed, whereas the addition of the same amount of **(S)-MA**

leads to a more than 20-fold fluorescence enhancement in the monomer emission of **(S,R)-14**. With the mirrored fluorescence responses toward the two enantiomers of MA, **(R)-MA** is able to increase the monomer emission intensity of **(R,S)-14** more intensively than **(S)-MA**. A particularly high enantiodiscrimination result of **(S,R)-14** for **(S)**- and **(R)**-MA has been obtained as $\Delta I_S / \Delta I_R = 46$. It is notable that both **(S)**- and **(R)**-**11** cannot induce any changes in the fluorescence emission of **(S,R)-14**, which indicates the key role of the α -hydroxyl group of MA on the interaction with **(S,R)-14**. In addition, the enantioselective recognition of HMA with **(R,S)-14** (1.0×10^{-5} M) in benzene/0.4% DME has been also reported by Li et al.⁶⁰ Similar to the enantioselective fluorescence response to MA, the monomer emission intensity of **(R,S)-14** can be increased more dramatically by **(R)-HMA** (4.0×10^{-3} M) than by the same amount of **(S)-HMA**, which results in a high enantioselectivity of 64 ($\Delta I_R / \Delta I_S$).

In view of the extremely high chiral recognition ability of bisbinaphthyl macrocycle **14** to MA, the utility of **14** for the chiral catalyst screenings has been tested through the asymmetric synthesis of the derivatives of MA.⁶¹ As shown in Figure 6, Li and co-workers tried to determine the best catalytic conditions for the asymmetric transformation from achiral aldehyde **17** to chiral α -hydroxylic acid **18** with trimethylsilyl cyanide (TMSCN) in the presence of $Ti(O^{\prime}Pr)_4$, and to chiral ligand **19** or diisopropyltartrate (DIPT) through the fluorescence monitoring of the ees of the samples separated from the reaction systems. In order to readily test the samples, a linear relationship between the fluorescence intensity differences ΔI [$\Delta I = (I_S / I_{S0}) - (I_R / I_{R0})$, where I_S and I_{S0} are the fluorescence intensities of **(S,R)-14** with and without the acid **18**, and I_R and I_{R0} are the fluorescence intensities of **(R,S)-14** with and without the acid **18**] and the ees of **18** has been established in a proper testing solution of THF/hexane/benzene (1:5.5:18.5). Thus one can read out the ees

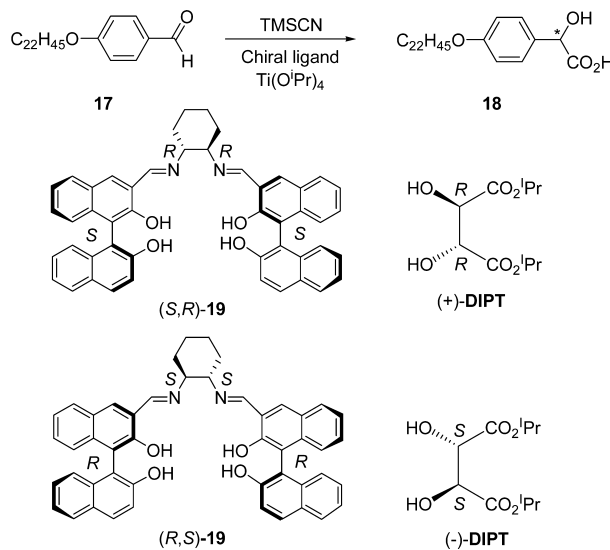


Figure 6. Asymmetric conversion of achiral aldehyde **17** to chiral α -hydroxylic acid **18** in the presence of the chiral ligands **19** or DIPT associated with $Ti(O^iPr)_4$.

from the fluorescence intensity changes of **14** in the presence of various samples of **18** and additionally determine the optimum catalytic conditions. For example, from the reaction in DCM with 40 mol % of (+)-DIPT as the chiral ligand in combination with 40 mol % of $Ti(O^iPr)_4$, the ee of the isolated sample of **18** has been determined to be 79% according to a ΔI of 1.92.

As an important research branch of binaphthyl-based enantioselective fluorescence sensing systems, PET-based monomeric binaphthyl sensors with the introduction of two chiral amines or amino alcohols into one BINOL molecule are receiving similar levels of interest from researchers as acyclic and cyclic bisbinaphthyl-based sensors. Certain types of the former sensors show much better results in enantioselective recognition events than the latter sensors. In an initial work, two simple monomeric binaphthyl compounds (*S*)-**20** and (*R*)-**20** (Figure 7) bearing two achiral benzylamino groups were reported by Lin et al.⁶² Interestingly, monomeric BINOL sensor **20** shows the opposite enantioselective fluorescence response toward the two

enantiomers of MA in contrast to bisnaphthyl sensor **8** in benzene solution. That is to say, (*S*)-MA enhances the fluorescence intensity of (*R*)-**20** much more intensively than that of (*S*)-**20**, and vice versa. A relatively good enantioselectivity with (*R*)-**20** has been calculated to be $\Delta I_S/\Delta I_R = 4.2$. The enantiodiscrimination behaviors of sensor **20** toward the enantiomers of *N*-benzyloxycarbonylphenylglycine (BPG) have also been investigated. Similarly, the fluorescence intensity of (*R*)-**20** can be increased more intensively by d-BPG than by L-BPG, which shows a relatively low enantioselectivity of $\Delta I_D/\Delta I_L = 2.0$.

Two diastereomeric monomeric BINOL probes (*S,R*)-**21** and (*R,R*)-**21** have been prepared by incorporating chiral MBAs into monomeric BINOL scaffolds, as shown in Figure 7. Surprisingly, with the introduction of the extra two chiral centers, (*R,R*)-**21** displays a reversed enantioselective behavior to the enantiomers of MA compared with sensor (*R*)-**20**; however, both the sensitivity and enantioselectivity are relatively lower ($\Delta I_S/\Delta I_R = 1.9$), which is due to the decrease of the association of (*R,R*)-**21** with MA induced from the steric hindrance of extra methyl. On the other hand, a much greater enantioselectivity toward d- and L-BPG with (*R,R*)-**21** has been observed, with $\Delta I_D/\Delta I_L = 5.1$. However, compound (*S,R*)-**21** exhibits much lower enantioselectivity toward either S/R-MA or L/D-BPG, which demonstrates that the compatibility between the extra chiral center and the chiral configuration of BINOL scaffold in (*R,R*)-**21** is much better than that in (*S,R*)-**21** for enantioselective bindings with chiral substrates.

Subsequently, the other two diastereomeric isomers of compounds **21**, (*S,S*)-**21** and (*R,S*)-**21** (Figure 7), were also synthesized by Feng and co-workers for the fluorescent enantioselective recognition of the *N*-Boc-protected α -amino acids.⁶³ The enantioselective fluorescence recognition of *N*-Boc-proline (Pro) has been conducted in a mixed solvent of DCM/hexane (3:7) containing 1.2% THF. The enantioselective enhancement of the fluorescence intensity of **21** in the presence of the two enantiomers of *N*-Boc-Pro is maximized at the monomer emission wavelength of 365 nm. A good enantioselectivity toward d- and L-N-Boc-Pro with sensor (*S,S*)-**21** has been obtained with $\Delta I_D/\Delta I_L = 6.6$. On the contrary, (*R,S*)-**21** displays a higher enantioselectivity toward L- and d-N-Boc-Pro

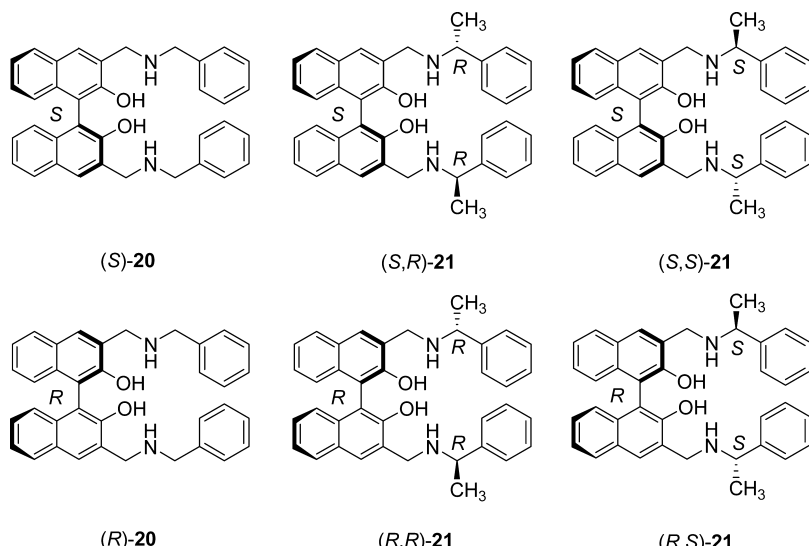


Figure 7. Enantiomeric compositions of monomeric binaphthyl compounds **20** and the structures of four diastereomeric isomers of compound **21**.

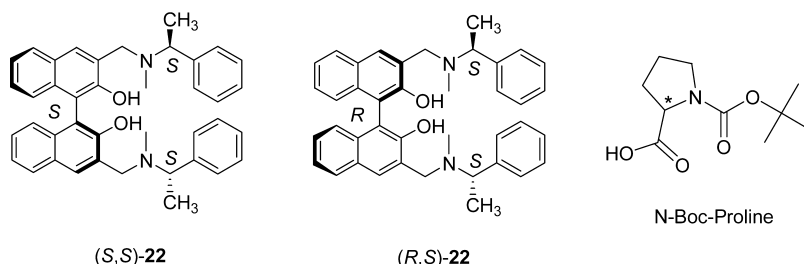


Figure 8. Structures of two diastereomeric isomers of compound **22** and N-Boc-proline (Pro).

with $\Delta I_L/\Delta I_D = 10.4$. Similarly, two contrast compounds (*S,S*)-**22** and (*R,S*)-**22** (Figure 8) in which the amine protons are substituted by methyls have been also investigated for the chiral recognition of *N*-Boc-Pro. As expected, neither (*S,S*)-**22** nor (*R,S*)-**22** showed enantioselectivity with the fluorescence enhancement responses to the two enantiomers of *N*-Boc-Pro, which indicates the fundamental role of the chiral amine hydrogen in the enantioselective hydrogen bond interaction between *N*-Boc-Pro and sensor **21**.

Very recently, by linking cyclohexane-1,2-diamine derivatives **23** to BINOL fluorophore, Cheng and co-workers have synthesized monomeric BINOL compounds **24** (Figure 9) as

(R,R)-**24** more intensively than D-Boc-Phg. With a 1:1 binding form, the chiroselectivity toward D- and L-Boc-Phg with (R,R)-**24** has been calculated by $(K_D F_D)/(K_L F_L)$ as 14.31, where K represents the association constant of (R,R)-**24** with D- or L-Boc-Phg and F stands for the maximum fluorescence enhancement of (R,R)-**24** in the presence of D- or L-Boc-Phg. As a contrast, one diastereomer of **24**, compound (S,R)-**24**, has been also obtained by incorporating (1*R*,2*R*)-cyclohexane-1,2-diamine into the (S)-BINOL scaffold. However, compound (S,R)-**24** exhibits a much lower enantioselectivity toward D- or L-Boc-Phg at $(K_D F_D)/(K_L F_L) = 1.29$, which indicates that the chirality cooperation of (R,R) or (S,S) is more harmonious for enantioselective binding with N-Boc-protected amino acids than that of (R,S) or (S,R).

In order to acquire more unique and outstanding chiral recognition effects, some chiral amino alcohols have been also used by Pu and co-workers for the design of novel monomeric binaphthyl chiral sensors. Recently, Liu et al. have reported an extraordinary chiroselective sensing system **2S** (Figure 10) for visually differentiating the two enantiomers of MA using the enantioselective formations of **2S**-MA complex precipitates.

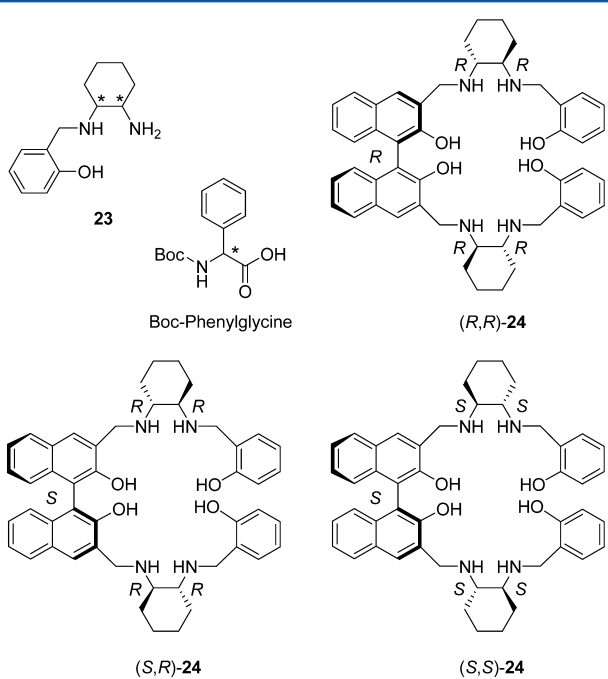


Figure 9. Structures of compound **23** and Boc-Phg as well as the three diastereomeric isomers of compound **24**.

novel unsymmetrical salan fluorescent chiral probes for the chiroselective recognition of N-Boc-protected amino acids such as Boc-phenylglycine (Boc-Phg), Boc-alanine (Boc-Ala), Boc-valine (Boc-Val), and Boc-phenylalanine (Boc-Phe). Among these, the two enantiomers of Boc-Phg can be enantioselectively discriminated much more distinctly with (R,R) -24.⁶⁴ Experimentally, D-Boc-Phg has been found to increase the fluorescence intensity of (R,R) -24 more efficiently than L-Boc-Phg does. Furthermore, with the mirrored fluorescence response, the enantiomer of (R,R) -24, (S,S) -24, displays a reversible chiroselective behavior toward the two enantiomers of Boc-Phg. In other words, L-Boc-Phg enhances the fluorescence of

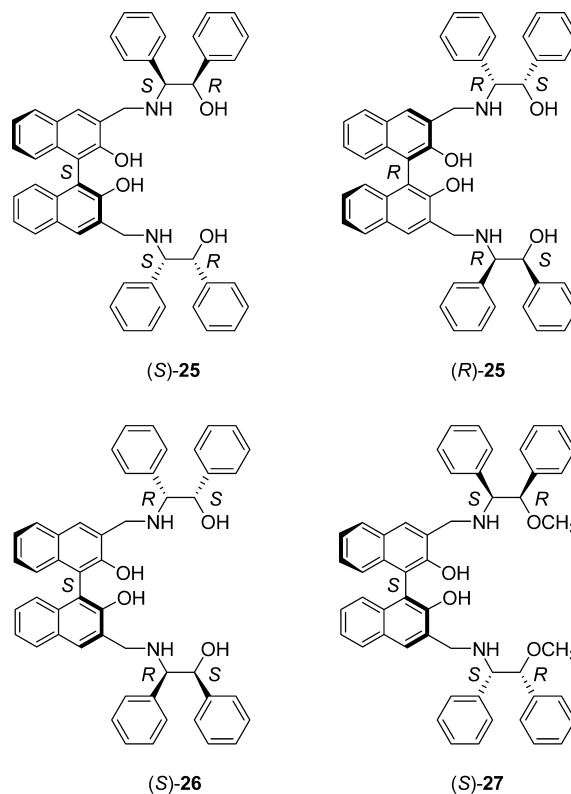


Figure 10. Structures of the two enantiomers of compound **25** as well as the structures of compounds **26** and **27**.

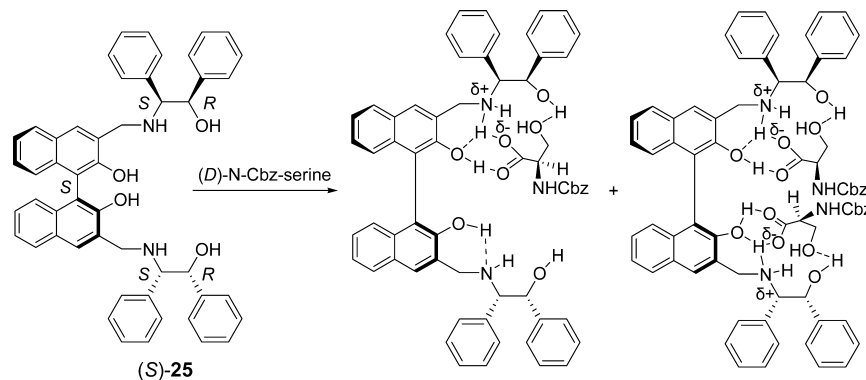


Figure 11. Proposed binding structures of the (S)-25 complexes associated with D-N-Cbz-Ser.

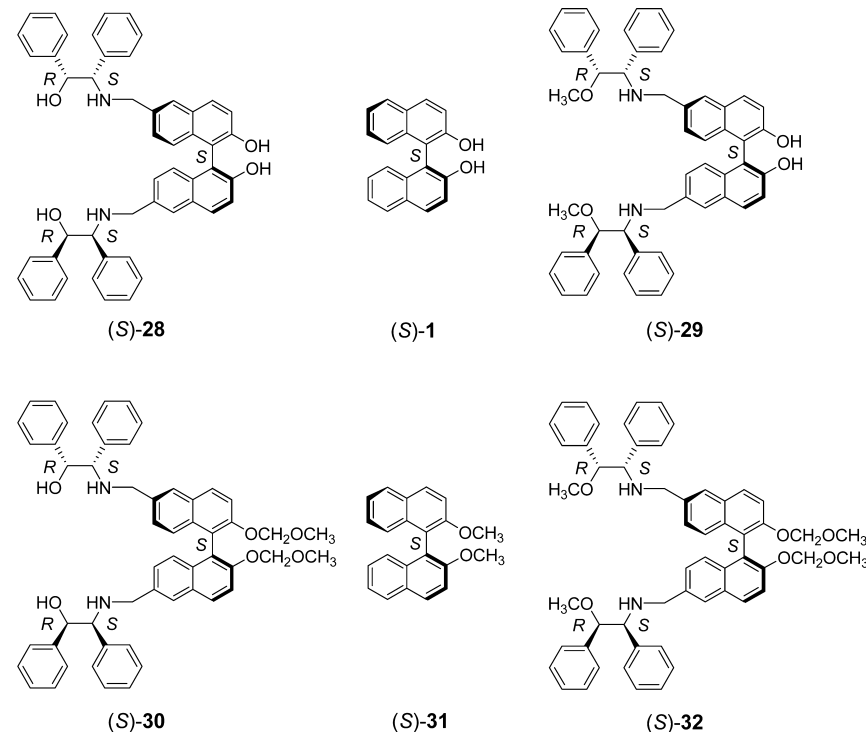


Figure 12. Structures of monoBINOL derivatives (S)-1 and (S)-28 through (S)-32.

followed by strong fluorescence enhancements at the monomer emission wavelength.⁶⁵ It has been demonstrated that when a solution of (S)-25 (5.0×10^{-4} M) is treated with more than 3.0×10^{-3} M of (S)-MA in benzene containing 0.4 vol. % DME, a white suspension forms immediately, whereas the treatment of (S)-25 with (R)-MA under the same conditions does not lead to any changes. With an enantioselective precipitation response, (R)-MA can cause (R)-25 to precipitate out of benzene, but (S)-MA cannot. It has been demonstrated by ^1H NMR experiments that the isolated precipitate is a 1:4 complex of (S)-25 with (S)-MA. In addition, up to 950-fold fluorescence enhancement at 367 nm has been observed with the formation of the (S)-25/(S)-MA suspension, but the fluorescence intensity of (S)-25/(R)-MA remains close to the background fluorescence intensity of (S)-25. It has been proposed that the configuration compatibility of (S)-25 with (S)-MA as well as the strengthening of the structural rigidity of (S)-25 is responsible for the solid-state fluorescence enhancement. As two contrast compounds, (S)-26 and (S)-27 have been prepared as well (Figure 10). Neither (S)-26 nor (S)-27 can cause (S)/(R)-MA to precipitate from benzene, which

alludes to the critical role of the cooperation between the chiral configurations of the BINOL scaffold and amino alcohol moieties in the enantioselective precipitate formation as well as the indispensability of the hydroxyl protons of amino alcohols in the hydrogen bond interactions.

Sensor (S)-25 can be also used for the chiroselective detection of chiral amino acid derivatives such as *N*-carbobenzyloxy-serine (*N*-Cbz-Ser).⁶⁶ It has been found that the enantioselective fluorescent responses of sensor (S)-25 to the two enantiomers of *N*-Cbz-Ser are dominant at the excimer emission, affording a high chiroselectivity at $\Delta I_D/\Delta I_L = 12.5$. ^1H NMR experimental results indicate both 1:1 and 1:2 binding forms exist in the mixture of the (S)-25 complexes with (D)-N-Cbz-Ser. Two postulated structures of the complexes have been proposed as shown in Figure 11.

As a structural analogue of (S)-25, monoBINOL derivative (S)-28 has been also fabricated by incorporating (1*R*,2*S*)-2-amino-1,2-diphenylethanol into the 6,6'-positions of the (S)-BINOL scaffold (Figure 12).⁶⁷ Because of the larger distance between the amine groups and the BINOL hydroxyl groups in

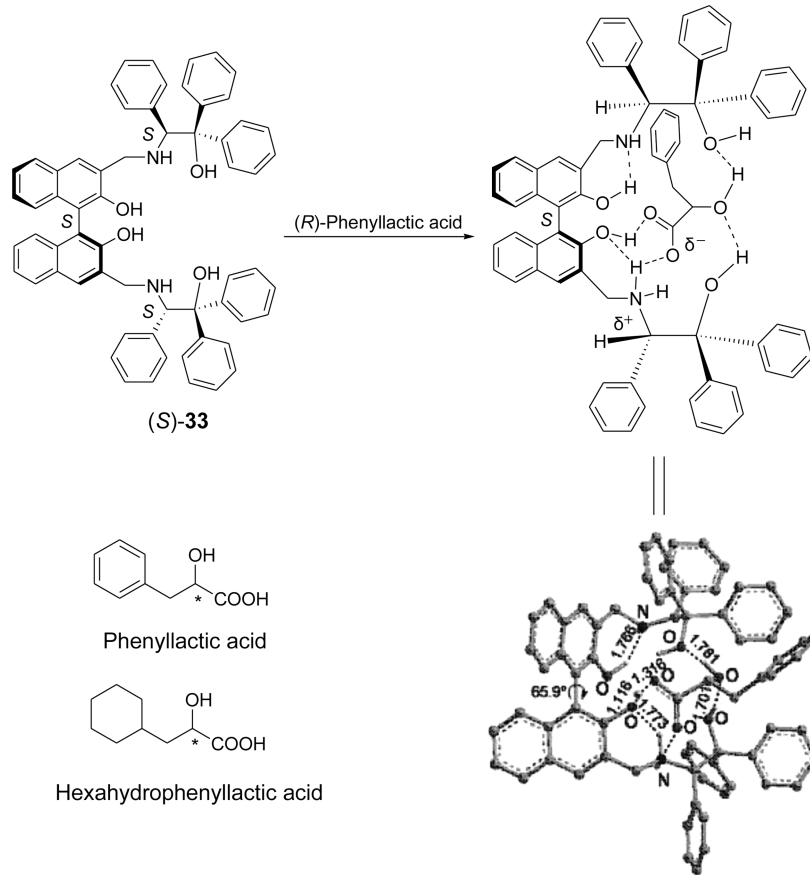


Figure 13. Optimized structure of the proposed 1:1 complex of (S)-33 with (R)-PL, and the structures of PL and hexahydrophenyllactic acid.

6,6'-substituted compound (S)-28, intramolecular hydrogen bonds are not formed between them and the amino alcohol moieties are allowed to rotate readily following the methylene linker. This causes (S)-28 to show distinctive fluorescence patterns in contrast to compound (S)-25. (S)-25 has both the monomer and excimer emission bands in its fluorescence spectrum, but (S)-28 only fluoresces at the monomer emission (379 nm) in benzene. Furthermore, the background fluorescence intensity of (S)-28 is much stronger than that of (S)-25. Additionally, even though (S)-28 has a similar fluorescence spectrum to that of (S)-1, no PET fluorescence quenching processes have been demonstrated to occur between the amine groups and the BINOL fluorophore.

In order to investigate the effect of each functional group on the fluorescence properties of (S)-28, the contrast compounds (S)-29, (S)-30, (S)-31, and (S)-32 have been also prepared (Figure 12). It has been found that the fluorescence quantum yields of the BINOL hydroxyl-protected compounds (S)-30, (S)-31, and (S)-32 (49%, 65%, and 46%, respectively) are similar to each other and much greater than those of the BINOL hydroxyl-unprotected compounds (S)-28, (S)-1, and (S)-29 (6%, 2%, and 6%, respectively) in benzene. This indicates that the BINOL hydroxyl groups influence the fluorescence properties of these monoBINOL derivatives much more readily than either amine groups or the amino alcohol hydroxyl groups do. As a chiroselective fluorosensor, (S)-28 also exhibits enantioselective precipitation responses with significant fluorescence enhancements toward the two enantiomers of MA. ¹H NMR experiments indicate the precipitates isolated from analytical systems are 1:3 complexes of (S)-28 with either (S)-MA or (R)-MA. More

notably, the fluorescence enhancement has been observed in (S)-28/(R)-MA complex but not in (S)-28/(S)-MA complex, suggesting an inverse enantioselective interaction in contrast to that of (S)-25.

Recently, another monoBINOL chiroselective sensor (S)-33 (Figure 13) has been derivatized from compound (S)-25 by substituting the hydrogens from the alpha carbons of the two amino alcohol hydroxyl groups in (S)-25 with two phenyl groups.⁶⁸ The additional phenyl substituents next to the amino alcohol hydroxyl groups improve the steric selective effect of the sensor for chiral acid substrates. Sensor (S)-33 shows high chiroselective behaviors to MA and/or HMA as well as other α -hydroxycarboxylic acids. Especially for some acid substrate, a novel fluorescent responding mode of enhancement/diminished for chiroselectivity with sensor (S)-33 has been observed at the monomer emission. For instance, the exposure of (S)-33 to the (R)-enantiomer of phenyllactic acid (PL) in benzene (DME, 0.4% v/v) can lead to a significant enhancement of the monomer emission intensity of (S)-33, whereas (S)-PL induces a fluorescence quenching at the monomer under the same conditions. Additionally, a high chiral selectivity of $I_R/I_S = 11.2$ [I_R or I_S : fluorescence intensity of (S)-33 in the presence of (R)- or (S)-PL] has been obtained. A 1:1 binding form between the host (S)-33 and the guest (R)-PL has been indicated from the ¹H NMR experimental results. Thus, an optimized structure of a 1:1 complex of sensor (S)-33 with (R)-PL calculated by B3LYP/6-31G on Gaussian 03 software has been proposed. As shown in Figure 13, all of the amino alcohol hydroxyl groups of (S)-33 participate in the multiple hydrogen bondings, ensuring that the complex formed has enhanced structurally rigidity, which is

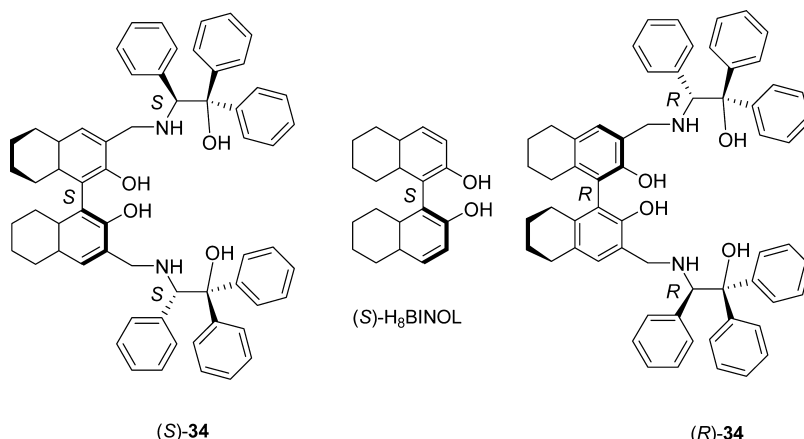


Figure 14. Structures of the two enantiomers of compound 34 as well as the chiral configuration of (S)-HgBINOL.

responsible for the chiroselective fluorescence enhancement. Moreover, sensor (S)-33 displays a much higher chiroselectivity toward the two enantiomers of hexahydrophenyllactic acid at the monomer emission, showing the I_R/I_S ratio as high as 22.8, which indicates that this sensing system with bulky substituents is more suitable for the enantioselective binding of chiral hydrogenated-phenyl acid substrates.

As a hydrogenated analogue of compound (S)-33, sensor (S)-34 (Figure 14) has been also shown to achieve good chiral recognition of MA.⁶⁹ Compound (S)-34 emits at 390 nm in CH₂Cl₂, which is much longer than the emission of (S)-H₈BINOL (323 nm). The formation of the intramolecular hydrogen bonds between the nitrogen atoms of the amino alcohol moieties and the H₈BINOL hydroxyl groups in (S)-34 has been proposed to be responsible for the red-shifted emission wavelength. The interaction of MA with (S)-34 can open the intramolecular hydrogen bonds as a result of the protonation of the nitrogen atoms of the amino alcohol moieties by the carboxyl protons of MA in order to recover the short wavelength emission of the H₈BINOL moiety accompanied by fluorescence enhancements. It has been discovered that (R)-MA intensifies the short wavelength emission of (S)-34 much more dramatically than (S)-MA, indicating that the complex formed between (R)-MA and (S)-34 is more rigid than the (S)-MA/(S)-34 complex. A good chiroselectivity was obtained at $\Delta I_R/\Delta I_S = 3.5$.

In addition, compound (R)-34, the enantiomer of sensor (S)-34, was chosen to cooperate with compound (S)-33 as a pseudoenantiomeric partnering sensing system for the simultaneous measurement of the concentration and the enantiomeric composition of MA.⁷⁰ In CH_2Cl_2 , (R)-MA can induce a much greater fluorescence enhancement of (S)-33 at the long wavelength emission ($\lambda_A = 374 \text{ nm}$) with a chiroselectivity as high as $\Delta I_R / \Delta I_S = 26$. On the other hand, (S)-MA can result in a much greater fluorescence enhancement of (R)-34 at the short wavelength emission ($\lambda_B = 330 \text{ nm}$) with an enantioselectivity of $\Delta I_S / \Delta I_R = 3.6$. In order to determine both the concentration and the enantiomeric composition of MA, two relationships have been established in a 1:1 mixed sensing system of (S)-33 and (R)-34 with a total sensor concentration of $2.0 \times 10^{-4} \text{ M}$ in CH_2Cl_2 . The first relationship is between $(I_A/I_{A0} - I_B/I_{B0})$, $(I_{A0}$ and I_{B0} represent the background emission intensities of (S)-33 and (R)-34, and I_A and I_B represent the fluorescence intensities of (S)-33 and (R)-34 in the presence of MA, respectively, at λ_A and λ_B) and the enantiomeric proportion of MA with the total acid substrate concentration in a certain range. The second

relationship is between $(I_A/I_{A0} - I_B/I_{B0})$ and the total concentration of the acid substrate with different enantiomeric proportions of MA. Therefore, the concentration and the enantiomeric composition of a MA sample can be determined simultaneously by using these two relationships in one test of the fluorescence intensity in this pseudoenantiomeric partnering sensing system.

More recently, Pu and Yu et al. have discovered that a single molecular system **35** can be used to simultaneously determine the concentration and the enantiomeric composition of *trans*-1,2-diaminocyclohexane (DACH) in one fluorescence test.⁷¹ Compound **35** is a nonfluorescent species. Upon exposure of **35** to DACH in CH₂Cl₂, fluorescence with two emission peaks at 370 nm (λ_1) and 438 nm (λ_2) was switched on due to the reaction of the DACH amino groups with the trifluoromethyl carbonyl moiety of **35** via the nucleophilic addition, as shown in Figure 15. Interestingly, (*R,R*)- and (*S,S*)-DACH similarly enhanced the fluorescence of (*S*)-**35** at λ_1 , but at λ_2 , (*R,R*)-DACH had a great effect on the fluorescence enhancement of (*S*)-**35** compared to (*S,S*)-DACH. For sensor (*R*)-**35**, there exists mirrored fluorescence responses toward DACH at λ , for

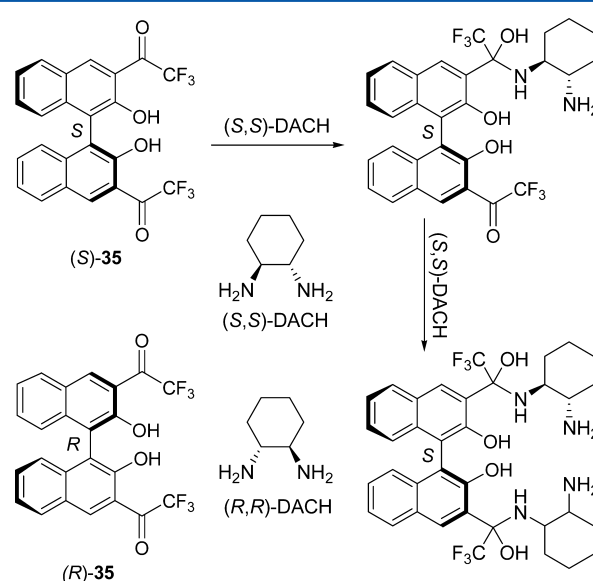


Figure 15. Structures of the two enantiomers of compound **35** and DACH; the proposed interaction mode between (*S*)-**35** and (*S,S*)-DACH through the nucleophilic addition.

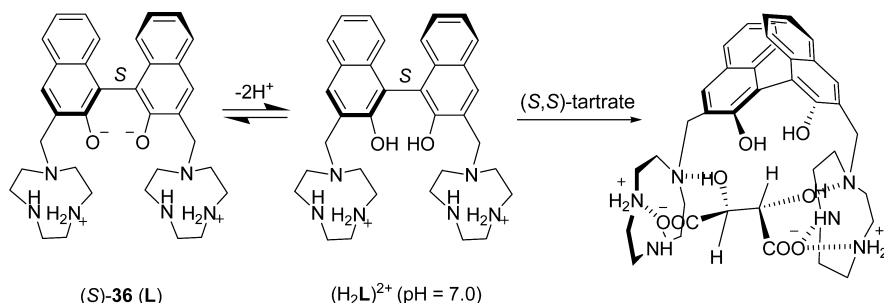


Figure 16. Zwitterionic structure of compound (S)-36 and the proposed interaction mode between (S)-36 and (S,S)-tartrate at pH 7.0.

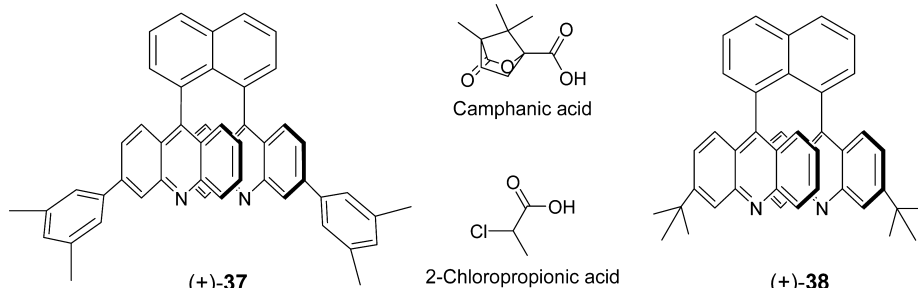


Figure 17. Structures of axially chiral 1,8-diheteroarylnaphthalene derivatives (+)-37 and (+)-38 and the structures of camphanic acid and 2-chloropropionic acid.

chiral recognition. Furthermore, it has been found the fluorescence intensity ratio (I_1/I_2) of the two emission peaks of (S)-35 only correlates to the enantiomeric proportion of DACH represented by (S,S)-DACH%. And the fluorescence intensity at λ_1 (I_1) only relies on the concentration of DACH. Therefore, the enantiomeric composition of an unknown sample can be readily determined based on the relationship between I_1/I_2 and (S,S)-DACH%. Then, through the correlation of I_1 and I_1/I_2 to the DACH concentration, the concentration of both (S,S)- and (R,R)-DACH can be simultaneously determined in one fluorescence test.

It is well-known that most of the reported chiral acid analytes, including α -hydroxycarboxylic acids and amino acids, involved in chiral recognition events are water-soluble and biologically important. Therefore, selective detection of these bioactive acids in aqueous media is physiologically necessary, but is also a challenging task for artificial fluorescent sensors to undertake. Due to the competition of the formation of hydrogen bonds from the protic solvent, it is disadvantageous for the BINOL sensors presented above, which are based only on hydrogen bondings, to recognize water-soluble acid substrates in aqueous solutions. Hence, design of the fluorescent chemosensors with appropriate interaction modes for chiral recognition in water is highly desirable. To this end, Bencini and co-workers have devised and synthesized a monoBINOL chiroselective fluorescent sensor (*S*)-36 (**L**) with the installation of two polyammonium hosts ($[9]\text{aneN}_3$ = 1,4,7-triazacyclononane) on one (*S*)-BINOL molecule for the chiroselective recognition of (*S,S*)-tartaric acid based on multiple hydrogen bondings associated with charge–charge interactions in water.⁷² It has been shown that, at pH 7.0, (*S*)-36 exists in its $(\text{H}_2\text{L})^{2+}$ form with the protonation of two secondary amine groups of $[9]\text{aneN}_3$, as shown in Figure 16, and the existing form of tartaric acid (TA) is anionic, which enables the two negatively charged carboxylates to interact with the positively charged amine groups through electrostatic interaction. Additionally, the α -hydroxyl groups of TA can

bind with the tertiary amine groups via hydrogen bonding. The chiral configuration enables (S)-36 to bind with the chiral acid enantioselectively based on these two associated interactions. With respect to fluorescence responses upon binding with tartrates, sensor (S)-36 displays a very high chiroselectivity toward (S,S)-tartrate with a dramatic fluorescence enhancement of approximately 8-fold at 420 nm over (R,R)-tartrate in water, indicating that the (S)-36 complex formed with (S,S)-tartrate is more stable than the (S)-36/(R,R)-tartrate complex.

3.1.2. 1,8-Diheteroaryl naphthalene-Derived Chemosensors.

SUBSTRATE: The substituted 1,8-diheteroarylnaphthalene derivatives are one class of atropisomeric compounds with inherent fluorescence. The introduction of two bulky heteroaryl substituents into both peri-positions of the naphthalene core leads to anti and meso-syn conformers due to the hindered rotation of the substituted barriers about the carbon–carbon single bonds.⁷³ Specifically, the C₂-symmetric anti-isomer can be separated into two enantiomers, and the conformationally stable and rigid structures with one-dimensional flexibility make them suitable for chioselective interactions with chiral substrates. In recent years, a series of 1,8-diheteroarylnaphthalene-derived compounds such as 1,8-diacyridyl or 1,8-diquinolylnaphthalenes and their N,N'-dioxides have been developed by Wolf and co-workers as promising fluorescent chiral sensors.

1,8-Bis(3,3'-(3,5-dimethylphenyl)-9,9'-diacridyl)naphthalene 37 (Figure 17) has been described by Mei and Wolf as the first example of the enantioselective discrimination of a wide range of chiral carboxylic acids, including amino acids, aliphatic acids, arylalkanoic acids, and halogenated carboxylic acids.⁷⁴ The C_2 -symmetric cleft that was formed can cause sensor 37 to chiroselectively accommodate the enantiomers of acid guests with its two antiparallel acridyl pockets via hydrogen bonding, which induces different extent of fluorescence quenching. The enantioselectivity can be calculated by the ratio of the Stern–Volmer constants based on a 1:1 or 1:2 binding mode of the diastereomeric complexes. For instance, the enantioselectivity

toward the two enantiomers of camphanic acid with (+)-37 has been obtained as $K_{SV}(R)/K_{SV}(S) = 4.5$ (K_{SV} represents the Stern–Volmer constant). Additionally, the enantioselectivity toward N-Boc-Pro has been observed through changes in fluorescence lifetime.⁷⁵ Upon treatment of (+)-37 with the (S) or (R) enantiomer of N-Boc-Pro, the fluorescence lifetime of 37 has been transduced from 18.8 ns to 7.5 and 6.8 ns, respectively. As an analogue of compound 37, sensor 38 with tert-butyl substituents on two acridly rings has been synthesized and used to determine both the total concentration and the enantiomeric composition of unknown samples of certain chiral carboxylic acids.⁷⁶ The accuracy of the concentration and enantiomeric purity has been determined in a test of six samples of 2-chloropropionic acid to be within $\pm 2\%$ and $\pm 3\%$, respectively.

1,8-Diacridylnaphthalene *N,N'*-dioxide fluorosensor 39 (Figure 18) has been developed for the chiroselective sensing of

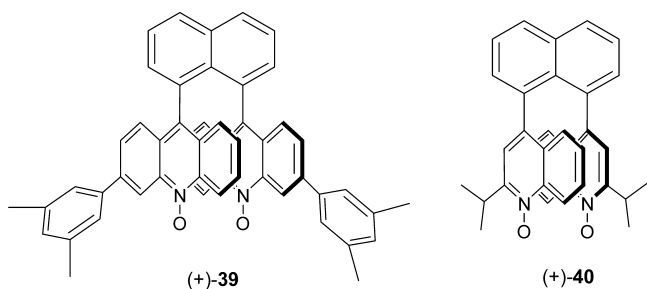


Figure 18. Structures of axially chiral 1,8-diheteroarylnaphthalene derivatives (+)-3 and (+)-4.

chiral hydrogen bond-donating substrates.⁷⁷ Interestingly, sensor 39 displays a fluorescence quenching response to amino acid derivatives but fluorescence enhancement behaviors to chiral diamines. The increase in the rigidity of 39 by the formation of the complexes with diamines is thought to be responsible for the fluorescence enhancement, and the fluorescence quenching is ascribed to the nonradiative relaxation of the formed diastereomeric complexes. Sensor 39 can be also utilized for the determination of both enantiomeric purity and concentration of diamine or carboxylic acid analytes with good accuracy.⁷⁸ Another example of 1,8-diquinolynaphthalene *N,N'*-dioxide, 40 (Figure 18), has been reported by Tumambac and Wolf as a promising fluorescence chiral sensor for the high-throughput screening (HTS) of asymmetric reactions.⁷⁹ This type of chiral sensor displays a good chiroselectivity toward the enantiomers of *trans*-1, 2-diaminocyclohexane (DACH) with a $K_{SV}(R,R)/K_{SV}(S,S)$ value of 4.9. Subsequently, sensor 40 has been applied

in the screening of the lipase-catalyzed acylation reactions of DACH with *Candida antarctica*. Compared with the HPLC analytical results, the fluorescence chiral analysis with sensor 40 exhibits a maximum error of 8%.

Upon coordinating two equivalents of the bidentate ligand *N,N'*-dioxide 39 to scandium(III), a novel metal complex chiral sensing system has been established (Figure 19).⁸⁰ The recognition mechanism of this system is based on a ligand displacement strategy. When enantiopure complex $\text{Sc}[\text{N},\text{N}'\text{-dioxide } 39]_2$ is treated with chiral substrates, ligand 39 can be chiroselectively replaced from the scandium center in two exchange steps, which involve a semireplaced intermediate complex accompanied by corresponding colorimetric responses. This sensing system has been shown to be suitable for the enantioselective and quantitative detection of unprotected amino acids, amino alcohols, amines, and carboxylic acids in aqueous media. Recently, Wolf and co-workers have expanded their ligand exchange method to the stereoselective UV detection of the anti and meso-syn conformers of DACH.⁸¹ To this end, the syn and anti isomers of ligand 39 have been separated and coordinated to scandium(III) to establish the stereoselective sensing systems, which displays UV charge transfer (CT) absorption at 390 nm. As a result, the ligand *syn*-39 can be replaced from the metal center by the racemic DACH much more efficiently than by the meso-syn DACH, according to the different degrees of the UV-CT band disappearances. Moreover, in terms of the linear relationship between the UV absorption changes and the diastereomeric composition, unknown samples of DACH can be evaluated rapidly with good agreement within 5% accuracy. In addition, enantiopure $\text{Sc}[\text{anti}-(-)\text{-}39]$ has been also prepared for the discrimination between the syn isomer and the anti enantiomers of DACH by the colorimetric changes, and the sequence of the displacement efficiency has been obtained as meso-syn DACH > (R,R)-DACH > (S,S)-DACH.

3.1.3. Other Inherently Chiral Fluorophore-Based Chemosensors.

Aside from binaphthyl and 1,8-diheteroarylnaphthalene-derived fluorophores, other inherently chiral fluorescent molecules have been rarely reported for the enantioselective sensing and recognition. One limited example of 2,15-dihydroxy-hexahelicene (HELIXOL), 41 (Figure 20), has been described as the fluorescent sensor for the chiral detection of amines and amino alcohols.⁸² Compared with BINOL 1, sensor 41 possesses a higher fluorescence quantum yield, which can offer relatively higher sensitivity and selectivity to chiral quenchers. For instance, sensor (−)-41 exhibits a good enantioselectivity toward the two enantiomers of alaninol, with $K_{SV}(R)/K_{SV}(S) = 4.5$. The establishment of the linear correlation

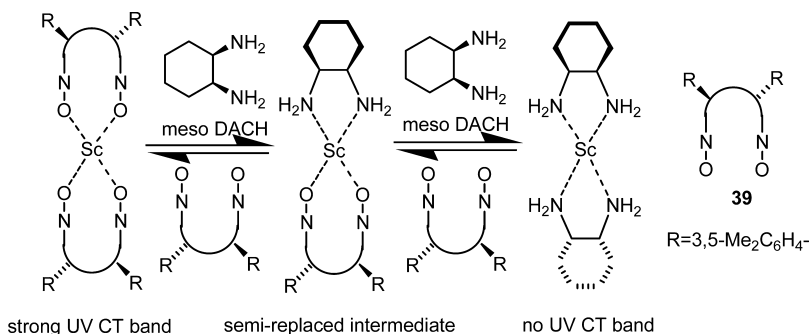


Figure 19. Ligand displacement mechanism of the $\text{Sc}[\text{N},\text{N}'\text{-dioxide } 39]_2$ sensing system for the *meso*-DACH.

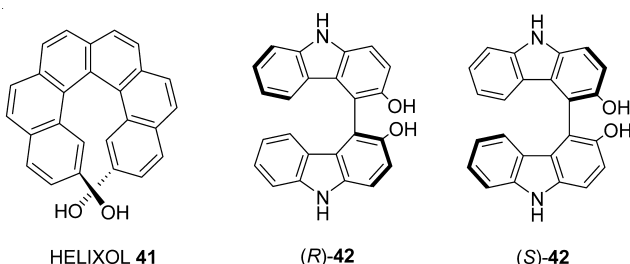


Figure 20. Structures of HELIXOL **41** and the two enantiomers of BICOL **42**.

of the Stern–Volmer constant with the enantiomeric purity makes HELIXOL a promising enantioselective sensor.

As a more recent example, the two enantiomers of a dimeric hydroxycarbazole derivative (BICOL), **42** (Figure 20), have been separated in order to study on selective binding with right-handed B-DNA or left-handed Z-DNA.⁸³ The computer-aided molecular modeling with molecular docking techniques indicates that these two axially chiral enantiomers show different binding behaviors to B- or Z-DNA even in the same binding sites. In practice, the treatment of (*S*)-**42** to B-DNA induces an increase in the fluorescence intensity of (*S*)-**42**, whereas Z-DNA reduces its fluorescence intensity. However, (*R*)-**42** displays similar fluorescence quenching responses to both B- and Z-DNA due to the fact that Z-DNA resembles B-DNA, which is caused by the accommodation of (*R*)-**42** in the minor groove of Z-DNA. These investigations suggest that BICOL **42** should be a promising fluorescent chiral scaffold for the design of DNA chiral sensors.

In addition, two bis(oxazolinyl)phenols **43** and **44** (Figure 21) were reported as fluorescent chiral receptors for various amines.⁸⁴ The receptor **43** showed fluorescence enhancements toward butylamine and several arylethylamines, whereas they showed fluorescence quenching toward secondary and branched amines. The unique fluorescence enhancements were attributed to an increased conformational restriction at the excited state, at which a proton transfer complex between the host and guest forms is stabilized in a tripodal hydrogen bonding mode. Enantiomeric α -chiral organoamines induced different fluorescent intensity changes in **44**. In ACN, the Stern–Volmer constants with (*R*)- α -methylbenzylamine and (*S*)- α -methylbenzylamine were determined as 1290 and 770 M⁻¹, respectively.

3.2. Chiral Probes with Particular Binding Units

The binding unit of a colorimetric or fluorescent chemosensor acts as the receptor due to its abilities to interact with a targeted molecule or ion and transmit the binding event to the signal reporting unit (chromogenic or fluorogenic reporter) via some transduction mechanism and pathway for the detectable signal output. The receptors of different structures generally recognize

the specific type of guests. For instance, aza(crown) ether host is enthusiastic over the interaction with cation guests by hydrogen bondings, whereas thio(urea) is the particular receptor for anion substrates. These receptors also emerge in the design of enantioselective sensors. However, in most cases, the receptor that is used is achiral in essence, and must cooperate with certain foreign chiral source as the steric barrier to achieve the preferable interaction with one of the enantiomers of a chiral substrate. Theoretically, in either the "receptor-reporter" or "receptor-spacer-reporter" approaches for the chiral sensor design, the chiral barriers can be introduced into each constitutional component with a rational distance between the chiral center and the binding site for the optimal chiral discrimination efficiency. Besides, among the cases, the use of enantioselective indicator displacement assays (eIDAs) is a special and efficient alternative, in which the chirogenic component is fixed beside the receptor moiety in order for the enantioselective replacement by the chiral analytes. In practice, a number of successful enantioselective chemosensors with particular binding units have been developed recently for the fluorimetric or colorimetric determination of important chiral analytes.

3.2.1. Crown or Azacrown Ether-Based Chemosensors.

(Aza)crown ethers are most important cation receptors or carriers. They have a unique architectural feature that allows them to form various complexes with cationic species such as alkali metals, alkaline-earth metals, and even organic ammonium ions. Primary ammonium guests can bind to crown ethers via hydrogen bonds between their $\text{N}^+ \text{-H}$ bonds and the free electron pair atoms in (aza)crown ethers (oxygen or nitrogen atoms). Besides, for the chiral crown hosts, the steric arrangement leads to a reorganization of the chiral cavity, whereby enantioselectivity is determined by the different matching degree for the two enantiomers of a guest. Since the initial work of Cram et al. on the use of chiral crown ethers in enantiomeric recognition,⁸⁵ chiral receptors based on these macrocycles have continued to receive increasing attention. Herein, the recent progress on the colorimetric and fluorescent spectroscopic methods for the enantioselective sensing using (aza)crown ethers as receptors will be covered.

Wang et al. synthesized four novel chiral 22-crown-6 ethers bearing hydroxyl side groups, **45a**, **45b**, **46a**, and **46b**, which were derived from rosin acid and BINOL (Figure 22).⁸⁶ Their enantioselectivities toward protonated primary amines and amino acid methyl ester salts were examined by UV-vis titration methods in CHCl₃/MeOH (2:1). The representative K_D/K_L values of 1-(1-naphthyl)ethylamine hydrochloride salts and 1-phenylethylamine hydrochloride salts are as follows: 1.80 and 6.02 for **45a**; 2.55 and 1.47 for **45b**; 2.03 and 1.61 for **46a**; 5.99 and 2.01 for **46b**.

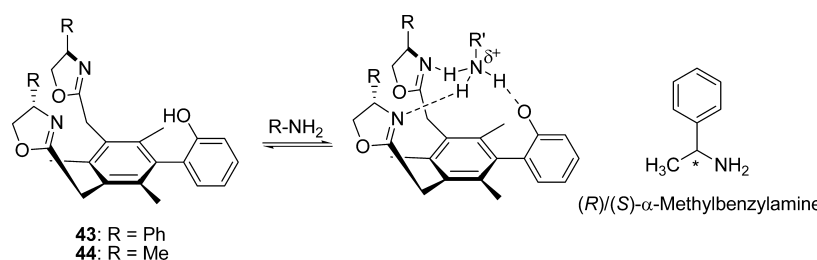


Figure 21. Structures of phenol-containing bis(oxazolines) **43**, **44**, and α -methylbenzylamine and the proposed binding modes of **43** and **44** with amines

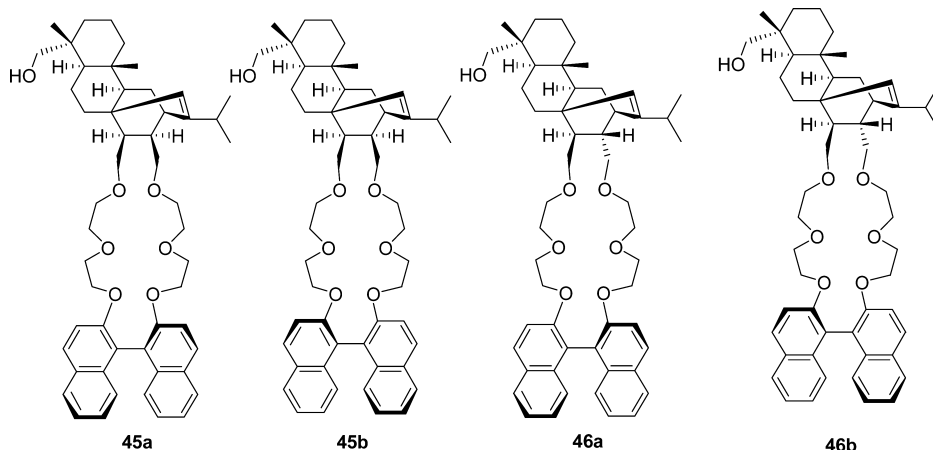


Figure 22. Structures of chiral crown ether derivatives from rosin acid and BINOL.

The Hyun group recently reported a new colorimetric chiral receptor **47** (Figure 23), which consists of three different

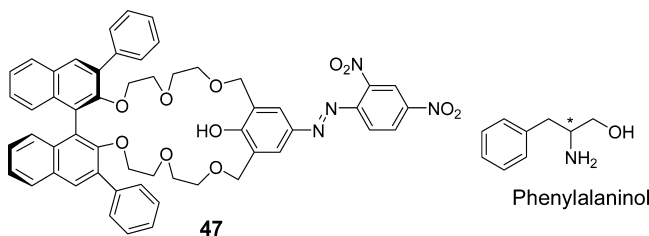


Figure 23. Structure of chiral receptor **47** and phenylalaninol (PA).

functional sites: the chromophore (2,4-dinitrophenylazophenol dye), the binding site (crown ether), and the chiral barrier (3,30-diphenyl-1,10-binaphthyl group).⁸⁷ This chiral receptor **47** was applied to the recognition of the two enantiomers of primary amino alcohols and amines in acetonitrile (ACN). Among the guests examined, the two enantiomers of phenylalaninol (PA) showed distinct differences in their absorption maximum wavelength ($\Delta\lambda_{\max} = 43.5$ nm) and association constants ($K_S/K_R = 2.51$). In addition, a striking color difference was observed by the naked eye upon the addition of PA. Receptor **47** showed a light green color, and the addition of (R)-PA and (S)-PA induced pink and blue colorimetric changes, respectively.

Karnik et al. reported a furo-fused BINOL-based chiral crown, (R)-(-)-**48**, as an enantioselective chiral sensor for phenylethylamine and ethyl ester of Val (Figure 24).⁸⁸ This chiral receptor

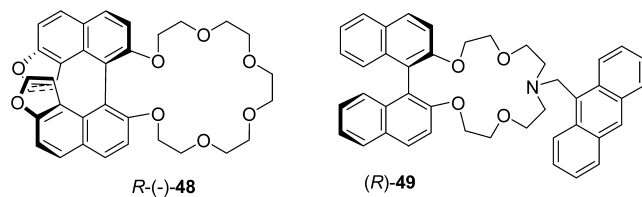


Figure 24. Structures of chiral receptors (R)-(-)-**48** and (R)-**49**.

(R)-(-)-**48** showed a fluorescence enhancement difference of 2.97 times between two enantiomers of phenylethylamine and 2.55 times between two enantiomers of ethyl ester of Val. The association constant (K) of (R)-(-)-**48** for (S)-(-)-phenylethylamine was calculated as $6.08 \times 10^5 \text{ M}^{-1}$, and K for (R)-(+)-phenylethylamine using (R)-(-)-**48** was calculated to be 5.38

$\times 10^4 \text{ M}^{-1}$. The ratio of association constants for two diastereomeric complexes of two enantiomers of phenylethylamine was found to be 11.30. For enantiomers of ethyl ester of Val, the ratio was calculated as 7.02. In this receptor, the fusion of furan to BINOL resulted in a highly stereodiscriminating backbone for the chiral crown developed.

Hyun and co-workers reported an azacrown-anthracenefluorophore (R)-**49** as fluorescent chemosensor for metal ions and chiral recognition (Figure 24).⁸⁹ This new fluorescent receptor exhibited large fluorescent changes with aqueous Hg^{2+} , Cu^{2+} , and Zn^{2+} . The chiral recognition of these receptors with chiral ammonium guests was also examined. The hydrogen perchlorate salts of (R)-2-phenylglycinol and the (S) isomer were used for the chiral recognition of receptor **49** in ACN. Based on the fluorescent titrations of receptor **49**, the association constants for the (R)-2-phenylglycinol and (S)-2-phenylglycinol were calculated as 4.5×10^4 and $3.45 \times 10^4 \text{ M}^{-1}$, respectively. The ammonium groups bound in the azacrown ring could block the PET mechanism from the benzylic nitrogen to anthracene group, which can induce fluorescence enhancements. Moderate selectivity (1.3 times) for the hydrogen perchlorate salt of (R)-2-phenylglycinol over the (S)-isomer was observed.

Huszthy and co-workers synthesized two enantiopure BODIPY-linked azacrown ether chemosensors (*S,S*)-**50** and (*S,S*)-**51**, which were prepared by reacting 3-chloro-5-methoxy BODIPY with new enantiopure monoaza-18-crown-6 ether ligands bearing two methyl and isobutyl groups on their chiral centers, respectively (Figure 25).⁹⁰ These BODIPY (boron dipyrromethene difluoride) derivatives exhibited pronounced off-on-type fluorescence changes (more than 10-fold) to some metal ions and chiral primary aralkyl ammonium ions, Ca^{2+} and Pb^{2+} in particular. However, only moderate enantioselectivity toward the enantiomers of α -phenylethyl ammonium perchlorate (PEA) was observed, which was attributed to the relatively high flexibility of chiral ligand (*S,S*)-**51**. The same group extended their work to acridinone moiety. Two new receptors (**52a** and **52b**) have a modular (fluorophore-methylene spacer-azacrown receptor) structure in order to display fluorescence response in the presence of various cations by blocking the PET process. Receptor (*S,S*)-**52a** showed high selectivity toward Cu^{2+} with almost 10-fold fluorescence enhancement upon complexation.⁹¹ Receptor (*S,S*)-**52b** also showed nice selectivity toward Cu^{2+} and Pb^{2+} . The enantiomers of 1-(1-naphthyl)-ethylammonium perchlorate (NEA) and potassium mandelate were examined for chiral recognition study. Unfortunately, there

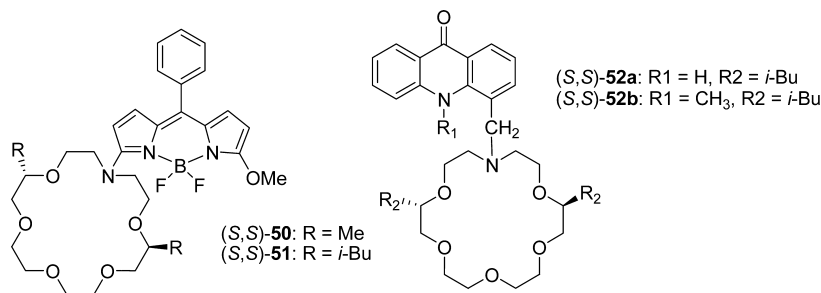


Figure 25. Structures of chiral receptors 50–52.

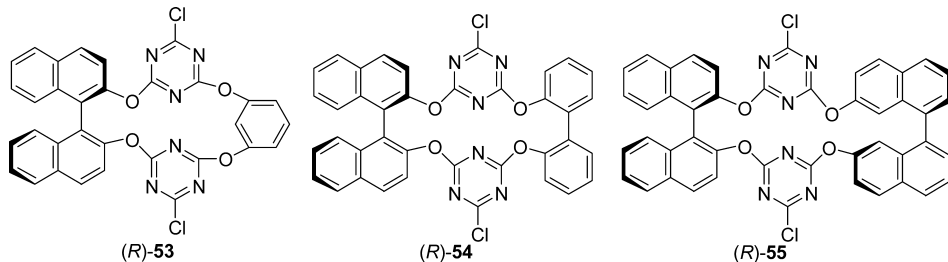


Figure 26. Structures of triazine-based bisbinaphthyl crown ethers 53–55.

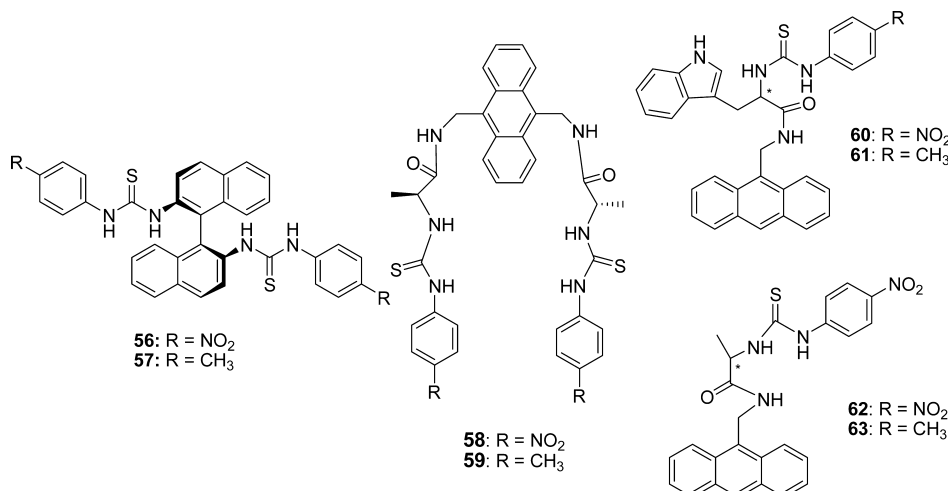


Figure 27. Structures of chiral receptors 56–63.

was not any enantiomeric recognition even though fluorescence enhancements were observed with these chiral guests in DCM/methanol (97:3) and ACN/water (97.5:2.5).

Xu et al. reported on triazine-based bisbinaphthyl crown ethers oxacalix[2]arene[2]bisbinaphthyls (R)-53, (R)-54, and (R)-55 and (S)-53, (S)-54, and (S)-55 (Figure 26), and their enantioselective recognition could be studied by fluorescence titration and ¹H NMR spectroscopy.⁹² When the solution of (R)-53 in CHCl₃ was excited at 366 nm, (R)-53 gave a characteristic emission spectrum with a monomeric naphthyl maximum at approximately 418 nm. The interactions of these chiral receptors with various α -aminocarboxylic acid anions were studied and were found to show highly enantioselective fluorescent recognition of α -aminocarboxylic acid anions. The fluorescence emission of (R)-53 upon addition of the (R)-Ala anion was enhanced by a factor of 5.4-fold, but there was very little fluorescence enhancement at 418 nm when (R)-53 interacted with (S)-Ala under the same conditions.

3.2.2. Thiourea- or Urea-Based Chemosensors. Most common neutral anion receptors utilize their binding sites to form N–H \cdots anion hydrogen bonds such as thiourea, urea, amide, pyrrole, etc. Among them, (thio)urea and its substituted derivatives are more attractive because they offer double hydrogen bonding sites with both high affinity and selectivity to anion hosts. In this section, chiral optical receptors bearing thiourea or urea groups will be covered.

He et al. reported on two chiral fluorescent receptors 56 and 57 based on (R)-1,1'-binaphthylene-2,2'-bisthiourea and on their chiral recognition properties for enantiomeric mandelate anions based on fluorescence changes and molecular modeling (Figure 27).⁹³ Addition of the L- and D-mandelate anions caused considerable increases in the fluorescent intensity. The L-enantiomer showed a larger fluorescence enhancement of 56 compared to the D-enantiomer. More specifically, upon addition of D-mandelate to the solution of receptor 56 in DMSO, the fluorescent peak at 437 nm increased gradually. Receptor 56 showed better enantioselective recognition ability than 57.

He et al. reported on anthracene-based chiral fluorescent receptors **58** and **59** bearing two thiourea and two amide groups, respectively (Figure 27).⁹⁴ Upon addition of anions in DMSO, the fluorescence emission intensities of **58** at 429 nm decreased with the concomitant appearance of a new peak at 538 nm. The distinct colorimetric change from light yellow to orange-red allowed for the naked-eye detection. Receptors **58** and **59** showed good enantioselective recognition for the L-enantiomers of the chiral guests, such as L/D-malate, L/D-aspartate, and L/D-glutamate, with the $K_{\text{ass}}(\text{L})/K_{\text{ass}}(\text{D})$ values from 2.18 to 9.65.

The chiral optical anthracene derivatives containing thiourea and amide groups **60–63** were also synthesized by He and co-workers (Figure 27).⁹⁵ The different increasing efficiencies ($\Delta I_L/\Delta I_D = 1.8$) were observed when L- and D- α -Phe were added to the receptor **60**. The association constants (K_{ass}) of **60** with L-Phe and D-Phe were calculated as $(2.96 \pm 0.16) \times 10^4$ and $(5.26 \pm 0.25) \times 10^3 \text{ M}^{-1}$, respectively, with an enantioselectivity ($K_{\text{ass}}(\text{L})/K_{\text{ass}}(\text{D})$) of 5.63. Upon the addition of L- and D-Phe, the intensity of the absorption band at 370 nm decreased with the appearance of a new absorption band at 475 nm.

The He group synthesized chiral receptors **64** and **65** based on (S)-BINOL and thiourea units (Figure 28).⁹⁶ The chiral

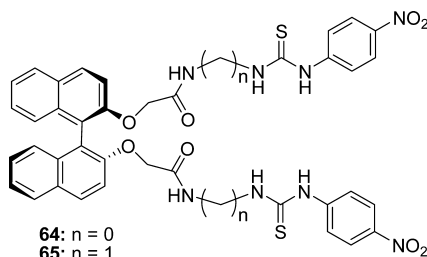


Figure 28. Structures of chiral receptors **64** and **65**.

recognition of these receptors was examined by fluorescence, UV-vis, and ^1H NMR spectra for chiral anions, such as D- and L-Phg anion, D- and L-mandelate, and D- and L-malate. When either D- or L-mandelate anions were added into the solution of receptor **64** or **65**, the fluorescence quenching phenomenon was observed. More dramatic changes were observed for UV-vis absorptions; upon the addition of D- or L-mandelate anions to receptor **64**, the absorption at 336 nm was decreased gradually, and the peak at 278 nm was increased gradually, and a new absorption peak at 412 nm was dramatically enhanced. The obvious color change of receptor **65** was observed by the naked eye when the enantiomers of mandelate anions were added. In addition, receptor **65** showed a good enantioselective recog-

nition ability ($K_{\text{ass}}(\text{L})/K_{\text{ass}}(\text{D}) = 13.6$) for the enantiomers of the mandelate anion.

Four linear thiourea anion receptors **66a**, **66b**, **67**, and **68** (Figure 29) derived from simple amino acid were synthesized by He et al.⁹⁷ Their bonding properties toward various chiral N-protected amino acid anions were examined by using UV-vis and fluorescence changes. Receptors **66a**, **67**, and **68** showed excellent enantioselective recognition abilities toward N-Boc-protected Ala anion based on the UV-vis changes. For example, the characteristic absorption peak of the host **66a** at 360 nm was decreased gradually with a red shift (about 10 nm) and a new absorption peak at 482 nm was produced upon the addition of N-Boc-protected Ala. In addition, obvious differences in the solution color (colorless to yellow) were observed with the N-Boc-Ala anion, which could be distinguished directly by the naked eye. The association constants (K_{ass}) for **66a** and the N-Boc-Ala anion were calculated as $K_{\text{ass}}(\text{L}) = 192.7 \text{ M}^{-1}$ and $K_{\text{ass}}(\text{D}) = 519.7 \text{ M}^{-1}$ with the D/L selectivity of 2.70.

Qing et al. reported four ferrocenyl macrocyclic derivatives, **69** and **70**, containing anthracene fluorophores (Figure 30).⁹⁸ The fluorescent properties of these receptors have been studied in three organic solvents, ACN, CH_3Cl , and DMSO, in both the absence and presence of phenyl amino alcohols. Solvent comparative experiments indicated that ACN was the most appropriate solvent to detect fluorescent changes. Very interestingly, all receptors showed selective fluorescence changes with L- or D-phenylglycinol. A unique and strong emission band (450–570 nm) was attributed to the intermolecular exciplex between the anthracene moiety in the receptor and guest. These special fluorescence enhancement phenomena were only observed with phenylglycinol, while other species could not induce such obvious changes. Accordingly, these receptors could easily discriminate phenylglycinol from other similar species.

As shown in Figure 31, the glucopyranosyl unit was adopted as a chiral barrier of two new anthracene thiourea derivatives, **71** and **72**, which were reported as fluorescent chemosensors for the chiral recognition of amino acids.⁹⁹ The association constants of **71** with D- and L-t-Boc Ala were calculated to be 1.18×10^4 and $2.16 \times 10^3 \text{ M}^{-1}$, respectively, with a $K_{\text{D}}/K_{\text{L}}$ value of 5.5. On the contrary, the association constants of **71** with D- and L-t-Boc Ala were calculated as 2.3×10^3 and $2.39 \times 10^4 \text{ M}^{-1}$, respectively, with a $K_{\text{D}}/K_{\text{L}}$ value of 10.4. These intriguing opposite D/L binding affinities for **71** and **72** were attributed to the unique without (or with) H- π interaction between the anthracene moiety and the methyl groups, which was supported by extensive high-level theoretical calculations as well as 2D NOSEY NMR experiments.

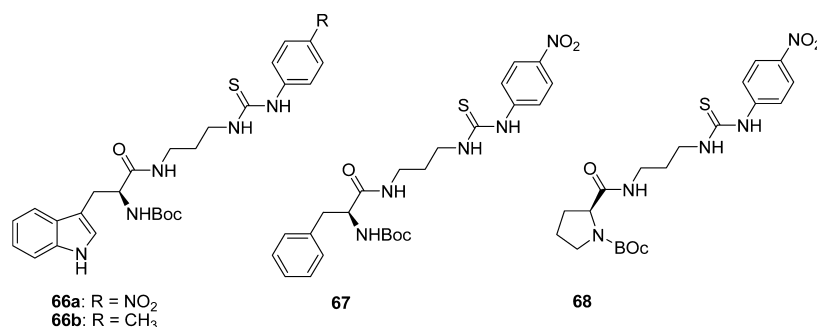
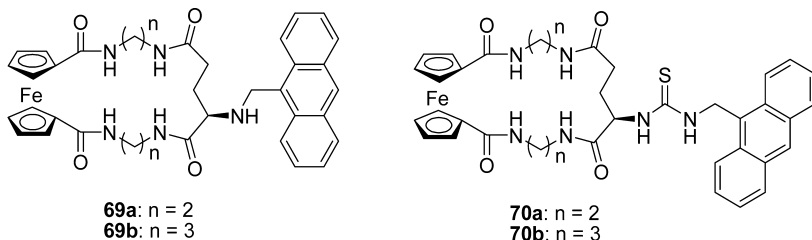
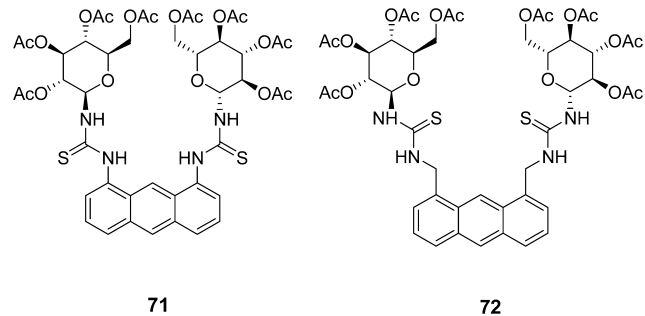
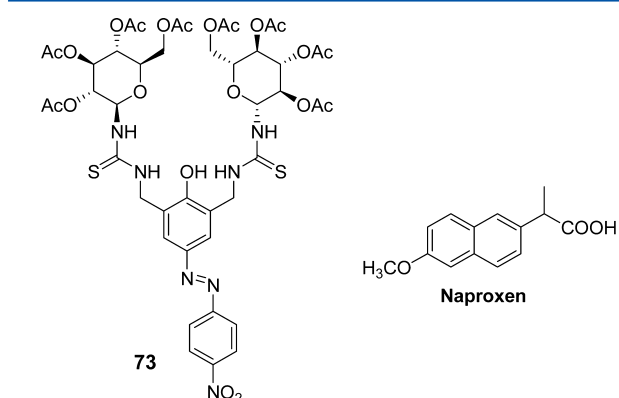


Figure 29. Structures of receptors **66–68**.

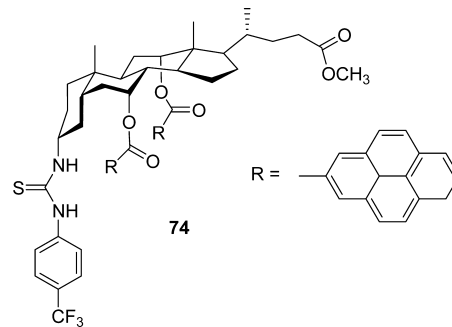
**Figure 30.** Structures of the ferrocenyl macrocyclic derivatives **69** and **70**.**Figure 31.** Chemical structure of **71** and **72**.

Yoon and co-workers also used these glucopyranosyl units as chiral barriers for a colorimetric anion sensor **73** for chiral recognition (Figure 32).¹⁰⁰ Large bathochromic shifts (~ 145 nm) with CH_3CO_2^- , F^- , and H_2PO_4^- in ACN, which were attributed to the deprotonation of the azophenol and a photoinduced charge transfer (PCT). Receptor **73** was further examined for chiral amino acid derivatives and chiral carboxylates. The association constants of **73** with L- and D-t-Boc threonine were calculated as 6.89×10^4 and $2.2 \times 10^4 \text{ M}^{-1}$, respectively, with a K_L/K_D value of 3.13. The D/L selectivity for t-Boc Ala of receptor **73** was observed as 3.6. Receptor **73** also displayed a moderate selectivity for the (S) enantiomer of naproxen ([2-(6-methoxynaphth-2-yl)propionic acid]), a non-steroidal anti-inflammatory drug (NSAID), over the (R) isomer.

**Figure 32.** Structures of **73** and naproxen.

nm) with CH_3CO_2^- , F^- , and H_2PO_4^- in ACN, which were attributed to the deprotonation of the azophenol and a photoinduced charge transfer (PCT). Receptor **73** was further examined for chiral amino acid derivatives and chiral carboxylates. The association constants of **73** with L- and D-t-Boc threonine were calculated as 6.89×10^4 and $2.2 \times 10^4 \text{ M}^{-1}$, respectively, with a K_L/K_D value of 3.13. The D/L selectivity for t-Boc Ala of receptor **73** was observed as 3.6. Receptor **73** also displayed a moderate selectivity for the (S) enantiomer of naproxen ([2-(6-methoxynaphth-2-yl)propionic acid]), a non-steroidal anti-inflammatory drug (NSAID), over the (R) isomer.

The Chan group synthesized a chiral fluorescent receptor **74** based on cholic acid for the chiral recognition of anions (Figure 33).¹⁰¹ Receptor **74** displayed enantioselective recognition for mandelate, with an enantioselective discrimination of ~ 5.0 , which was confirmed by the fluorescence in ACN and a ^1H NMR spectroscopic method. The $\pi-\pi$ interaction between the pyrenyl group of **74** and the phenyl group of (S)-mandelate or (L)-

**Figure 33.** Structure of **74**.

phenylalanine anion was attributed to enhance the binding interaction between the host and the guest.

As shown in Figure 34, Chan and co-workers reported chiral fluorescent receptors **75** and **76** for trifunctional amino acids (Figure 34).¹⁰² The addition of D-Ser (10 equiv) induced a fluorescence quenching effect ($\sim 80\%$). The binding constant of **75** with D-Ser was calculated as $(2.26 \pm 0.17) \times 10^3 \text{ M}^{-1}$, which was slightly larger than that of **75** with D-threonine ($[1.82 \pm 0.14] \times 10^5 \text{ M}^{-1}$), D-lysine ($[1.37 \pm 0.11] \times 10^5 \text{ M}^{-1}$), and D-tyrosine ($[1.94 \pm 0.09] \times 10^5 \text{ M}^{-1}$). Receptor **75** also showed better affinity for the D amino acids with high K_D/K_L values from 6.7 to 8.9. In contrast to host **75**, on the other hand, receptor **76** displayed opposite enantioselectivity toward Ser, threonine, lysine (Lys), and tyrosine with K_L/K_D values from 6.2 to 8.1.

Costero et al. prepared four new chiral ligands, cyclohexane-based naphthylthioureas (−)-77, (+)-77, (−)-78, and (+)-78 (Figure 35).¹⁰³ Complexation constants and stoichiometries have been determined using fluorescence changes for L- and D-aspartate, L- and D-glutamate, and L- and D-tartrate, which are all TMA(teramethylammonium) salts. While chiral receptors containing two thiourea groups form 1:1 complexes with the dicarboxylates examined, receptors containing only one thiourea group show 2:1 stoichiometries except with tartrate. Solutions of either (−)-78 with a large excess of L-aspartate or (+)-78 with a large excess of D-aspartate can be used for enantiomeric discrimination between L- and D-aspartate.

The Costero group also reported two other cyclohexane-based naphthylthiourea chiral ligands (+)-(1*R*,2*R*)-79 and (−)-(1*S*,2*S*)-79 (not shown) as enantioselective sensors for different dicarboxylates by UV and fluorescence spectroscopy (Figure 35).¹⁰⁴ Comparative studies carried out with these ligands and receptors, (+)-(1*R*,2*R*)-80 and (−)-(1*S*,2*S*)-80 (not shown), demonstrated that the presence of the ethoxycarbonyl groups in these latter compounds is essential to provide a 1:1 stoichiometry. In addition, this complex stoichiometry induced significant differences in their fluorescence emissions. Unique excimer bands in the fluorescence spectra were observed in the case of 1:1 complexes; however, this type of emission is absent

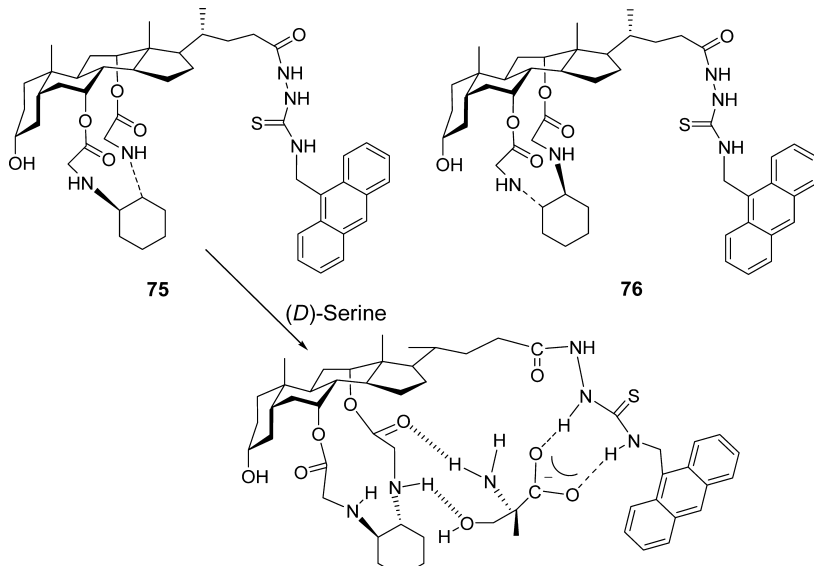


Figure 34. Structures of fluorescent sensors **75** and **76** and the proposed binding mode of host **75** with D-Ser.

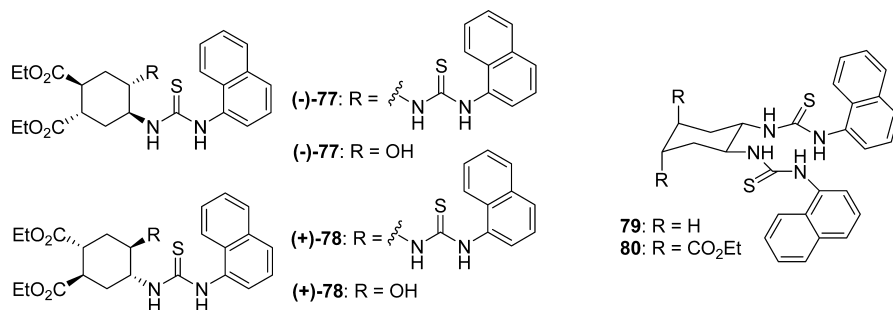


Figure 35. Structures of cyclohexane-based naphthylthiourea receptors **77–80**.

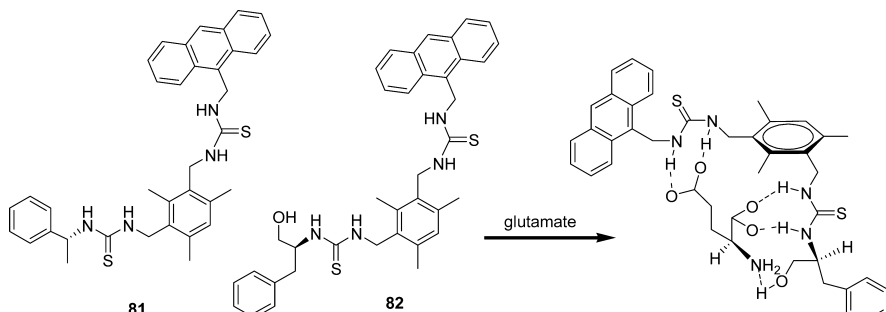


Figure 36. Structures of fluorescent chiral receptors **81** and **82** and the proposed binding mode of host **82** with glutamate.

with 2:1 stoichiometries. The rigid dicarboxylate moiety also plays a key role in enhancing the enantioselective selectivity.

In 2011, Chan and co-workers continued their interest in this research direction and reported two new sensing probes **81** and **82** (Figure 36).¹⁰⁵ Operating on the PET mechanism, the host fluorescence emission band at 413 nm was quenched gradually upon the addition of the guest. As revealed by the respective association constants, sensor **81** showed the highest affinity to isophthalate ($K_a = (6.25 \pm 0.61) \times 10^4 \text{ M}^{-1}$) in ACN. The preorganization of sensor **82** permits three site binding with the guests leading to enhanced complexation with aspartate and glutamate. The chiral recognition ability of the sensors, however, is only moderate.

New coumarin-based chiral thiourea sensor **83** (Figure 37) was reported to be an enantioselective fluorescent chemosensor for N-Boc-protected Pro, which displayed low background

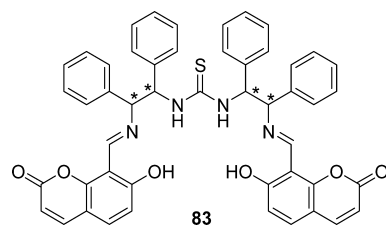


Figure 37. Structure of chiral coumarin-thiourea derivative **83**.

fluorescence and fluorescence enhancement with 18-nm blue shifts on addition of *N*-Boc-protected Pro (Pro).¹⁰⁶ The net fluorescence intensity increase of **83** by *N*-Boc-D-Pro was found to be 4.55 times that of *N*-Boc-L-Pro (i.e., the enantiomeric difference ratio, $E_f = (I_D - I_0)/(I_L - I_0)$, was 4.55).

(*S*)-2-Hydroxy-2'-(3-phenyluryl-benzyl)-1,1'-binaphthyl-3-carboxaldehyde **84** was reported as a selective fluorescent chemosensor for tryptophan (Trp; Figure 38).¹⁰⁷ The binol

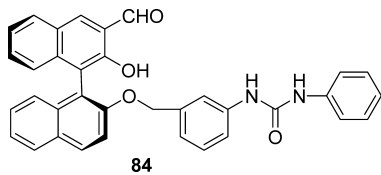


Figure 38. Structure of chiral receptor **84**.

carboxaldehyde **84** exhibited a high selective fluorescence enhancement at 351 nm with L-Trp over various other examined L- α amino acids. In addition, **84** displayed a good enantioselectivity toward L-Trp over D-Trp through different fluorescence enhancement factors. The enhancing efficiency (I/I_0) increased by ~7-fold with the addition of 14 equiv of D-Trp, while increased by 18-fold with 14 equiv of L-Trp.

Self-sorting has been defined as the ability to differentiate between the self and nonself. Sijbesma et al. demonstrated the formation of segregated enantiomeric dynamic rods in water from the self-sorting of chiral *trans*-1,2-bisureido cyclohexane-based bolaamphiphiles (Figure 39).¹⁰⁸ Both exciplex and FRET

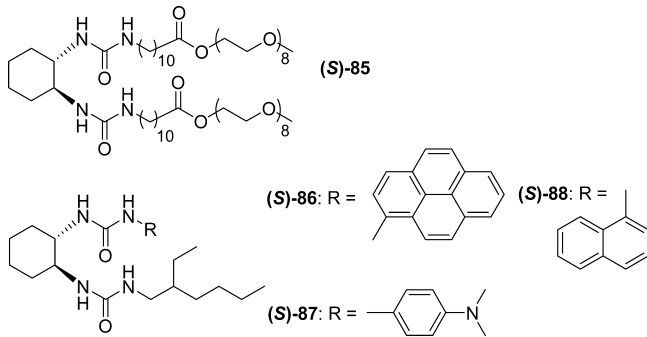


Figure 39. Structures of chiral *trans*-1,2-bisureido cyclohexane-based bolaamphiphiles **85–88**.

were used as versatile tools to probe chiral self-sorting. For example, in 2-mM aqueous solutions of USU containing either 0.5 mol % (*S*)-**85** or 15 mol % (*S*)-**86**, an exciplex band was not observed. However, upon mixing these solutions, a broad band at 490–510 nm appeared, which demonstrated the dynamic nature of the micelles. In addition, fluorescence resonance energy transfer (FRET) between the naphthalene probe (*S*)-**87** (as the donor) and (*S*)-**85** (as the acceptor) was utilized; increased energy transfer was attributed to the increased fraction of pyrene that is within a few nanometers of naphthalene.

3.2.3. Schiff-base-derivatized chemosensors. A chiral Schiff-base receptor, 4-methyl-2,6-bis-[*(2*-hydroxy-1-phenylethylimino)methyl]phenol, (*R,R*)-**89** (Figure 40), was reported as a highly enantioselective fluorescent chemosensor for α -hydroxycarboxylic acids, such as MA.¹⁰⁹ The fluorescence intensity of (*R,R*)-**89** increased by 122-fold with (*S*)-MA, while (*R*)-MA enhanced the intensity only 42 fold. The association

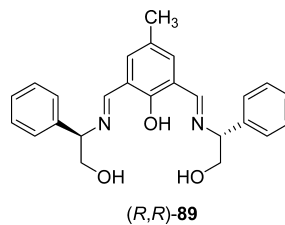


Figure 40. Structure of chiral receptor (*R,R*)-**89**.

constant K was evaluated as $7.2 \times 10^2 \text{ M}^{-1}$ for (*R,R*)-**89** with (*S*)-MA. The corresponding value for the system (*R,R*)-**89** with (*R*)-MA was reported as $1.8 \times 10^2 \text{ M}^{-1}$.

Calixarene-like chiral salenmacrocycles (*S,S,S,S,S,S*)-**90a–f** and (*S,S,S,S,S,S*)-**91a–f** were prepared for the enantioselective fluorescent recognition of MA derivatives (Figure 41).¹¹⁰ When (*S,S,S,S,S,S*)-**90d** was treated with (*R*)- or (*S*)-MA (**92a**), a significant fluorescence enhancement was observed at 527 nm. (*R*)-MA induced a 28-fold increase in the fluorescence intensity of a chiral salenmacrocycle, whereas (*S*)-MA caused only a 14-fold fluorescence enhancement with $E_f = 2.0$ (E_f is the enantiomeric fluorescence difference ratio = $(I_S - I_0)/(I_R - I_0)$). This highly enantioselective fluorescent response makes chiral salenmacrocycles useful for the enantioselective fluorescent recognition of some MA derivatives.

3.2.4. Amino Acid- or Peptide-Based Sensors. Amino acids are well-known to be the basic units of proteins, some of which are necessities in the human body for performing some critical functions. The use of amino acid units as the building blocks for the construction of the chiral receptors affords two main functions. First, amino acids are naturally occurring chiral sources; second, the amide and peptidic bonds are excellent hydrogen bond donors as the binding sites. Recently, several amino acid derivatives have been synthesized as pseudopeptidic fluorescent sensors for enantioselective recognition study.

For example, Hua et al. reported a series of C_2 -symmetrical macrocycles containing pyridyl units **93** (Figure 42) and their molecular recognition of these homochiral macrocycles for amino acid derivatives by IR, FAB-MS, fluorescence and UV-vis.¹¹¹ In particular, the macrocycle **93** exhibited significant chiral recognition toward the enantiomers of D- and L-alanine methyl ester hydrochlorides. The association constants of the macrocycle **93** with D-Ala-OMe•HCl and L-Ala-OMe•HCl were calculated as $K_D = 8.12 \times 10^2 \text{ M}^{-1}$ and $K_L = 2.03 \times 10^3 \text{ M}^{-1}$ with the selectivity ratio of 2.5.

He et al. reported two chiral anthracene derivatives, **94** and **95**, for the chiral recognition of the receptors (Figure 42).¹¹² The results demonstrated that the receptors and tetrabutylammonium mandelate formed a 1:1 complex in DMSO. Upon addition of D- or L-mandelate, the fluorescence emission intensities of receptor **94** at 418 and 441 nm gradually increased. Receptor **95** showed a moderate selectivity for the D-mandelate anion over the L enantiomer, which was attributed to the relatively greater rigidity of the receptor **95**. In addition, chiral fluorescence receptors **96** and **97** were also synthesized and their chiral recognition properties were studied with bis(tetrabutylammonium) dibenzoyl tartrate using ^1H NMR and fluorescence spectra.¹¹³ In particular, receptor **96** showed an high enantioselectivity ($K_{\text{ass}}(\text{D})/K_{\text{ass}}(\text{L}) = 6.2$) toward the enantiomers of bis(tetrabutylammonium) dibenzoyl tartrate in DMSO.

Kubik et al. reported the synthesis and binding properties of carbohydrate receptor **98**, which contains two boronic acid

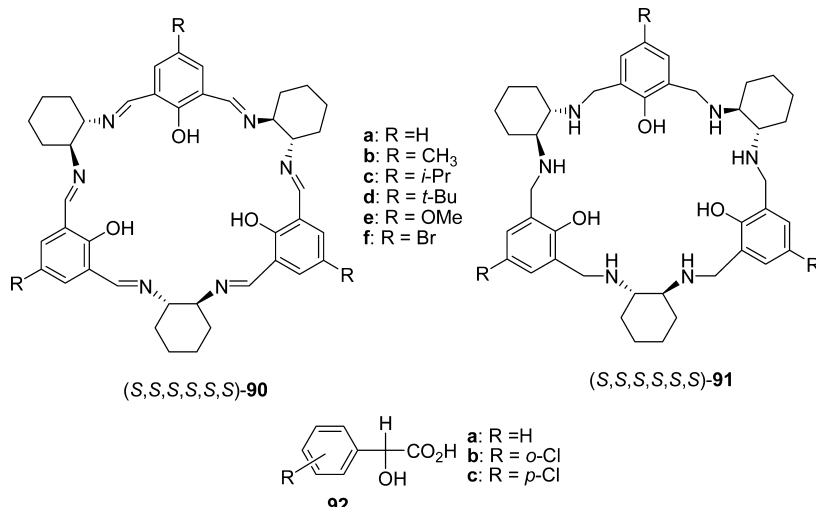


Figure 41. Structures of chiral receptors **90** and **91** and guests **92**.

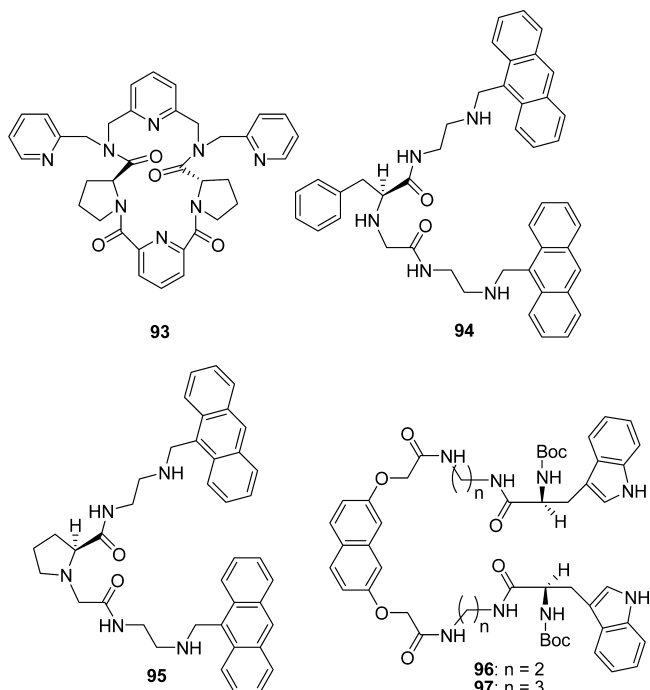


Figure 42. Structures of chiral receptors **93**–**97**.

binding sites and a cyclotetrapeptide cavity (Figure 43).¹¹⁴ The binding affinity toward D-glucose is significantly higher than toward L-glucose, which could be confirmed based on fluorescence quenching effects. Receptor **98** forms stable 1:1 complexes with D-glucose ($K_a = 2.48 \times 10^4 \text{ M}^{-1}$) and L-glucose

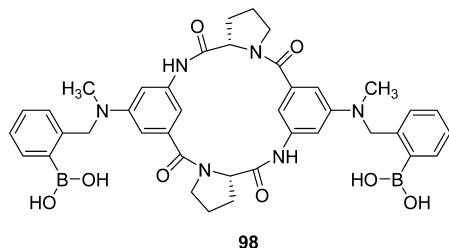


Figure 43. Structure of chiral receptor **98**.

($K_a = 1.19 \times 10^4 \text{ M}^{-1}$) in water/methanol (1:1) at pH 11.7. The ratio of the stability constants $K_a(D)/K_a(L)$ was 2.1. Thus, **98** showed high affinity and selectivity in glucose recognition combined with good enantioselectivity in aqueous solution.

Pseudopeptidic naphthalenophane **99** was synthesized as a selective receptor for N-protected aromatic amino acids (Figure 44).¹¹⁵ Mass spectrometry, NMR, fluorescence, and molecular modeling techniques have been adopted to explain its interactions and selectivity. The careful comparison of NMR data and theoretical calculations could confirm the selectivity toward aromatic amino acids and the L enantioselectivity. Fluorescence titrations of **99** and the enantiomers of Z-Phe-OH provided a fluorescence ratiometric response.

Galindo and co-workers reported eight pseudopeptidic fluorescent receptors (**100a–c**, **101a–c**, **102**, and **103**) for the molecular recognition of amino acids (as Z-protected derivatives).¹¹⁶ As shown in Figure 44, these receptors are either macrocyclic or open chain derivatives based on the naphthalene chromophore. The preferential binding of all the receptors for Phe over aliphatic amino acids (Ala and Val) was observed. Among these fluorescent receptors, two macrocyclic receptors **100a** and **100b** in particular showed exciplex emissions, fluorescence quenching at 390 nm, and fluorescence enhancement at 340 nm, which indicates that **100a** and **100b** are fluorescent ratiometric sensors for Phe. As a proof of concept, **100a** and **100b** were further utilized as analytical tools for the identification of model samples enriched with Phe, which mimics the relatively high concentrations of Phe found in the pathology phenylketonuria (PKU).

BINOL derivatives bearing a stryptophan unit have been prepared and studied for their enantioselective recognition of N-Boc-protected amino acid anions (Figure 45).¹¹⁷ The receptors (*S*)-**104a** and (*S*)-**104b** and (*R*)-**104a** and (*R*)-**104b** all showed good chiral recognition ability toward the enantiomers of the Ala and Phe anions, which were attributed to the preorganized structure of the chiral center of binaphthyl unit. Particularly, the association constants (K_{ass}) were different ($K_{\text{ass}}(S) = 4.91 \times 10^4 \text{ M}^{-1}$; $K_{\text{ass}}(R) = 8.29 \times 10^3 \text{ M}^{-1}$), yielding a selectivity of 5.92 for the Phe anions.

3.2.5. Imidazolium-Based Chemosensors. In contrast to the well-known types of hydrogen bond donors for anion binding, such as amide, pyrrole, urea, etc., imidazolium derivatives have been utilized as anion receptors via ($\text{C}-\text{H}$)⁺...

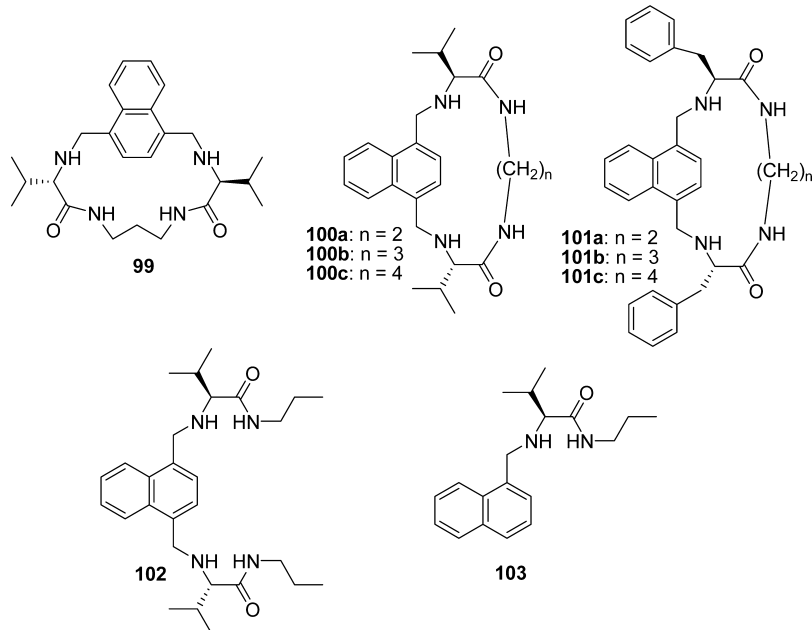


Figure 44. Pseudopeptidic receptors **99–103**.

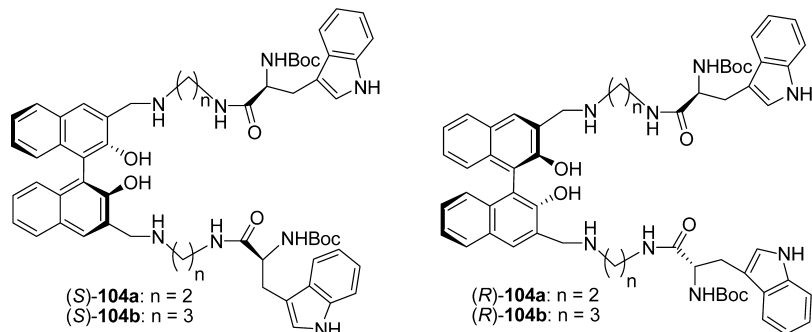


Figure 45. Structures of receptors **(S)-104a** and **(S)-104b** and **(R)-104a** and **(R)-104b**.

X^- ionic hydrogen bonding. Recently, various imidazolium derivatives have been synthesized and studied as selective anion receptors.^{118,119}

Yu et al. reported BINOL-bisimidazolium derivatives **(R)-105** and **(S)-106** as fluorescent chemosensors for anions (Figure 46).¹²⁰ In ACN, F^- ($\lambda_{\text{max}} = 474 \text{ nm}$) and CH_3CO_2^- ($\lambda_{\text{max}} = 454 \text{ nm}$)

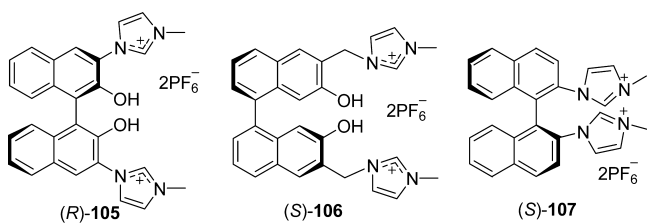


Figure 46. Structures of chiral hosts **(R)-105**, **(S)-106**, and **(S)-107**.

nm) induced large bathochromic-shifted fluorescent emission peaks of **(R)-105** among the various anions. In addition, unique colorimetric changes from colorless to yellow for F^- and colorless to pale yellow color for CH_3CO_2^- . Both hosts **(R)-105** and **(S)-106** showed chelation-enhanced fluorescence quenching effects with amino acid derivatives. **(R)-105** displayed a high binding affinity for the *t*-Boc Ala anion, with a K_L/K_D value of 4.5.

On the other hand, **(S)-106** showed a moderate selectivity (K_D/K_L of 2.9) with *t*-Boc Ala anion in ACN.

Binaphthyl derivative **(S)-107** bearing a bisimidazolium group was investigated by Yoon et al. as a fluorescent chemosensor for chiral anion recognition (Figure 46).¹²¹ The expected strong $(C-H)^+-X^-$ hydrogen bonding between the imidazolium moieties and carboxylate was further confirmed by ^1H NMR in CD_3CN . Upon the addition of chiral guests (2 equiv), **(S)**-mandelate induced a larger downfield shift (δ 8.12 to 8.43 ppm) of imidazolium C–H in host **(S)-107** than that of **(R)**-isomer (δ 8.12 to 8.39 ppm). K_S over K_R for **(S)**- and **(R)**-2-phenylbutylate was reported as ~ 1.5 , which was confirmed by ITC titrations and fluorescent titrations. The chiral selectivity of **(S)-107** was further confirmed by theoretical calculations.

$1,1'$ -Binaphthyl-based imidazolium chemosensors **((R)-108**, **(R)-109**, and **(R)-110a–c**) were synthesized and their binding affinities as well as chiral selectivities were studied (Figure 47).¹²² Among the eleven α -amino acids investigated in the aqueous solutions module, the highly selective recognition of tryptophan (Trp) was observed via synergistic effects of multiple hydrogen bonding and electrostatic interactions. These results also supported that the C-2 hydrogen on the imidazolium ring plays a key role as a hydrogen bond donor. A 1:1 complex between the host and tryptophan was confirmed by the UV–vis, fluorescence, and mass spectrometry data. The binding affinity

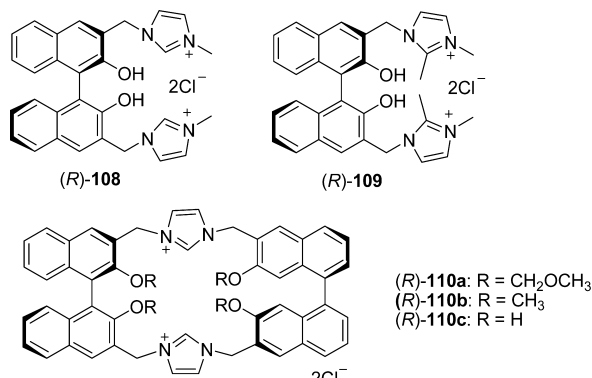


Figure 47. Structures of 1,1'-binaphthyl-based imidazolium chemo-sensors 108–110

and selectivity of the cleft-like receptor (*R*)-**108** with L-Trp were better than those of (*R*)-**109–110a–c**. Even though selectivity for tryptophan over various aromatic amino acids was not excellent, the macrocyclic (*R*)-**110a** displayed a remarkable enantioselectivity for the two enantiomers of tryptophan, with a K_D/K_t value of 6.2.

Xie et al. synthesized two kinds of novel chiral molecular tweezers from *(L)*-Ala, *(L)*-Phe, and *(L)*-glutamic acid, in which imidazolium pincers played a key role as the main binding site for amino acids (Figure 48).¹²³ The enantioselective recognition of

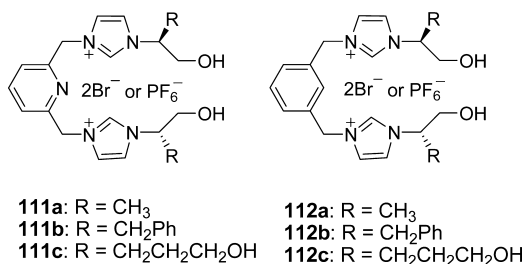


Figure 48. Structures of chiral molecular tweezers **111a–c** and **112a–c**.

(*L*)- and (*D*)-amino acid derivatives by these molecular tweezers was investigated by UV spectroscopic titration experiments. Due to the hydrogen bonding interaction between pyridine nitrogen and amino acid, the chiral molecular tweezers **111a–c** displayed better chiral selectivity than **112a–c**. For example, the host **111b**

(PF₆⁻ salt) showed high enantioselectivity for *N*-Boc protected histidine methyl ester with a K_L/K_D value of 5.10.

3.2.6. Phenylboronic Acid-Based Chemosensors. Due to the unique ability to covalently bind with polyols, phenylboronic acids can be used to monitor polyhydroxy analytes, such as sugars and α -hydroxyl carboxylic acids, in aqueous solutions, which is advantageous for the molecular recognition in biological systems.^{124–127} In recent years, development of boronic acid-based chiral probes for enantioselective recognition has captured considerable interest. James and co-workers have developed several enantioselective fluorescent phenylboronic acid-based probes with nonconjugated tertiary amine groups as the modulator of the fluorescent transduction via the photoinduced electron transfer process (PET) for the detection of important chiral compounds. In general, PET-based boronic acid sensors are divided into two types, a sensing system based on (1) the acceptor-photoinduced electron transfer effect (a-PET) in which the nonconjugated amino group serves as the donor of the electron transfer (ET) and (2) the donor-photoinduced electron transfer process (d-PET) in which the fluorophore acts as the ET donor.^{128–130} Since the discrimination between a-PET and d-PET sensors is the electron transfer orientation of the excited electron, the choice of an appropriate fluorophore and the reasonable modification of the electron-accepting moiety are generally crucial considerations in the PET sensor design. Evidently, the use of the electron-donating fluorophore, as well as the introduction of electron-withdrawing groups into the electron-accepting moiety of sensor is preferable for the design of a d-PET sensing system. In addition, the theoretical calculations based on density functional theory can be employed to aid PET sensor design via the prediction of the electron transfer direction.

Because of the intrinsically axial chirality, BINOL derivatives can be used readily to devise chiral fluorescent boronic acid-based probes for the chiral recognition of chiral polyhydroxyl compounds. Moreover, the sensing mechanism of BINOL-based boronic acid chiral probes is generally based on a-PET. In early work, James and Shinkai et al. designed chiral fluorescent probe 113 (Figure 49) through the introduction of two molecular boronic-acid binding sites to one BINOL molecule for the enantioselective discrimination between D- and L-glucose.¹³¹ Based on this work, the enantioselective recognition of chiral sugar acids including TA (tartaric acid) across a broad pH range with (R)- and (S)-113 was investigated by Zhao et al.¹³²

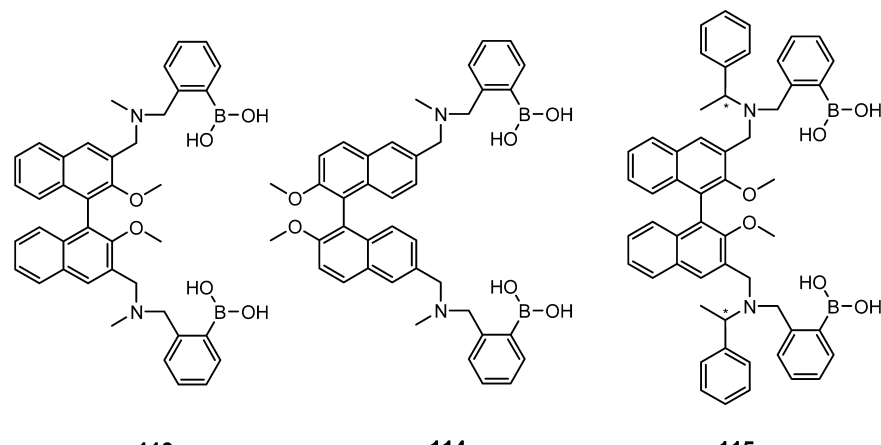


Figure 49. Structures of BINOL-based chiral fluorescent bisboronic acid probes **113–115**

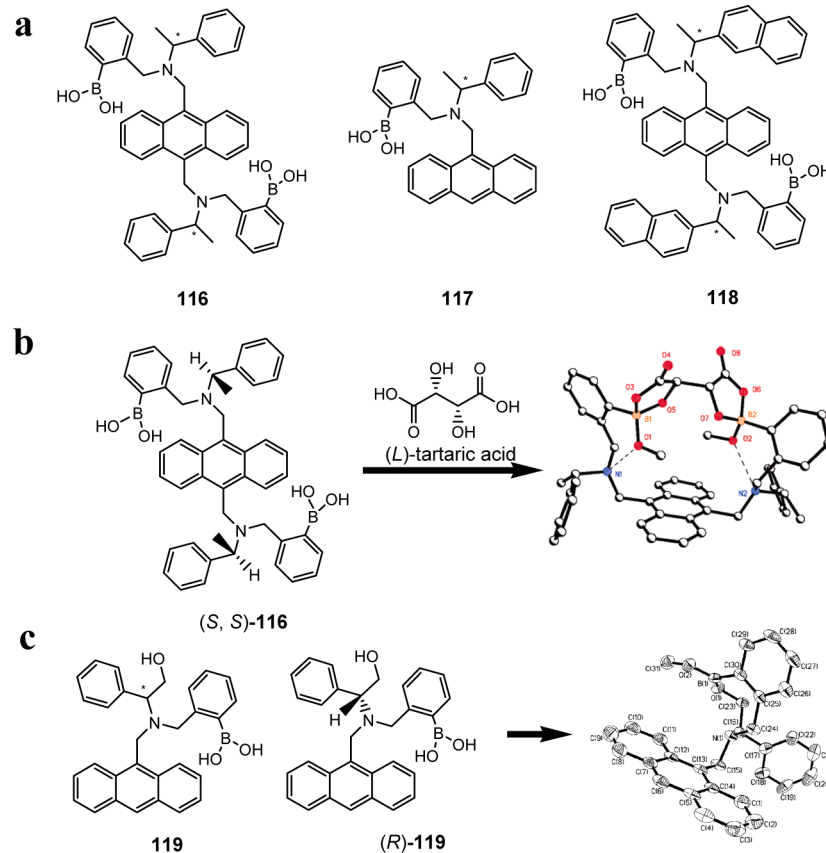


Figure 50. Anthracene-based chiral fluorescent probes. (a) The structure of probes **116–118**, (b) the formation of *(S,S)*-**116** complex with *L*-TA, and (c) the structure of probe **119** and the single crystal structure of *(R)*-**119**.

Different from those reported chiral probes whose enantioselectivities are based on only one fluorescent response mode, probe **113** displays a novel fluorescent transduction profile of enhancement/diminishment for the enantioselective discrimination between *D*- and *L*-TA at pH 3–7. At pH 5.6, enhancement of the emission intensity of *(S)*-**113** is observed upon addition of *L*-TA, whereas the fluorescence intensity is reduced by *D*-TA. With the mirrored response, the fluorescence intensity of *(R)*-**113** is enhanced by *D*-TA, but reduced by *L*-TA. Moreover, probe **113** exhibits a good enantioselectivity toward TA at pH 8.3 only with the response of fluorescence enhancement. For *D*-TA the enantioselective response is shown as a $K_R F_R / K_S F_S$ (where K is the binding constant, and F represents the maximum fluorescence enhancement) of $(71 \pm 23):1$ and $1:(42 \pm 13)$ for *L*-TA.

Recently, another BINOL-based bisboronic acid probe **114** was synthesized by Liang et al. with chiral 2,2'-dimethoxy-*N,N'*-dimethyl-1,1'-binaphthalene-6,6'-dimethanamine as the chiral precursor reacted with 2-formylphenylboronic acid (Figure 49).¹³³ A remarkable enantioselectivity toward *D*-sorbitol with *(R)*- and *(S)*-**114** has been observed as $K_R / K_S = 1:35$ at pH 9.0.

There is only one chirogenic center in either **113** or **114**, and the distance between the chirogenic center and the boronic-acid binding site is relatively large, which influences their performance on the chiral recognition of diverse analytes. Therefore, in order to improve the enantioselective performance of BINOL-based boronic acid probes, Li et al. introduced another chirogenic center from chiral α -phenylethylamine to 1,1'-bisnaphthol molecule to give four diastereoisomeric bisboronic acid chiral probes, *(R,R)*-**115**, *(R,S)*-**115**, *(S,R)*-**115**, and *(S,S)*-**115**, in

which the first letter stands for the chirogenic center of BINOL and the second letter stands for the chirality of α -phenylethylamine (Figure 49).¹³⁴ Each diastereoisomeric probe displays better enantioselectivity toward the enantiomers of TA, with the similar fluorescence response as probe **113** shows. However, different from **113** which shows no enantioselectivity toward *D*-sorbitol, the diastereoisomeric probes can be employed to recognize *D*-sorbitol at pH 7.0. For example, in the presence of *D*-sorbitol the enhancement in fluorescence intensity is observed for *(S,S)*-**115**, but diminishment for *(S,R)*-**115**. Moreover, the similar diastereoselectivity response for *D*-sorbitol has been also shown with *(R,R)*-**115** and *(R,S)*-**115**.

In addition, to tackle the limitations of the BINOL-based bisboronic acid probe, such as the emission in UV region and the large distance between the chirogenic center and binding site of the receptor, Zhao et al. devised chiral fluorescent anthracene-based bisboronic acid probe **116** and monoboronic acid probe **117** by incorporating chiral α -phenylethylamine group to anthracene fluorophore (Figure 50), for the enantiodiscrimination of sugar acids including TA.¹³⁵ It has been indicated by pH titrations that **116** and **117** are a-PET probes whose fluorescent intensity is enhanced at acidic pH but diminished at neutral/basic pH due to the protonation of amine/boronic acid moiety. The fluorescence transduction efficiency is as high as 10-fold upon switching pH from 2 to 12. It has been found by binding titrations that **116** displays excellent enantioselectivity in binding with TA. At pH 8.3, upon addition of *L*-TA, *(S,S)*-**116** exhibits an 8.24-fold enhancement in emission at 429 nm upon excitation at 365 nm, whereas the addition of *D*-TA leads to only a 1.5-fold fluorescence enhancement. The addition of *D*-TA to *(R,R)*-**116**

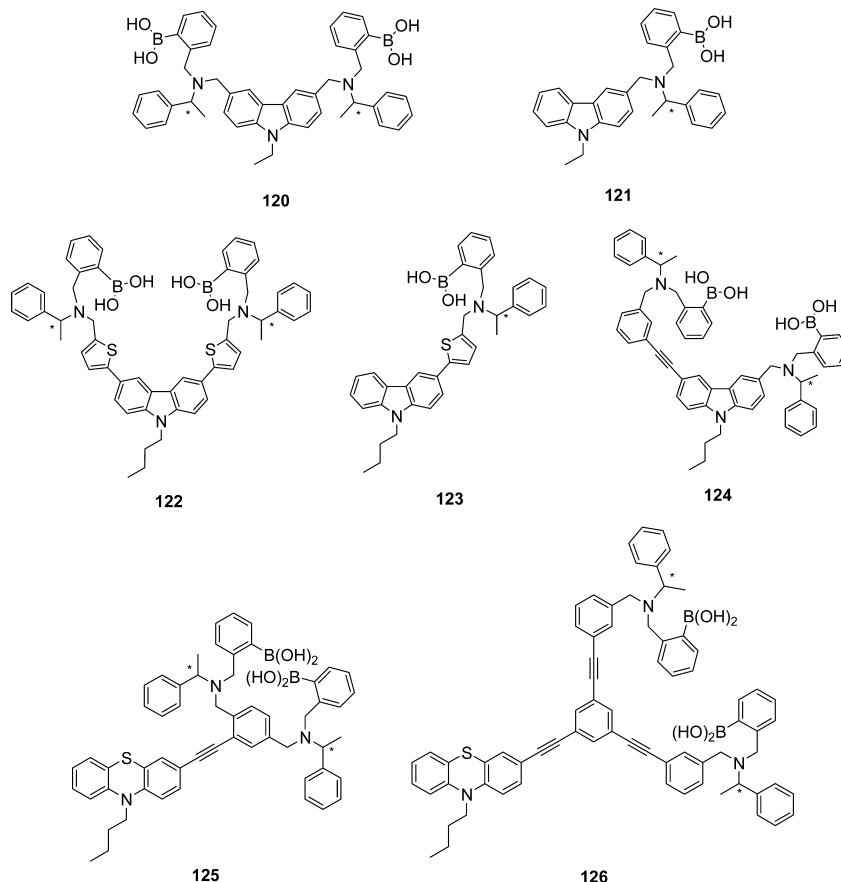


Figure 51. Structures of carbazole-based and phenothiazine-based chiral fluorescent bisboronic acid probes **120–126**.

aqueous solution induces 8.87-fold fluorescence enhancement, whereas only 1.5-fold increase in emission occurs upon the addition of L-TA. Thus, a mirroring of the fluorescence response for the two enantiomers of the probe **116** has been observed when treated with the enantiomers of TA. At pH 7.0, the enantioselectivity defined as K_R/K_S is obtained as 490:1 for D-TA and as 1:550 for L-TA. Although probe **116** shows the high ability for chiral discrimination of TA, there is no enantioselectivity for probe **117**. It has been shown by single crystal structure that the formation of 1:1 cyclic complex between probe **116** and TA (Figure 50b) is the key in the enantioselective discrimination between D- and L-TA. This is the reason that monoboronic acid probe **117** cannot utilize to detect TA enantioselectively. For sugar acids, enantioselective discrimination for certain sugar alcohols is also observed with probes (S,S)- and (R,R)-**116**. At pH 8.3, probe **116** shows a high enantioselectivity for D-mannitol, as shown using the ratio of binding constants, $K_S/K_R > 2000$.¹³⁶

With chiral 1-(naphthalen-2-yl)ethylamine as the chirogenic center, Zhao and James designed another chiral fluorescent anthracene-based bisboronic acid probe **118** (Figure 50).¹³⁷ Probe **118** also displays a high enantioselectivity toward the enantiomers of TA; however, the chirally fluorescent response is not based on the PET mechanism as a result of the formation of the naphthylene-anthracene excimer. Thus, the ability to restrict the interaction between the naphthalene and anthracene fluorophores becomes the key in the enantioselective discrimination between D- and L-TA. At pH 2.5, (R,R)-**118** exhibits a dramatic fluorescence enhancement of the anthracene fluorophore upon excitation at 370 nm in the presence of D-TA, but

addition of L-TA to (R,R)-**118** results in little changes of fluorescence intensity. For (S,S)-**118**, there exists a mirrored response model compared with (R,R)-**118**; that is, the fluorescence intensity of (S,S)-**118** is enhanced more dramatically by L-TA than by D-TA.

In addition to chiral fluorescent anthracene-based bisboronic acid probes, Chi et al. recently reported a novel anthracene-based monoboronic acid probe **119** containing 2-amino-2-phenylethanol as the chirogenic component (Figure 50).¹³⁸ The chiral recognition of mono α -hydroxyl carboxylic acids, such as MA and lactic acid (LA) by probe **119** has been investigated by fluorimetric titration experiments. As a result, (R)- and (S)-**119** exhibit a remarkable enantioselectivity for D-MA in ACN, with a $K_R K_S / K_S K_S$ of 1:2.8, and a mirrored response enantioselectivity for L-MA of 3.0:1. Moreover, the enantioselective discrimination between D- and L-LA with **119** has been tested as 1:2.4 and 2.9:1, respectively. However, no enantiodiscrimination between the enantiomers of mono α -hydroxyl carboxylic acids was observed with **117** instead of **119**. The additional hydrogen bond offered by the hydroxyl group of **119** is critical for the enantioselectivity, which is indirectly proven by the event of no enantioselectivity in aqueous solution. In particular, it has been found that the fluorescence response of **119** with the binding of mono α -hydroxyl carboxylic acids is time-dependent, because unfastening the intramolecular boronic acid ester cyclic structure (Figure 50c) is a slow process. Therefore, probe **119** also displays significantly kinetic enantioselectivity with different apparent binding rate constants (K_{app}) of diastereomeric complexes. Experimentally, the kinetic

enantiodiscrimination between (*R*)- and (*S*)-**119** for *D*-MA is 1.5:1, whereas for *L*-MA enantioselectivity of 1:1.4 is observed.

Owing to their strong background fluorescence at acidic pH, most a-PET-based boronic acid probes show little fluorescence response when binding with analytes in acidic media. Therefore, the chiral fluorescent boronic acid probes based on the d-PET mechanism have been developed recently to enantioselectively recognize acidic chiral compounds, such as TA, in the acidic region. In 2009, Han et al. devised novel carbazole-based bisboronic acid probe **120**, which contains two chiral amine/phenylboronic acid units at the 3 and 6 positions of a carbazole core, and 3-substituted monoboronic acid chiral probe **121** (Figure S1).¹³⁹ pH titration experiments have demonstrated a lower fluorescence intensity at acidic pH than that at basic pH due to the d-PET effect arising from the protonation of the amine/boronic acid moiety of **120**, which is supported by DFT/TDDFT calculations. By using **120** as the chiral fluorescence probe, enantioselective discrimination between *D*- and *L*-TA can be achieved with the response of fluorescence enhancement at pH 2.0–6.0. For instance, at pH 5.6, (*S,S*)-**120** exhibits a larger increase in emission at 375 nm upon excitation at 307 nm in the presence of *L*-TA than that in the presence of *D*-TA, with the enantioselectivity ($K_D F_D / K_L F_L$) of 1:1.8. When using (*S,S*)-**120**, the mirrored effect is observed with the enantioselectivity of 1.7:1. In addition, the fluorescence transduction profile of enhancement/diminishment for the chiral recognition of TA is observed with **120**. For example, at pH 7.0, the fluorescence of (*S,S*)-**120** is enhanced by *L*-TA but diminished by *D*-TA, with the enantioselectivity of (-1.0):(+1.6). A mirrored response for (*R,R*)-**120** is obtained with the enantioselectivity of (+1.6):(-1.0), where the positive sign indicates enhancement of fluorescence intensity and the negative sign indicates diminishment of fluorescence intensity. Although monoboronic acid probe **121** shows similar pH titration results to that of **120**, no enantioselectivity toward TA was observed with (*R*)- and (*S*)-**121** because of their inability to form the 1:1 cyclic complex with TA. Probe **120** is the first d-PET-based bisboronic acid chiral probe that has some drawbacks, such as shorter excitation/emission wavelength (307 nm/375 nm) and a much lower PET efficiency (only 0.25-fold).

To improve the performance of **120**, Wu et al. designed chiral fluorescent bisboronic acid probe **122** by using 3,6-dithiophen-2-yl-9H-carbazole as the fluorophore core in which the thiophene unit not only acts as the efficient π -conjugation expander of the carbazole, but also serves as the promoter of the electron-donating ability of the fluorophore (Figure S1).¹⁴⁰ It has been found by pH titration experiments that **122** displays a much higher contrast ratio (~3.0 fold) of d-PET effect and much longer excitation/emission wavelength (349 nm/413 nm) compared to **120**. The monoboronic acid chiral probe **123** with a longer excitation/emission wavelength compared to **121** was also prepared. Furthermore, improved enantioselectivity with (*R,R*)- and (*S,S*)-**122** toward the enantiomers of TA has been found with the response of fluorescence enhancement in the acidic pH region. For instance, at pH 3.0, the fluorescence of (*S,S*)-**122** is enhanced by 2.64 fold in the presence of *D*-TA but by 3.55 fold in the presence of *L*-TA, with the enantioselectivity of $K_D / K_L = 1:2.5$. Conversely, a mirrored effect is observed with (*R,R*)-**122**, and the enantioselectivity of K_D / K_L is 1.5:1. Interestingly, chiral recognition of the enantiomers of MA is also observed by using (*R,R*)- and (*S,S*)-**122**. However, no enantioselectivity was observed with either monoboronic acid probe **123** or thiophene-unsubstituted bisboronic acid probe

120. Recognition of LA, which is another mono α -hydroxyl carboxylic acid without a phenyl group compared with MA was also investigated, but no significant enantioselectivity was found. Thus, in addition to considering the specific structure of MA, the thiophene unit becomes the key in the design of fluorescence chiral boronic acid probes for the enantioselective discrimination between *D*- and *L*-MA.

More recently, another carbazole-based chiral bisboronic acid probe **124** was prepared by Liu et al. with the ethynylene linker as the π -conjugation extender (Figure S1).¹⁴¹ An a-PET fluorescence intensity-pH profile with a 2.0-fold PET efficiency was reported by pH titration of **124**. However, different from normal a-PET probes that cannot work well in acidic media due to serious interference of the strong background emission, **124** displays a fluorescence enhancement response when binding with TA, and significant enantioselective discrimination between *D*- and *L*-TA is observed in the acidic pH region, which is proposed to be a hybrid a-PET/d-PET mechanism. On the other hand, a transition from the 1:2 open binding form to the unstable 1:1 cyclic binding form of the probe-TA complex was observed upon addition of excess TA, owing to the larger binding pocket of **124**.

Given that other fluorophores that possess an electron-donating nature, besides carbazole, can also be utilized to design d-PET-based probes, Wu et al. have assembled two phenothiazine based bisboronic acid chiral probes **125** and **126** (Figure S1).¹⁴² Compared to those carbazole-derived probes, **125** and **126** display a more improved performance, such as longer excitation/emission wavelengths (375/488 nm and 380/492 nm), larger stokes shifts (138 and 142 nm), and higher contrast ratio (~6.0 and ~8.0 fold) based on the d-PET effect. Furthermore, both **125** and **126** exhibit enhanced enantioselectivity toward the enantiomers of TA with the response of fluorescence enhancement in the acidic pH region. For instance, at pH 3.0, the enantioselectivity toward *D*- and *L*-TA with (*R,R*)-**125** is obtained as $K_D / K_L = 5.8:1$ with a mirrored response, the enantioselectivity is 1:4.8 with (*S,S*)-**125**. Compared with **125**, probe **126** displays a better enantioselectivity toward TA due to the larger binding pocket. At pH 4.0, the higher enantioselectivity with (*S,S*)-**126** toward *D*- and *L*-TA is obtained as $K_D / K_L = 11:1$ conversely, the selectivity with (*R,R*)-**126** is 1:10.5. Due to the larger binding pocket of **126** compared to that of **125**, a transition from the 1:1 cyclic binding form to the 1:2 open form of the **126**-TA complex is observed upon increase of the analyte concentration, which is shown by the mass spectroscopic analysis. In addition, it has been found that **125** and **126** can be also employed to recognize disaccharides and glycosylated steroids enantioselectively in neutral pH with the response of fluorescence diminishment. For example, at pH 7.4, (*R,R*)-**126** shows a moderate selectivity (K_R / K_S) of 2.9 toward maltose, and a significant selectivity (K_S / K_R) of 3.5 toward ginsenoside Re.

Apart from the traditional reporter (or indicator)-spacer-host (or receptor) sensing framework in the PET-based boronic acid chemosensors discussed above, the well-accepted chemosensing system with an indicator-receptor complex, in which either the indicator (chromophore or fluorophore) or the receptor is variable, can also be used for enantioselective recognition via the introduction of a chiral element into the receptor unit. The method involved in the chiral sensing system is referred to as enantioselective indicator-displacement assay (eIDA). Anslyn and co-workers developed a series of indicator displacement chiro-systems with pyrrolidine-boronic acid derivatives as the chiral receptors for the colorimetric or

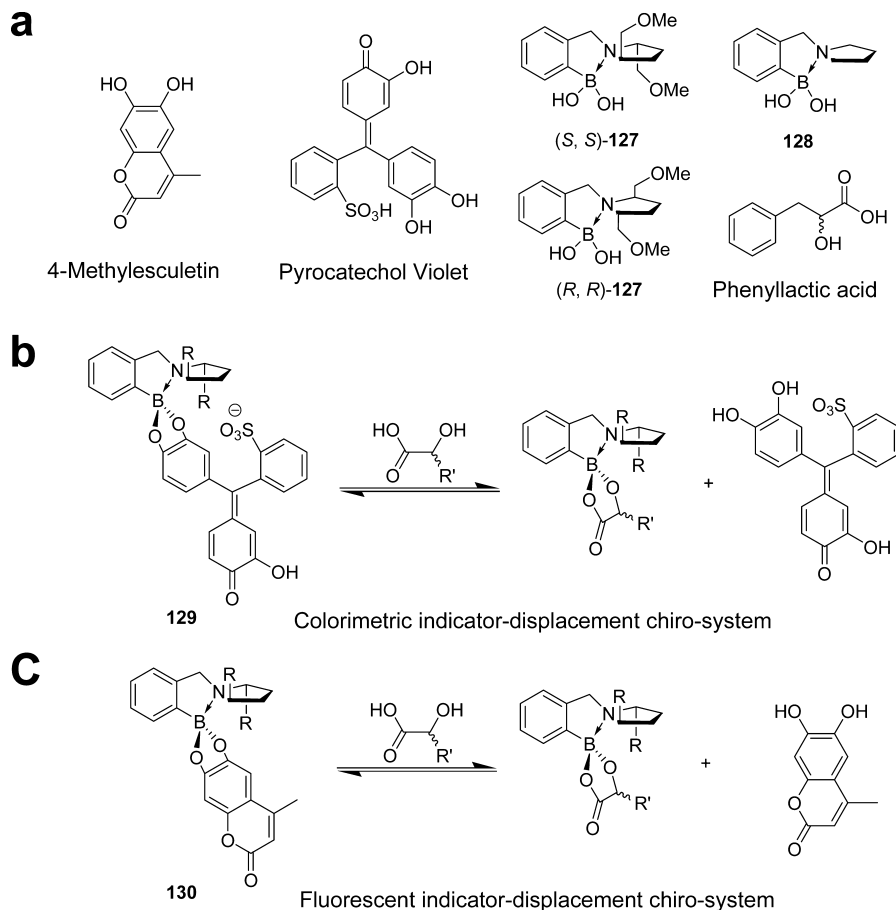


Figure 52. Indicator-displacement chiro-systems. (a) The structures of two indicators ML and PV, chiral and achiral boronic acid receptors **127** and **128**, and phenyllactic acid (PL). Colorimetric or fluorescent indicator-displacement chiral sensing systems **129** and **130** with (b) PV and (c) ML, respectively, as the reporters.

fluorescent detection of the *ee* of chiral analytes.^{143,144} As is shown in Figure 52, IDA approach is based on the event that analytes can take the place of the indicators from the receptors, which can cause changes in optical signals (UV-vis absorbance or fluorescence). Furthermore, the introduced chirality of the boronic acid receptors can lead the enantiomers of the chiral substrates to associate with the hosts in different degree. For instance, the UV-vis titrations of receptor **127** with the enantiomers of PL has indicated that the enantiodifferentiation between (*R,R*)- and (*S,S*)-**127** for d-PL, as represented by the ratio of the association constants (K_R/K_S), is 2.4:1, whereas for L-PL the ratio is 1:2.9. Thus, when the two enantiomers of PL are used to replace the indicator PV (pyrocatechol violet) from (*S,S*)-**127**, the displacement efficiency of L-PL is larger than that of d-PL. However, d- and L-PL show the same displacement efficiency for PV when using **128** as the achiral host. On the other hand, the similar enantioselectivity for PL has been also observed in the fluorescent displacement chiro-system **130** with 4-methylesculetin (ML) as the indicator (Figure 52c). On the basis of the optical detection results associated with the mathematical analysis of solution equilibria, the ees of unknown PL samples have been measured with the average errors of 0.17 and 0.13 respectively in chiro-system **129** and **130**.

3.3. α -Aromatic Cinnamylnitrile-Derivatized Chemosensors

Recently, a new class of organic compounds with an aggregation-induced emission (AIE) or aggregation-induced emission enhancement (AIEE) have been developed and explored as

fluorescent chemosensors. The Zheng group recently reported new chiral AIE-materials and their fluorescent recognition.

Chiral AIE-compounds containing a TA group were synthesized by the Zheng group (Figure 53).¹⁴⁵ **D**-**131** and **L**-

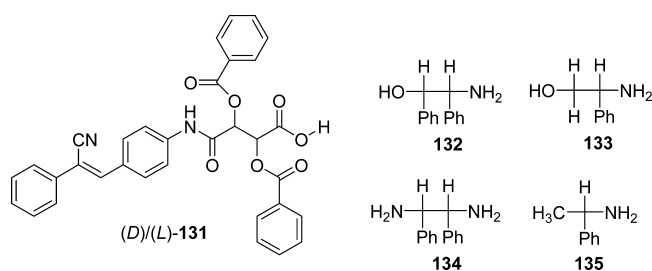


Figure 53. Structures of compounds **131**–**135**.

131 selectively aggregated with one enantiomer of a number of chiral amines, which induced strong fluorescence via AIE. The dramatic AIE character of **131** was observed. A suspension of **L**-**131** and (1*R*,2*S*)-**132** displayed a fluorescence intensity of 419, but the solution of **L**-**131** and (1*S*,2*R*)-**132** showed an intensity of only 1.6. A high enantiomer fluorescence intensity ratio of 262 ($I_{(1R,2S)-7}/I_{(1S,2R)-7}$) was observed. For amines **133**, **134**, and **135**, the same methodology with **L**-**131** gave $I_{(2S)-133}/I_{(2R)-133} = 10$, $I_{(1R,2R)-134}/I_{(1S,2S)-134} = 18$, and $I_{(R)-135}/I_{(S)-135} = 17$. This was used for the quantitative analysis of enantiomeric composition.

Chiral α -aromatic cinnamylnitrile derivatives (*R,R*)-136 and (*S,S*)-136 were synthesized as AIE-compounds by the same group (Figure 54).¹⁴⁶ Eighteen different chiral α -hydroxycarboxylic acids, including MA, 2-chloroMA, 3-PL, etc., were examined for enantioselective recognition. The fluorescence intensity ratio of two enantiomers ranged from 10 to 1.6×10^4 and could be used to determine the purity of the enantiomers. For example, the fluorescence intensity ratios (I_S/I_R) of the two enantiomers of MA was 1.68×10^4 .

The same group recently found that simple AIE-compounds 137a and 137b could show different fluorescence output intensity in gel, suspension, and precipitate in 1,2-dichloroethane (Figure 54).¹⁴⁷ A solution of 137a in 1,2-dichloroethane showed almost no fluorescence, but the addition of hexane into the solution emitted strong fluorescence with increase of aggregates in the suspension. In this work, the authors found that the mixture of 138 and a wide variety of carboxylic acids created excellent organogelators. Both the solution and gel of the mixture of (1*S,2R*)-138 and benzoic acid showed no fluorescence. However, after 20 mol % of 137a (relative to benzoic acid) was added, the gel exhibited strong fluorescence. For example, 137a in transparent gel from mixing (1*S,2R*)-138 and (S)-MA and in suspension from mixing (1*S,2R*)-138 and (R)-MA was light-emitting and the fluorescence intensity in the transparent gel was much less than that in the suspension. The fluorescence intensity ratio of 137a in suspension and in TGel arose from these two enantiomers of MA was 32. These AIE-mixtures could emit different intensity of fluorescence according to their gel, suspension, and precipitates formation, which were applied to fluorescence switches and quantitative determination of enantiomer composition.

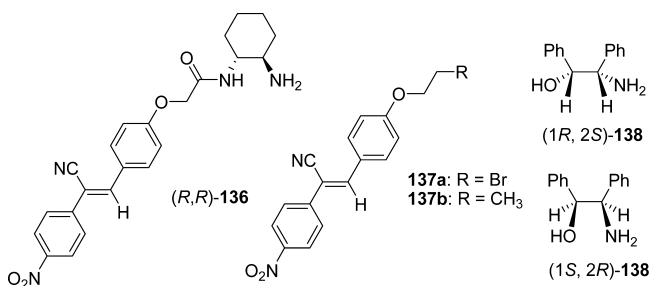


Figure 54. Structures of AIE-compounds 136 and 137 and chiral amino alcohol 138.

carboxylic acids, including MA, 2-chloroMA, 3-PL, etc., were examined for enantioselective recognition. The fluorescence intensity ratio of two enantiomers ranged from 10 to 1.6×10^4 and could be used to determine the purity of the enantiomers. For example, the fluorescence intensity ratios (I_S/I_R) of the two enantiomers of MA was 1.68×10^4 .

The same group recently found that simple AIE-compounds 137a and 137b could show different fluorescence output intensity in gel, suspension, and precipitate in 1,2-dichloroethane (Figure 54).¹⁴⁷ A solution of 137a in 1,2-dichloroethane showed almost no fluorescence, but the addition of hexane into the solution emitted strong fluorescence with increase of aggregates in the suspension. In this work, the authors found that the mixture of 138 and a wide variety of carboxylic acids created excellent organogelators. Both the solution and gel of the mixture of (1*S,2R*)-138 and benzoic acid showed no fluorescence. However, after 20 mol % of 137a (relative to benzoic acid) was added, the gel exhibited strong fluorescence. For example, 137a in transparent gel from mixing (1*S,2R*)-138 and (S)-MA and in suspension from mixing (1*S,2R*)-138 and (R)-MA was light-emitting and the fluorescence intensity in the transparent gel was much less than that in the suspension. The fluorescence intensity ratio of 137a in suspension and in TGel arose from these two enantiomers of MA was 32. These AIE-mixtures could emit different intensity of fluorescence according to their gel, suspension, and precipitates formation, which were applied to fluorescence switches and quantitative determination of enantiomer composition.

4. CHIRAL PROBES WITH MACROCYCLIC NON-FLUORESCENT RIGID SCAFFOLDS

4.1. Calixarene-Based Chemosensors

Due to their readily stereoselective synthesis, multiple position modifications, and conformationally rigid structures, calixarenes have been intensely and extensively used as ideal functionalized host platforms in various areas such as asymmetric synthesis, drug separation and delivery, molecular recognition and sensing, and nanotechnologies.¹⁴⁸ Two methods exist in order to accomplish chirogenic derivatization of the calixarene-based scaffolds: (1) direct introduction of various foreign chiral sources, such as amino acids, chiral amines, amino alcohols, the inherent fluorophore BINOL, etc., onto the reactive narrow or wide rim and (2) inherent chiral species, which is based on the absence of a plane of symmetry or an inversion center in the molecule as whole.¹⁴⁹ In practice, all the calixarene-based chiroselective fluorosensors covered in this section belong to the former case.

Some impressive work has been published by He and co-workers. In 2005, Liu et al. synthesized chiral calix[4]arenes containing hydrazide and dansyl groups (dansyl = 5-(dimethylamino)-1-naphthalenesulfonyl) and examined them for their enantioselective recognition abilities by the fluorescence and ^1H NMR in CHCl_3 (Figure 55).¹⁵⁰ Both 139a and 139b showed excellent enantioselectivities to the N-protected Ala or Phe anions. More specifically, the different quenching efficiencies ($\Delta I_L/\Delta I_D = 5.0$) indicated that receptor 139a had good enantioselective recognition between L- and D-Ala anions. An excellent enantioselectivity $K_{\text{ass}}(\text{L-Phe})/K_{\text{ass}}(\text{D-Phe}) = 10$ was observed for compound 139a.

He et al. also reported anthracene derivatives of chiral calix[4]arenes 140a and 140b (Figure 56), which displayed good chiral recognition abilities toward the enantiomers of D- and L-tetrabutylammonium malate with $K_D/K_L = 4.34$ and 10.41 for 140a and 140b, respectively.¹⁵¹ The receptors' preorganization property, steric effect, relative rigidity, structure-complementary with guest, and multiple hydrogen bonding were attributed to the enantioselective recognition of malate. They prepared host 141a and 141b as colorimetric chemosensors for α -Phg anions.¹⁵² $K_L/K_D = 4.76$ for 141a and $K_D/K_L = 2.84$ for 141b were obtained via UV absorption changes in DMSO. Furthermore, the color of the solution clearly changed from colorless to saffron upon the addition of α -Phg anions.

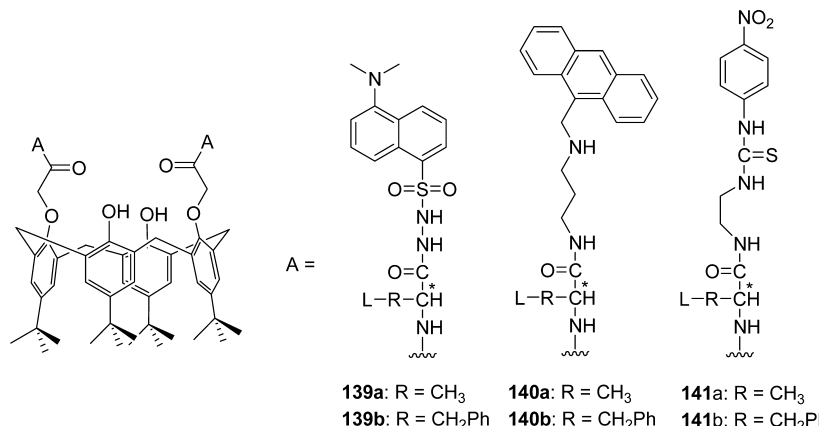


Figure 55. Structures of chiral calixarene derivatives 139–141.

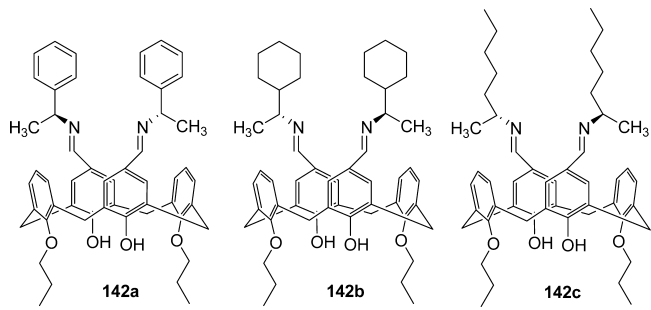


Figure 56. Chiral Schiff-base derivatives of calix[4]arenes **142a–c**.

The Yilmaz group prepared chiral Schiff-base derivatives of calix[4]arenes **142a–c** from the reaction of 5,17-diformyl-25,27-dipropoxy-26,28-dihydroxycalix[4]arene with (S)-(–)-1-phenylethylamine, (R)-(–)-1-cyclohexylethylamine, and (R)-(–)-2-heptylamine, respectively (Figure 57).¹⁵³ The spectrophotometric titrations show that a relatively good enantioselective recognition ability was obtained with receptor **142b** toward (R)- and (S)-phenylethylamine compared to hosts **142a** and **142c**. More specifically, (R)-1-phenylethylamine was 2.67 times more stable than the (S) isomer and $\Delta\Delta G = 2.43 \text{ kJ mol}^{-1}$ in CHCl_3 .

Recently, two armed chiral calix[4]arenes (**143a–c** and **144a–b**) functionalized at the lower rim with chiral amino-naphthol units have been also prepared by the Yilmaz group.¹⁵⁴ Among these hosts, UV-vis spectroscopic studies indicate that chiral receptors **143b** and **144b** show strong binding and good recognition ability for the enantiomers of dibenzoyltartaric acid with K_L/K_D values of 2.27 and 1.40, respectively. In addition, chiral calix[4]arenes **143b** and **144b** were used as chiral NMR solvating agents to determine the enantiomeric purity of MA.

In addition, a series of tri-O-alkylated inherently chiral fluorescent calix[4]crowns in the cone conformations and a series of tetra-O-alkylated inherently chiral fluorescent calix[4]-crowns in the partial cone conformations have been synthesized (Figure 58).¹⁵⁵ By condensing with chiral auxiliary (S)-BINOL, the resulting diastereomers could be separated via preparative TLC. For example, diastereomers of **147a–c** were separated on preparative TLC and then hydrolyzed to provide enantiomerically pure **146a–c**. The same methods were applied to **150a–c**, and then pure enantiomers of **149a–c** were obtained. Among these enantiomers, a tetra-O-alkylated chiral calix[4]crown-6 in the partial cone conformation **149c** showed considerable enantioselective recognition selectivity toward chiral leucinol.

From the fluorescence titration experiments, the association constant (K_a) of the 1:1 complex formation was obtained as 50 M^{-1} for D-leucinol and 143 M^{-1} for L-leucinol, according to the Stern–Volmer plot.

Diamond and co-worker reported calixarene **151** as a fluorescent molecular sensor for chiral amines based on their size and chirality (Figure 59).¹⁵⁶ Based on the fluorescence quenching studies, calixarene **151** did not show any significant enantiomeric selectivity for short chain amino alcohols, such as phenylglycinol in methanol. On the other hand, excellent selectivity was observed for a longer chain amino alcohol, phenylalaninol (PA). In chloroform a new emission band at a longer wavelength (440 nm) was observed only with (R)-PA and not with the (S) enantiomer. The fluorescent properties of this calixarene in the presence of PA were quite solvent dependent. While enantiomeric selectivity was observed in methanol at 227 nm, no discrimination was achieved in ACN.

4.2. Calixpyrrole-Based Chemosensors

Although calixpyrroles are attractive anion hosts, there is only one example that involves the enantioselective receptor design that has been reported to date. Lee et al. synthesized a new set of chiral receptors, namely the BINOL-strapped calix[4]pyrroles (**R**-**152** and (S)-**152** (Figure 60).¹⁵⁷ (R)-2-Phenylbutyrate ((R)-PB) or (S)-2-phenylbutyrate ((S)-PB; as the tetrabutylammonium salt) were used to examine their chiral recognition. The association constants for the binding of (R)- and (S)-PB to (S)-**152** ($K_a(R) = 9.8 \times 10^3$ and $K_a(S) = 1.0 \times 10^5 \text{ M}^{-1}$) were obtained with the ITC instrument. The resulting association constants K_a were found to be 10-times larger in the case of the (S)-PB compared to the (R) enantiomer. Based on the density functional theory (DFT) calculations, (S)-**152**·(S)-PB is computed to be 5.5 kcal mol^{–1} more stable than (S)-**152**·(R)-PB. In the optimized structure of (S)-**152**·(S)-PB, stabilizing π – π interactions were observed between the benzene ring of the guest and one of the naphthyl groups of the host (as well as by the pyrrole NH-carboxylate anion hydrogen bonds). No such π – π interactions were observed in the case of (S)-**152**·(R)-PB.

4.3. Cyclodextrin-Based Chemosensors

As the most extensively used chiral selectors in modern chiral drug separation technologies, cyclodextrins (CDs) are inherently chiral macrocyclic hosts because all of their glucopyranosidic units remain the D form.^{158,159} Therefore, CDs can be used directly to accommodate chiral chromogenic guests enantioselectively in their hydrophobic cavities in order to induce UV

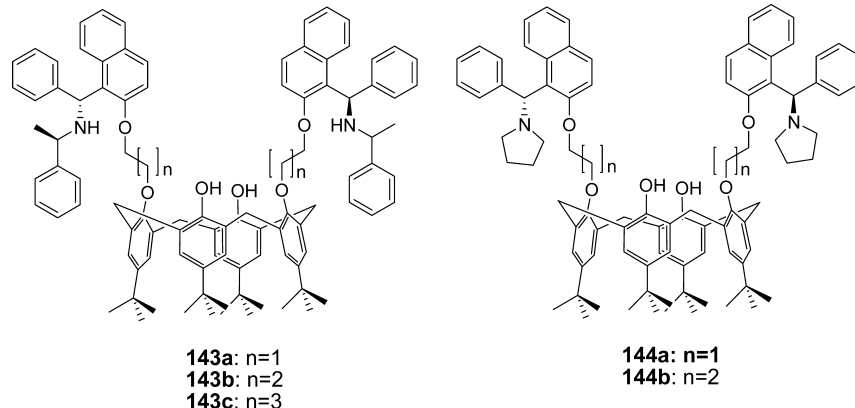


Figure 57. Structures of chiral calix[4]arenes **143a–c** and **144a–b**.

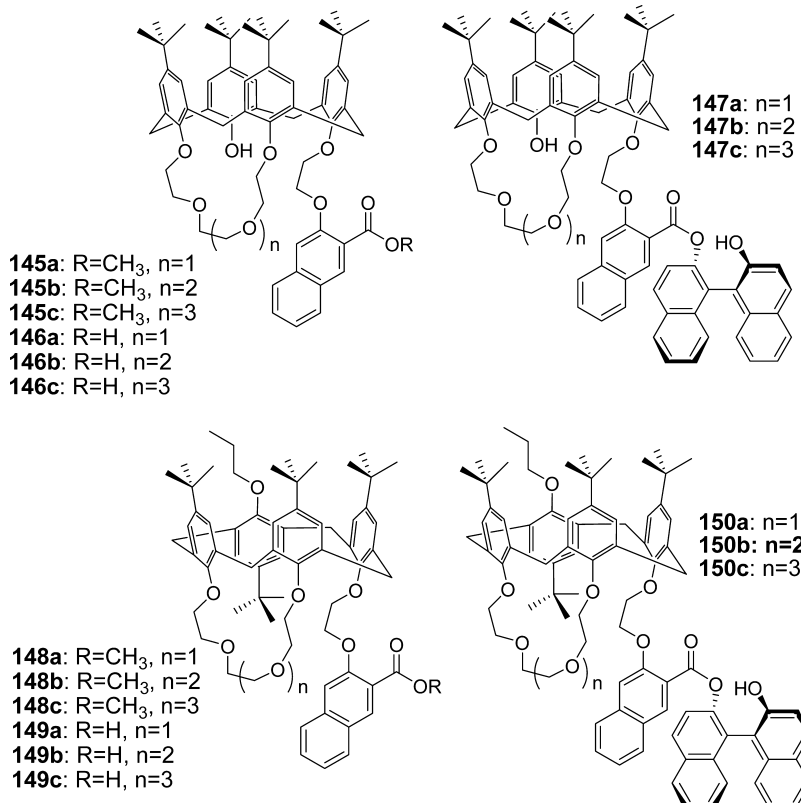


Figure 58. Structures of tri-O-alkylated inherently chiral fluorescent calix[4]crowns and tetra-O-alkylated inherently chiral fluorescent calix[4]crowns.

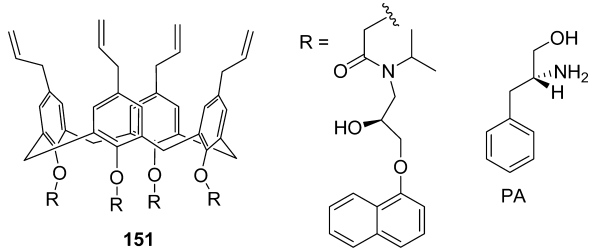


Figure 59. Structures of 151 and phenylalaninol (PA).

4.2 Calixpyrrole-based chemosensors

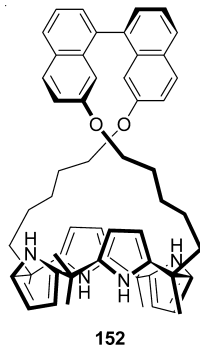


Figure 60. Structure of BINOL-strapped calixpyrrole 152.

spectral responses. For the design of the cyclodextrin-based fluorescent chiral sensory systems, inclusion of certain organic fluorophore in the CD cavity to establish the fluorescent binary complex receptor is an efficient alternative for the chiral recognition. In addition, another chiral sensor design strategy involving a certain amino acid as a linker/spacer between the CD

rim and the fluorophore has been also proposed for the chiral recognition by an enantioselective guest displacement assay, in which the fluorophore is located in the CD cavity due to the hydrophobic interaction. In some cases, a copper ion is allowed to participate in the chiral recognition process with the amino acid linker as the metal ligand in combination with the fluorophore self-inclusion system *via* a ligand exchange mechanism. Below, detailed examples will be summarized.

Recently, Ritter et al. prepared poly(*N*-isopropylacrylamide co-(D or L)-*N*-tryptophan-acrylamide), which was then examined for its chiral recognition with random methylated β -cyclodextrin (RAMEB-CD) (Figure 61).¹⁶⁰ It is well-known that poly-(*N*-isopropylacrylamide) [poly(NIPAAm)] is a typical thermoresponsive polymer exhibiting lower critical solution temperature (LCST) behavior in aqueous media at around 32 °C. Accordingly, selectivity could be confirmed by UV spectroscopy as well as by the DLS (dynamic light scattering) technique and turbidity method. The polymer with D enantiomer was found to interact more conclusively with the RAMEB-CD by UV spectroscopy. Correspondingly, the LCST increased by a few degrees after RAMEB-CD addition compared to the L enantiomer.

D'Anna and co-workers reported six binary complexes between three fluorophores (pyrene, xanthone and anthraquinone) and β -cyclodextrin (β -CD) or heptakis-(6-amino)-(6-deoxy)- β -cyclodextrin (am- β -CD) as chiral selectors for three α -amino acids, including phenylalanine (Phe), methionine (Met), and histidine (His; Figure 62).¹⁶¹ The effect of α -amino acids on the stability and stoichiometric ratio of the binary complexes has also been studied at two pH values (8.0 and 9.0). They also demonstrated that the binary complexes were in most cases stabilized by adding the ternary agent. The conditional constant (b_{2T}) values for ternary complexes (fluorophore-CD-amino

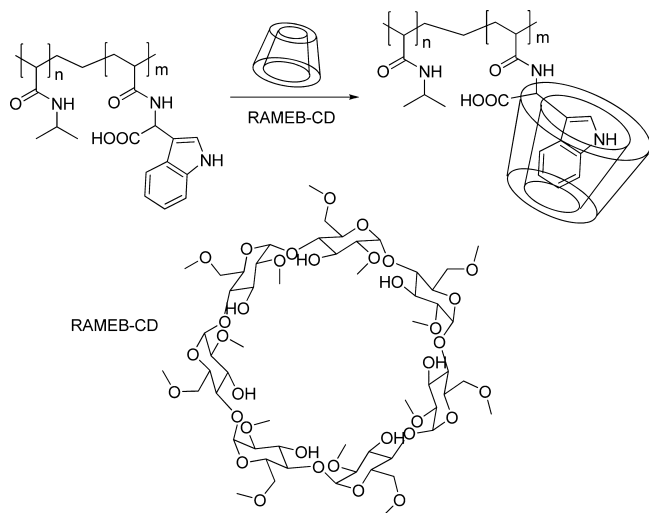


Figure 61. Proposed scheme for the inclusion of poly(NIPAAm)-Trp with RAMEB-CD.

acid), determined by means of fluorescence spectroscopy, showed that the binary complexes are suitable receptors for chiral recognition. The highest L enantioselectivity was 7.4, for Phe with Py/am- β -CD, while the highest L enantioselectivity was 5.6, for Met with Aq/ β -CD. The pyrene (Py)/am- β -CD complex has been emphasized as the chiral selector for Phe, Met and His. In particular, N- and O-protected α -amino acids were also examined. Generally, the trend of Phe > Met > His was observed.

A series of chiral N-dansyl-amino acid-modified β -cyclodextrins (β -CDs) were prepared as fluorescent chemosensors for chiral discrimination, in which an amino acid as a spacer improved binding affinities and chiral discrimination abilities of the chemosensors (Figure 63).¹⁶² D and L isomers of borneol, camphor, camphorquinone, and fenchone were utilized as analytes for chiral recognition. For example, L-N-dansyl-Phe-modified β -CD displayed high D selectivity for norbornane derivatives; on the other hand, D-N-dansyl-Phe-modified β -CD showed high L selectivity for menthol. Based on the microcalorimetric titration results, authors suggested that β -CD derivatives selectively accommodate the enantiomer which induced the least unfavorable entropy change when an inclusion complex was formed.

Corradini's group reported fluorescent monofunctionalized β -cyclodextrins 153–157 bearing a Cu²⁺ binding side arm and a dansyl group as enantioselective sensors for unmodified α -amino

acids.¹⁶³ In particular, authors found significant insights into the role of the cavity in the recognition process (Figure 64). Addition of D or L amino acids to the solution of 155 and 156 (0.1 M borate buffer, pH 7.3) induced enhancements of fluorescence emissions. Host 155 showed high enantioselectivity only with Pro; Val and Ser induced significant differences at low amino acid excess, while Leu (leucine) induced a significant difference only at 10:1 excess. When cyclodextrin 156 was used instead, good enantioselectivities for Pro, Val, Leu, Ser, Phe, and PhGly at all ratios were observed, while Lys and Tyr enantiomers were discriminated only at low molar excess values. Overall, cyclodextrin 156 was more enantioselective than 155, suggesting that the self-inclusion in the cyclodextrin cavity strongly increased the chiral discrimination ability of the Cu²⁺ complex.

Corradini's group also extended their work using β -CD derivatives containing L-Phe (S-158), L-PhGly (S-159), and L-Pro (S-160) moieties, as shown in Figure 65.¹⁶⁴ These hosts were used as enantioselective fluorescence chemosensors for the discrimination of enantiomers of the amino acids such as, Val and Pro, via a ligand exchange mechanism. In this paper, authors demonstrated a fast and effective detection method with high ee using fluorescence quenching by the copper(II)/amino acid complexes in a fluorescence microplate reader. Calibration of the fluorescence response as a function of enantiomeric composition could be obtained using the Stern–Volmer model with good linearity and fast evaluation of ee within 6% error.

5. METAL COMPLEX-BASED CHIRAL PROBES

Due to the large variety of metal–ligand affinity and complexation geometries, the interaction of analytes with metal complexes has been utilized for chiral recognition. In recent years, several metal ions, such as Cu²⁺, Zn²⁺, Ni²⁺, Cd²⁺, Pt²⁺, etc., have been employed in the design of the metal complex-based enantioselective sensing systems with various recognition and sensing strategies. In particular, the displacement of bound indicators has been intensively adopted since the binding to the ligands is commonly reversible. The Anslyn group has reported pioneering findings in this field.

Anslyn et al. reported indicator-displacement assays (IDAs) based on competitive dynamic metal coordination as shown in Figure 66.¹⁶⁵ Pyrocatechol violet (PV) was used as an indicator, which can effectively compete with the amino acid guest for open coordination sites on (S,S)-161-Cu²⁺. (S,S)-161-Cu²⁺ forms a 1:1 complex with PV resulting in a color change from pale yellow to intense blue and a UV absorption shift from 445 to 645 nm. The addition of an amino acid to the (S,S)-161-Cu²⁺/PV

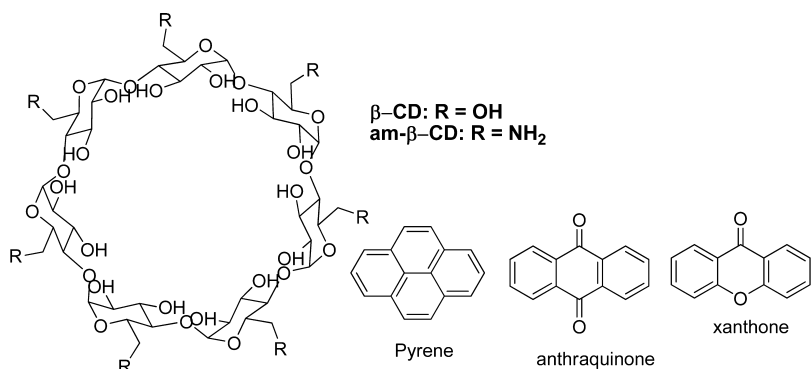


Figure 62. Constitutional components of the binary complexes between β -cyclodextrin or heptakis-(6-amino)-(6-deoxy)- β -cyclodextrin and three fluorophores.

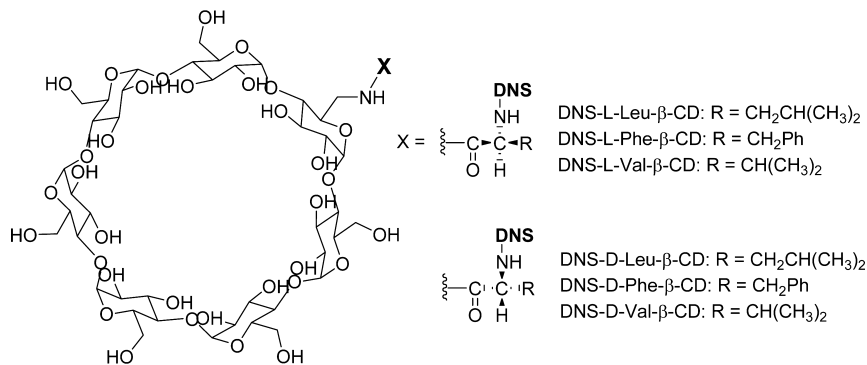


Figure 63. Constitutional components of chiral *N*-dansyl-amino acid-modified β -cyclodextrins.

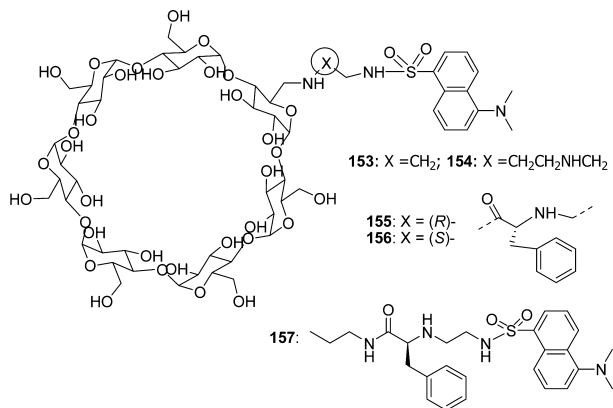


Figure 64. Structures of cyclodextrins 153–157 and structural elements considered in the design of enantioselective cyclodextrins.

complex can displace PV and can induce recovery of the spectral change. A consistent preference for D-amino acids was observed by about a factor of 2–2.5. Relationships between *ee* and absorbance were obtained in 1:1 MeOH/H₂O (50 mM HEPES buffer pH 7.0). The resultant *ee* versus *A* relationships were linear ($R^2 > 0.99$). This method allows for the measurement of free amino acid *ee*'s in protic media by visible spectroscopy.

Subsequently, Anslyn et al. extended the scope of the prior study by using an enantioselective eIDA (Figure 67).¹⁶⁶ One of the two chiral receptors ($[\text{Cu}^{2+}(162)]^{2+}$ or $[\text{Cu}^{2+}(162)]^{2+}$) and chrome azurol S (CAS), as the indicator, were used to

enantioselectively discriminate 13 α -amino acids in aqueous medium (MeOH:H₂O, 1:1, HEPES pH 7.5). Coordination of the indicator to the Cu metal center produced a blue solution with an absorbance band at 602 nm, while the free indicator produced a yellow solution with an absorbance band at 429 nm. $[\text{Cu}^{2+}((R,R)-162)]^{2+}$ was generally found to bind more strongly to L- α -amino acids, however in the case of aspartate, asparagine, and His, the D enantiomer was preferred by receptor $[\text{Cu}^{2+}((R,R)-163)]^{2+}$. Enantiomeric excess (ee) was determined for true test samples using ee calibration curves to demonstrate the capabilities of eIDAs. Analysis using receptor $[\text{Cu}^{2+}((R,R)-162)]^{2+}$ afforded an overall average error of 10.2%, whereas receptor $[\text{Cu}^{2+}((R,R)-163)]^{2+}$ showed an overall average error of 13.6%. The proposed method allowed for a potential HTS method for determining ee.

He and co-workers synthesized chiral fluorescent receptor 164, which showed a good selective binding ability to Cu²⁺ (Tris-HCl buffer, pH 7.4, MeOH/H₂O = 1:1) (Figure 68).¹⁶⁷ Then, the 164-Cu²⁺ complex was then prepared, which displayed an excellent enantioselective recognition ability for D,L-mandelate anions in aqueous solution. The binding constant for L-mandelate was calculated as 576 M⁻¹, whereas that of D-mandelate was only 38 M⁻¹. The resulting K_L/K_D value of 15.2 was reported with the 1:1 stoichiometry complex. The different fluorescence enhancements of complex 164-Cu²⁺ with the enantiomers of mandelate showed that the 164-Cu²⁺ complex can be used as an enantioselective fluorescent chemosensor for chiral mandelate anions in physiological pH conditions.

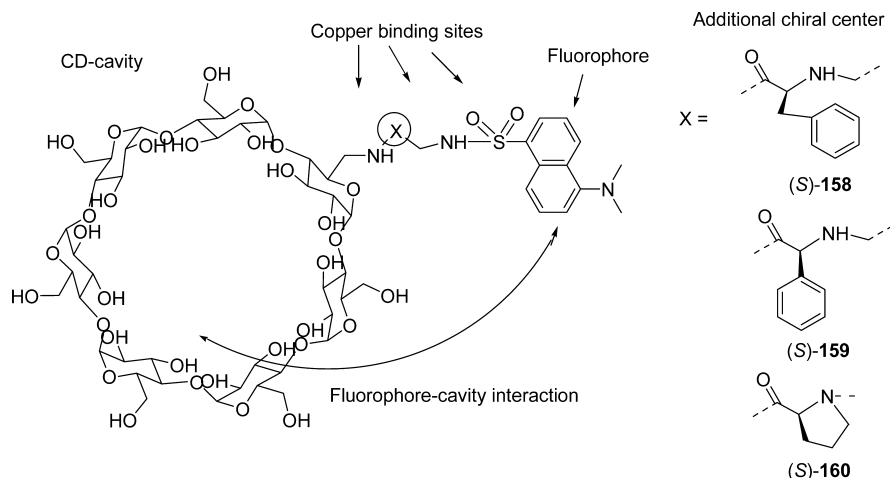


Figure 65. General scheme of enantioselective fluorescent cyclodextrins.

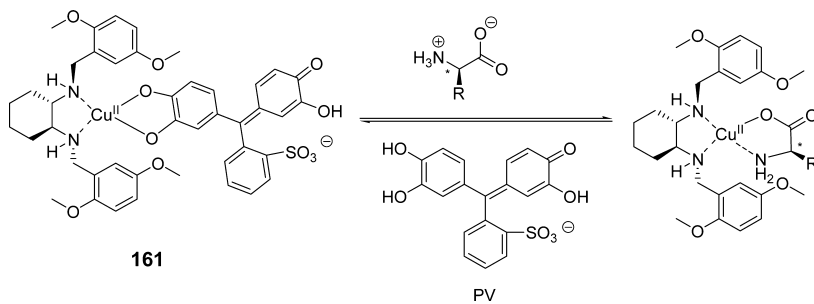


Figure 66. The proposed binding mode of host **161**, indicated (PV) with amino acids.

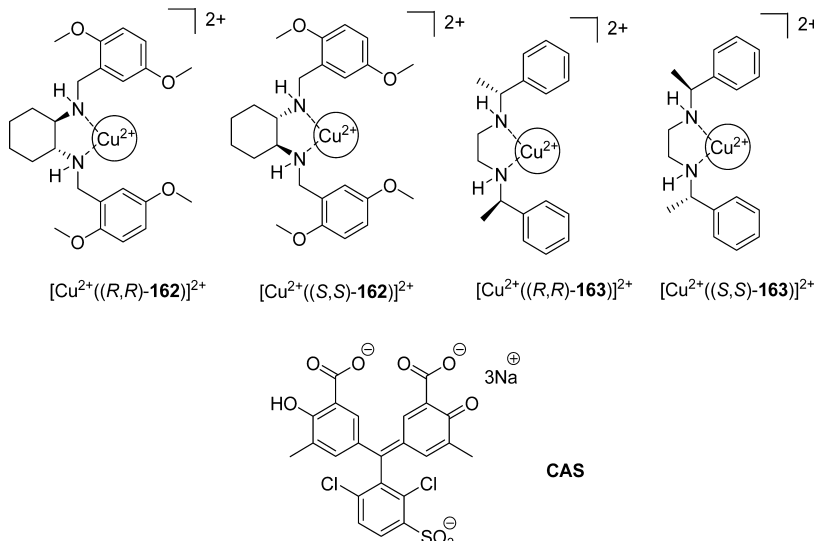


Figure 67. Structures of complexes and indicators (CAS).

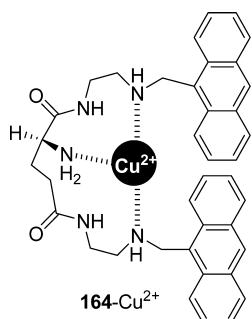


Figure 68. Structure of **164-Cu²⁺**.

Recently, the Pu group reported the preparation of a new chiral molecular gel from the sonication of a BINOL-terpyridine (*R*)-**165**-based Cu²⁺ complex (*R*)-**166** (Figure 69).¹⁶⁸ Study of

the interaction of the gel with chiral amino alcohols led to the discovery of unprecedented enantioselective gel collapsing. More specifically, a solution of (*R*)-phenylglycinol in CHCl₃ was added to a gel of (*R*)-**166** in CHCl₃, which was formed by sonication for 1 min. When the mixture was sonicated for 2 min, the gel remained stable. On the other hand, the addition of (*S*)-phenylglycinol collapsed the gel (*R*)-**166** under the same conditions. Compound (*S*)-**166**, the enantiomer of (*R*)-**166**, was also prepared for comparison, and the opposite enantioselective gel collapsing behavior was observed. The chiral complex (*S*)-**166** also showed significant enantioselective fluorescent enhancement in the presence of a variety of amino alcohols in solution. For example, (*S*)-phenylglycinol induced larger fluorescence enhancement compared to (*R*)-phenylglycinol.

Kwong et al. described a fluorescence macrocyclic receptor based on the Zn²⁺ complex of a C₂-terpyridine and a crown ether for the recognition of zwitterionic amino acids in a water/DMF (1:3, *v/v*) solution buffered with 10 mM of HEPES (pH 7.4; Figure 70).¹⁶⁹ Among the various amino acids, L-aspartate (*K* = 4.5×10^4 M⁻¹, ΔG_0 = 26.5 kJ mol⁻¹) and L-cysteine (*K* = 2.5×10^4 M⁻¹, ΔG_0 = 25.1 kJ mol⁻¹) showed the highest affinity toward receptor **167**. On the other hand, receptor **168** also exhibited 1:1 binding toward L-aspartate with *K* = 5×10^2 M⁻¹, which is ~90 times smaller than the *K* value of receptor **167**. This indicated that the Zn²⁺-tpy and the crown ether both play key roles in binding with carboxylate group and ammonium group of zwitterionic L-amino acids, respectively. Receptor **168** showed

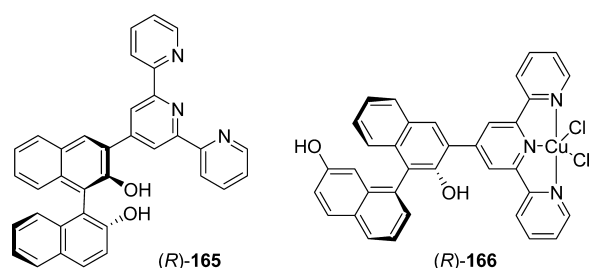


Figure 69. Structures of (*R*)-**165** and its Cu²⁺ complex (*R*)-**166**.

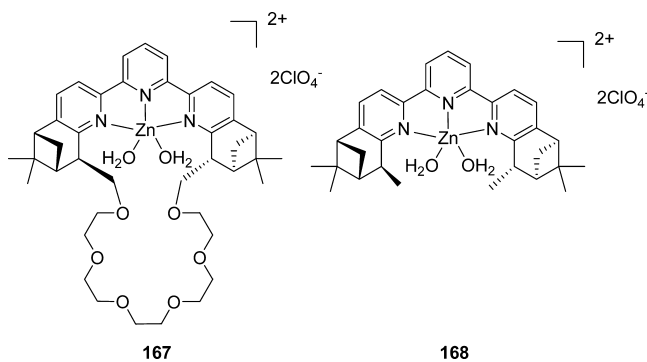


Figure 70. Structures of compounds 167 and 168.

enantioselectivity toward the D-amino acids with K_D/K_L value of 3.0.

More recently, Ihara et al. reported enantioselective recognition of amino acids by using a highly ordered chiral assembly of achiral porphyrin 169 on a chiral molecular gel (Figure 71).¹⁷⁰ The enantioselectivity for various amino acid

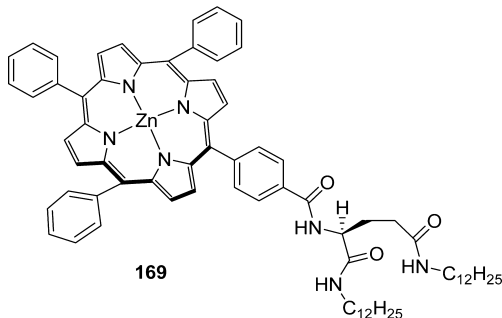


Figure 71. Structure of L-glutamide-functionalized zinc porphyrin 169.

methyl ester racemates, such as Ala-OMe, Leu-OMe, Phe-OMe, Lys-OMe, and His-OMe, was determined by monitoring the changes in the CD spectra and by fluorescence quenching. The best ee was observed for the His-OMe by monitoring the CD patterns and fluorescence quenching. The Stern–Volmer constants were calculated as $K_{SV}(L) = 26.3 \times 10^3 \text{ M}^{-1}$ and $K_{SV}(D) = 7.03 \times 10^3 \text{ M}^{-1}$.

Recently, the Feng group reported a new chiral sensor based on an *N,N'*-dioxide nickel(II) complex 170-Ni²⁺ that visually recognized a series of chiral (R)-hydroxycarboxylic acid enantiomers by coordination and self-assembly into nanospheres or nanofibers (Figure 72).¹⁷¹ With the help of various techniques, the morphologic structures of the colloid or suspension were also reported. In addition, this metal complex

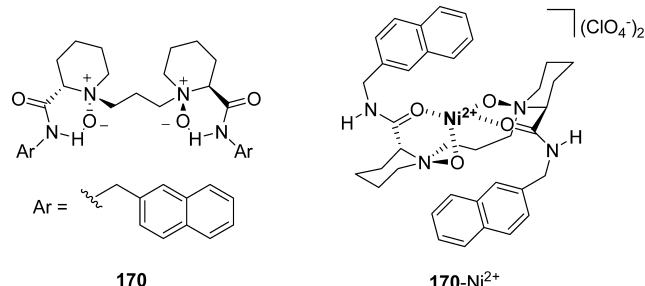


Figure 72. Structures of compound 170 and the 170-Ni²⁺ complex.

170-Ni²⁺ could recognize N-Boc-amino acids and chiral (R)-hydroxycarboxylic acids via highly enantioselective fluorescence changes. In particular, a highly enantioselective fluorescent response to MA was shown, the (S) enantiomer greatly enhanced the fluorescence intensity of 170-Ni²⁺, but the (R) isomer showed relatively little change in ACN, resulting in the enantiomeric fluorescence difference ratio of 10.3. Furthermore, they extended their work to HTS.¹⁷² In view of the highly enantioselective fluorescent recognition of chiral amines and amino alcohols, complex 170-Ni²⁺ was used to determine the concentration and ee value. Using a 96-well plate, HTS for enantiomer discrimination was realized.

Very recently, Lin et al. reported a highly porous and fluorescent metal–organic framework (MOF) 171, a cadmium carboxylate infinite chain secondary building unit, which was prepared from a chiral tetracarboxylate bridging ligand derived from BINOL 171 (Figure 73).¹⁷³ The fluorescence of 172 was quenched by four chiral amino alcohols, as shown in Figure 73, with Stern–Volmer constants of 4.9×10^2 to $3.12 \times 10^4 \text{ M}^{-1}$ and enantioselectivity ratios of 1.17–3.12. The highest enantiomeric quenching ratio [$K_{SV}(S)/K_{SV}(R)$] of 3.12 was observed for 2-amino-3-methyl-1-butanol. The fluorescence quenching of 172 was attributed to the H-bonding between amino alcohols and the binaphthol moieties decorating the MOF. A preconcentration effect inside the MOF channels induced higher detection sensitivity of 172, whereas the higher enantioselectivity of 172 was attributed to the enhanced chiral discrimination due to the cavity confinement effect and the conformational rigidity of the BINOL moieties in the framework.

Tsukube et al. synthesized a Na⁺ complex with cholesterol-armed cyclen 173, as shown in Figure 74.¹⁷⁴ Based on the light scattering, fluorescence, and TEM characterizations, a particularly stable self-aggregate in aqueous solution was reported, which was examined for sensing and detection of amino acid anions. In this work, various dansylamino acid derivatives (dansyl = 5-(dimethylamino)-1-naphthalenesulfonyl) were examined, which were nicely accommodated in the helicate aggregates to provide highly enhanced fluorescence signals and could be detected by the naked eye at 10^{-7} M level. The highest L/D selectivity was recorded as 2.2 in the case of the leucine derivative, while the highest D/L selectivity was reported as 2.0 with the Phg anion. As described above, dansylamino acid anions were stabilized by cyclen 173-Na⁺ complex via electrostatic attraction and hydrophobic interaction.

Parker et al. reported that the Δ-Eu, Gd, and Tb complexes of ligand 174 and 175 could bind selectively and reversibly to “drug-site II” in serum albumin (Figure 75).¹⁷⁵ During this process, their helicity was reversed to maximize binding. The binding process of the Δ-enantiomer to a binding site on serum albumin could be observed by inversion of the lanthanide circularly polarized luminescence. This example is described as the first report of chiral inversion following noncovalent protein association of a probe and these lanthanide complexes were reported as unique chiroptical probes for albumin, which showed potential application to image protein association in vitro or in vivo.

Recently, a simple colorimetric strategy for enantioselective detection of chiral secondary alcohols, which utilizes chiral ferrocene derivatives 176 and 177 as probes, has been devised by James et al. (Figure 76).¹⁷⁶ The recognition mechanism for this system involves hydrogen bond interactions between the imidazole nitrogens in 176 and 177 and the OH groups of alcohols, which are reflected in UV–vis spectral changes. For

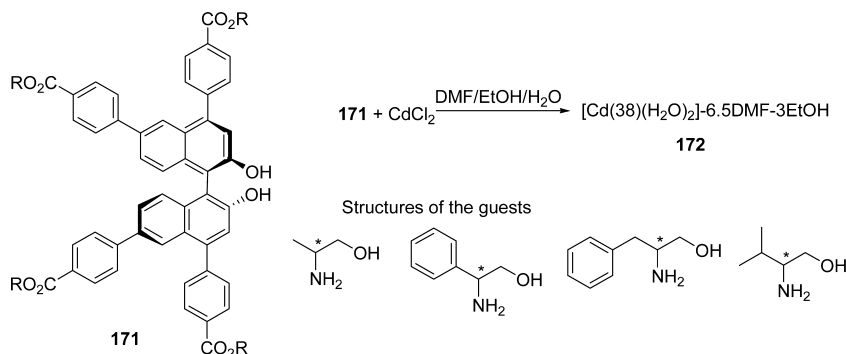


Figure 73. Structures of the chiral BINOL derivative of **171** and amino alcohol quenchers and the synthesis of **172**.

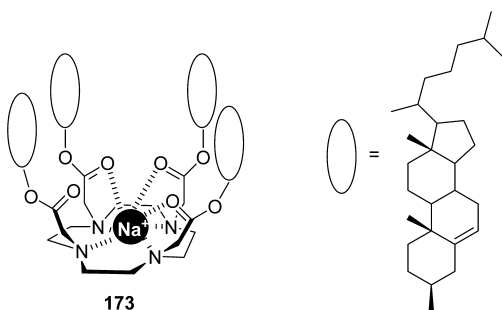


Figure 74. Structure of cholesterol-armed cyclen **173**-Na⁺ complex.

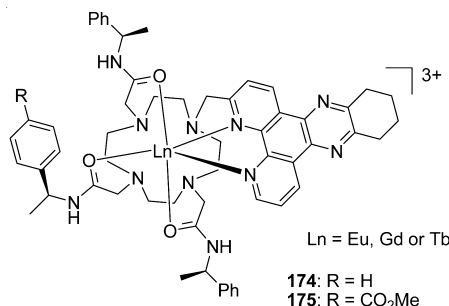


Figure 75. Structures of Δ -Eu, Gd, and Tb complexes of ligands **174** and **175**.

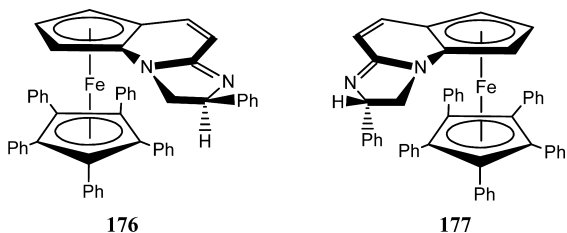


Figure 76. Structures of chiral ferrocene derivatives **176** and **177**.

instance, the visible absorption peak of **176** is red-shifted from 516 to 576 nm upon binding to the enantiomers of dimethyl tartrate (DT) in MeCN. Importantly, binding of **176** to the D-DT enantiomer induces a larger wavelength shift than does binding to the L-DT antipode. Similar results arose from studies with sensor **177**. In contrast, although eliciting a wavelength change, binding of the enantiomers of free tartaric acid (TA) to these probes does not display enantioselectivity. The results of an ¹H NMR study show that the observed colorimetric responses arising from interaction of **176** with D-DT and D-TA are caused by similar hydrogen bonding modes and that the lack of

selectivity of wavelength shifts observed for the enantiomers of TA results from an increased distances between the chiral centers in probe **176** and TA in the hydrogen bonded complex.

6. POLYMER-BASED CHIRAL PROBES

Functional polymers have been widely employed in a variety of fields including the electronics, electrical materials, aerospace and automobile industries as well as the life sciences. The use of functional polymers in the analyte-recognition area has taken advantage of several important optical sensing properties that these materials have that are not shared by small molecules, including ease of preparation, ready amplification of the recognition signal, enhancement of recognition efficiencies and selectivities, and simple implementation in fabrication in devices. In recent years, numerous polymer-based chemosensors have been developed for optical sensing of metal ions, anions, oxygen, H₂O₂, and temperature.¹⁷⁷ However, very few examples exist of the use of polymer systems for fluorescence or colorimetric based enantioselective sensing.

One recent example of the use of a polymer sensor was described by Cheng and co-workers, whose efforts focused on the two (*R,R*)-salen/salan-based chiral polymers **178** and **179** (Figure 77). (*R,R*)-Salen-based polymer **178** was prepared by copolymerization of (*R,R*)-1,2-diaminocyclohexane with 2,5-dibutoxy-1,4-di(5-tert-butylsalicylaldehyde)-phenylene. Reduction of **178** with NaBH₄ then formed (*R,R*)-salan-based polymer **179**. Both **178** and **179** were found to exhibit good selectivities for distinction between the two enantiomers of phenylglycinol via different degrees of fluorescence intensity enhancement. For instance, exposure of sensors **178** and **179** to (S)-phenylglycinol leads to a large increase in the fluorescence efficiency, whereas lesser changes in emission intensities take place when (R)-phenylglycinol is mixed with these probes. Quantitation of the enhancements leads to enantioselectivity ratios of 1.84 and 2.05 for sensor **178** and **179**, respectively.

Cheng, et al. have recently described two other similar salen/salan-based fluorescent chiral polymers **180** and **181**, containing ethyne groups in their backbones. (*R,R*)-Salen-based sensor **180** was observed to display good enantioselectivity in its fluorescence enhancement response to chiral α -hydroxyl carboxylic acids.¹⁷⁹ For example, addition of L-malic acid (L-MA) causes a significant increase in the fluorescence intensity of **180**, whereas only a small increase in the emission intensity of the probe occurs when D-MA is added. High fluorescence intensity ratios of 8.41 and 6.55 were found to be associated with the enantioselective responses of **180** to the antipodes of MA and lactic acid (LA), differences that can be detected using the naked eye under UV lamp irradiation. Interestingly, (*R,R*)-selen-based

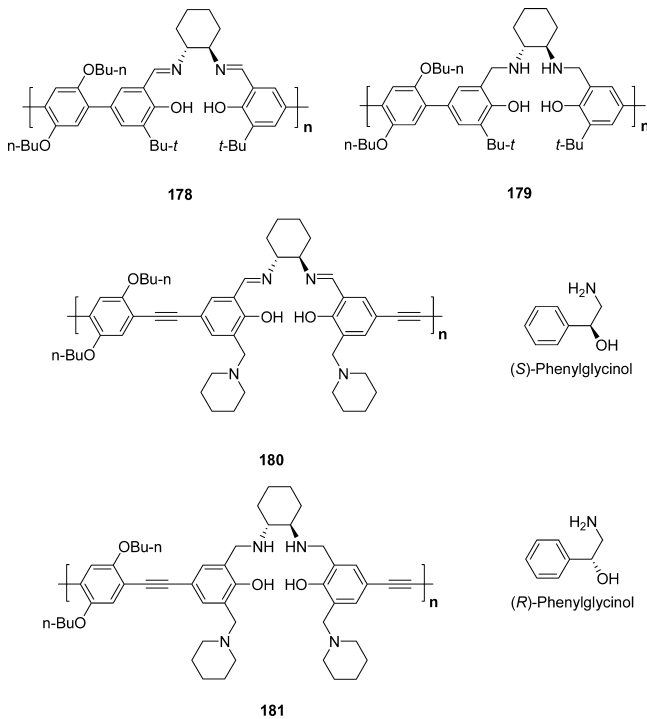


Figure 77. Structures of polymer sensors 178–181 and the two enantiomers of phenylglycinol.

sensor 180 displays a significant fluorescence quenching response to α -amino acids. This opposite response results from a different arrangement of the intramolecular hydrogen bonding array between an amine vs a hydroxyl group in the analytes and the phenol group in the polymers.

In additional studies, Cheng and co-workers synthesized two novel chiral polymers 182 and 183, which contain (S)-2,2'-binaphthol and (S)-2,2'-binaphthylidiamine moieties in the main polymer chains (Figure 78).¹⁸⁰ Sensor 182 displays enantioselective fluorescence enhancement behavior with an intensity ratio of 6.85 toward the enantiomers of phenylalaninol (PA), in which the PA-induced increase in fluorescence intensity is linearly correlated with the molar concentration ratios of the D and L

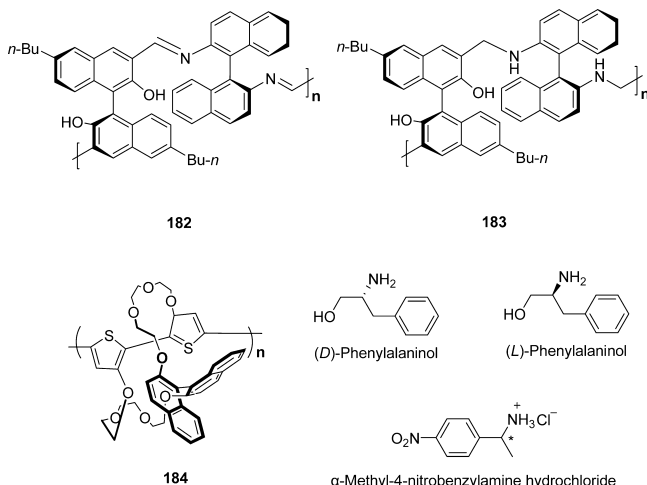


Figure 78. Structures of polymer sensors 182–184 and the two enantiomers of PA and the structure of α -methyl-4-nitrobenzylamine hydrochloride (MNBA).

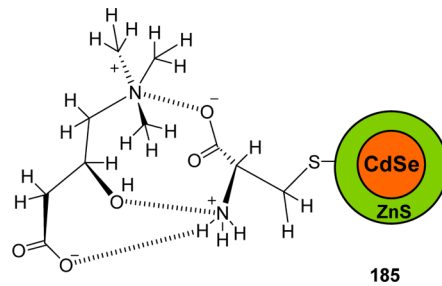


Figure 79. Proposed interaction mode between D-carnitine and L-Cys-capped QDs.

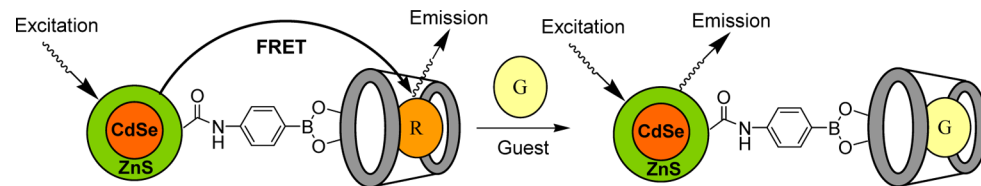
enantiomers. However, no obvious enantioselective response was observed by using polymer 183 as a chiral probe for PA.

More recently, Fukuhara and Inoue prepared the novel binaphthocrown ether-polythiophene conjugate 184 and demonstrated that it serves as a chromophoric/fluorescence sensor for enantioselective recognition of α -methyl-4-nitrobenzylamine hydrochloride (MNBA).¹⁸¹ Treatment of sensor 184 with (R)- and (S)-MNBA results in UV-vis spectral changes with different magnitudes that correspond to an enantioselectivity of 2.16. In addition, sensor 184 is capable of discriminating between (R)- and (S)-MNBA via an enantioselective fluorescence quenching response with a Stern-Volmer quenching constant ratio of 2.23.

7. NANOMATERIAL-BASED CHIRAL PROBES

The unique performances of functional nanomaterials on a nanoscale of 1 to 100 nm are encouraging researchers to make use of them in various areas ranging from our daily life to aerospace technology. In the chemical or biological sensing fields, either as the signal producers and transducers or controllers, nanomaterials have become the ideal building blocks for the construction of chemosensing systems due to their advanced optical, thermal, electrical, magnetic, and catalytic properties, which are caused by quantum effects and nanoscale structures. Over the past few decades, a large number of nanomaterial-based chemosensors have been used in the applications of biological and environmental monitoring, however the reports of chiral sensing systems based on nanomaterials, especially those with colorimetric or fluorimetric analyses, are few in number.^{182–186} A few nanomaterials including semiconductor nanocrystals, noble metal nanoparticles, polymeric nanoparticles, and 2D nanoscale grapheme have been developed in recent years for the design of fluorescent and colorimetric chiroselective sensing systems with the installation of the chirogenic components.

Semiconductor nanocrystals (NCs), i.e., quantum dots (QDs), are well-known, intriguing inorganic fluorophores due to their unique properties such as broad absorption and excitation spectra, narrow and size-tunable emission spectra, high photo bleaching threshold, and excellent chemical stability. Recently, a chiral sensing system 185 based on CdSe/ZnS nanocrystals capped at the surface with either of the two enantiomers of cysteine (Cys) have been fabricated for the enantioselective recognition of carnitine (Figure 79).¹⁸⁷ Selective interaction of L-Cys-capped QDs with D-carnitine via electrostatic interactions in conjunction with hydrogen bonding has been observed along with a significant fluorescence quenching, whereas L-Cys-capped QDs cannot decrease the fluorescence intensity of D-Cys-capped QDs, and vice versa. Based on these results, sensing system 185 can be used to determine the enantiomeric



186

Figure 80. FRET-based chiral sensing system based on β -CD-functionalized CdSe/ZnS nanocrystals.

composition of mixed enantiomeric carnitine samples with the errors less than 2.7%.

Another example involving a FRET-based displacement chiral sensing system **186** has been presented by jointing a β -cyclodextrin (β -CD) with Rhodamine B accommodated in its chiral cavity to phenylboronic acid-modified CdSe/ZnS QDs via a boronate linker (Figure 80).¹⁸⁸ In this FRET sensing system, Rhodamine B acts as the energy acceptor storing the excitation energy that is transferred by a radiationless process from CdSe/ZnS QDs. When replacing Rhodamine B from the inside of the β -CD cavity by a guest, the FRET effect can be eliminated, accompanied with the recovery of the donor fluorescence of CdSe/ZnS QDs and a decrease in the fluorescence intensity of Rhodamine B. It was found that this displacement chiral system can be used for the enantioselective differentiation between L-Phe and D-Phe with the enantioselectivity, as represented by the ratio of the association constants, of $K_L/K_D = 8.71$. The similar enantioselectivity toward the two enantiomers of tyrosine has been also obtained, with $K_L/K_D = 22$.

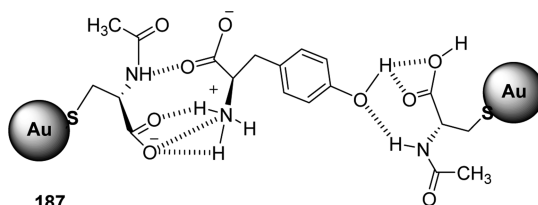
Noble metal nanocrystals, typically silver nanoparticles (AgNPs) and gold nanoparticles (AuNPs), are ideal inorganic chromophores for the design of the colorimetric sensing system due to their extremely high coefficients and the tunable surface plasmonic resonance properties. Accordingly, a chiral sensing system based on AgNPs with a nucleotide (ATP, GTP, CTP, and TTP) as the capping stabilizer has been prepared, and the enantioselective recognition and separation of the two enantiomers of Cys in aqueous solution has been achieved for the first time by using this sensing system as the colorimetric sensors.¹⁸⁹ The UTP-capped AgNPs have been found to be the most efficient chiroselective agents for Cys over the other nucleotide-capped nanoparticles. The exposure of UTP-capped AgNPs to D-Cys results in a significant aggregation of the nanoparticles accompanied by the color changes from yellow to red, but almost no changes occur to L-Cys. Furthermore, the enantioseparation can be realized by the centrifugation of a L,D-Cys aqueous solution in the presence of UTP-capped AgNPs. With the similar sensing strategy, a chiral system **187** (Figure 81) based on L-N-acetyl-cysteine (NALC) stabilized AuNPs has been used more recently for the chiroselective determination and enrichment of L-tyrosine (Tyr) with the colorimetric and

aggregation responses.¹⁹⁰ L-Tyr has been shown to selectively interact with NALC-AuNPs, resulting in the visual aggregation of AuNPs along with the UV-vis absorption spectral ratiometric changes, which can be observed via a significant red-to-purple color change. However, D-Tyr hardly induces any changes. Thus, L-Tyr can be isolated with D-Tyr from an aqueous solution of racemic Tyr via centrifugation.

Application of fluorescent polymer nanomaterials in biological and environmental sensing has attracted substantial attention because of their biocompatibility, low toxicity, environmental safety, and functional diversity. However, only one example has been presented to date relating to the use of fluorescent polymer nanocomposites for the chiral recognition study. The fabricated sensing system **188** (Figure 82) was created by functionalizing the polyacrylonitrile (PAN) nanoparticles with boronic acid (B) for the enantioselective detection of monosaccharides.¹⁹¹ Jang and co-workers found that the fluorescence of the B-PAN nanoparticles can be enantioselectively changed by binding the two enantiomers of a monosaccharide with their boronic acid moieties covalently aided with hydrogen bonding. For instance, D-galactose can induce the increase in the fluorescence intensity of the B-PAN nanoparticles, but L-galactose cannot do so. The d-PET effect was thought as the fluorescence transduction inducement.

8. CONCLUSIONS AND FUTURE PERSPECTIVES

The use of fluorescence and colorimetric chemosensors to detect chiral molecules has been a central focus of recent efforts in the field of sensor technologies, owing to the fact that enantiomerically pure compounds and drugs have unparalleled importance in bioscience, clinical medicine, and bionics areas. In the past decade, different building blocks and binding partners have been devised for the construction of structural frameworks of sensors that are required for optical signaling of chiral recognition. For this purpose, numerous fluorescence probes of different types that sense chiral guests have been devised and the recognition mechanisms of these systems have been subjected to detailed study. Among them, the small organic molecule-based chiral chemosensors are most widely studied in this topic. However, the most involved chiral recognition mechanism with these sensors is based on hydrogen bond interaction that is employed successfully in organic solvents but not in water. This confines these sensors to be used for the water-soluble chiral analyte detections and the chiral recognition applications in physiological environment. Therefore, the development of the chiral sensors that can be used efficiently in aqueous solutions, such as boronic acid-based sensors or electrostatic sensing systems, should be the focused task in this area. Other types of chiral sensors have been also developed to remedy some shortages of small organic molecule-based sensors from different aspects and improve on the sensing performances. For example, the polymer-based sensors have the capacities to amplify the chiral



187

Figure 81. Proposed interaction mode between L-Tyr and NALC-AuNPs.

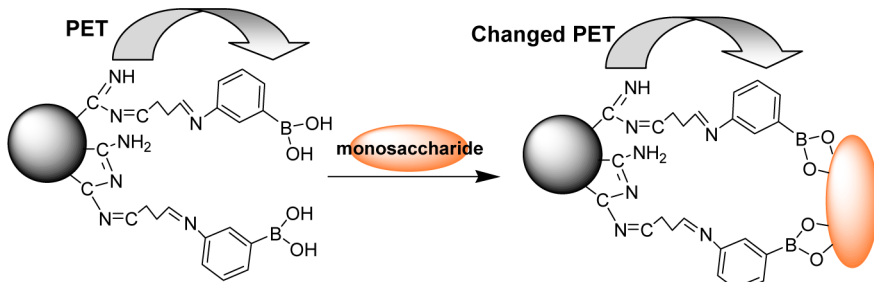


Figure 82. Fluorescent B-PAN nanoparticles based sensing system 188 for enantioselective interaction with monosaccharide sensing.

recognition signal further enhancing the sensitivity and the enantioselectivity. Those macrocyclic scaffolds can utilize their rigid structures to improve the enantioselectivity in the chiral recognition process. The nanomaterial-based sensing systems possess much excellent photophysical properties and higher stability. However, some of them own more or less drawbacks in practical applications. For instance, some of the metal complex-based sensors and semiconductor or noble metal nanocrystal-based sensors usually contain toxic metal ions, such as Cu^{2+} , Cd^{2+} , Au^{3+} , etc. which block their biological detection applications. The wrap of these toxic sensors by SiO_2 or polymeric nanocapsules may be the most common and important method to solve this problem. In addition, the low-toxic carbon nanomaterials should be the research focus on the development of new chiral fluorescent sensing systems in future.

It is well-known that the central issue associated with chiral molecule recognition is selectivity, gained from differential interactions that take place between probes and each of the enantiomers of chiral guests. For this purpose, a detailed understanding must be gained of how guest binding to the hosts occurs. As a consequence, theoretical calculations have become more commonly applied in developing structural models that can be used to guide the design of new fluorescent probes. Another goal of investigations in this area is the development of near-infrared absorbing and emitting chiral probes that can be applied to real time, *in vivo* detection of chiral guests deep inside tissues. Although this type of sensor may be difficult to construct owing to serious technical problems, their availability would represent a significant contribution to clinical medicine and disease diagnosis involving chiral biomolecules.

AUTHOR INFORMATION

Corresponding Author

*Phone: 82-2-3277-2400. Fax: 82-2-3277-2384. E-mail: jyoon@ewha.ac.kr.

Notes

The authors declare no competing financial interest.

Biographies



Xin Zhang was born in P. R. China in 1981. He received his Ph.D. in Applied Chemistry from Dalian University of Technology (China) in 2011. In 2012 he joined Professor Yoon's group at Ewha Womans University (Korea) as a postdoctoral fellow. His current research interests focus on molecular assemblies, fluorescent sensors design for the recognition and analysis of molecules of biological importance, and organic reagent for the bioimaging.



Jun Yin was born in Hubei province, P. R. China, in 1981. He received his Bachelor Degree in 2002 and Ph.D. degree in 2007 from CCNU. He began his postdoctoral research with Professor Jishan Wu and Chunyan Chi at National University of Singapore before he joined the College of Chemistry, CCNU in 2010. In 2012, as a research professor he began his research with Professor Juyoung Yoon at Ewha Womans University. He is now an associate professor at CCNU. His research interests focus on supramolecular self-assembly, fluorescent sensors, and organic conjugated molecular functional materials.



Juyoung Yoon received his Ph.D. (1994) from The Ohio State University. After completing postdoctoral research at UCLA and at Scripps Research Institute, he joined the faculty at Silla University in 1998. In 2002, he moved to Ewha Womans University, where he is currently a Professor of Department of Chemistry and Nano Science and Department of Bioinspired Science. His research interests include investigations of fluorescent chemosensors, molecular recognition, and organo EL materials.

ACKNOWLEDGMENTS

We acknowledge the National Research Foundation of Korea (NRF) grant funded by the Korea government (MSIP; No. 2012R1A3A2048814). We deeply thank previous and present group members.

LIST OF ABBREVIATIONS

ACN	acetonitrile
[9]aneN ₃	1,4,7-triazacyclononane
AIE	aggregation-induced emission
AIEE	aggregation-induced emission enhancement
AgNPs	silver nanoparticles
Ala	alanine
ALS	aromatic-linker-steroidal
AuNPs	gold nanoparticles
BINOL	1,1'-bi-2-naphthol
Boc	tert-butyloxycarbonyl
BODIPY	boron dipyrromethene difluoride
BPG	N-benzyloxycarbonylphenylglycine
CAS	chrome azurol S
Cbz	carbobenzoyloxy
β-CD	β-cyclodextrin
CT	charge transfer
Cys	cysteine
DACH	1,2-diaminocyclohexane
Dansyl	S-(dimethylamino)-1-naphthalenesulfonyl
DCM	dichloromethane
2D	two-dimensional
DFT	density functional theory
DIPT	diisopropyltartrate
DME	dimethoxyethylene
DLS	dynamic light scattering
DT	dimethyl tartrates
ee	enantiomeric excess
eIDA	enantioselective indicator-displacement assay
ET	electron transfer
FRET	fluorescence resonance energy transfer
HELIXOL	2,15-dihydroxy-hexahelicene
His	histidine
HMA	hexahydromandelic acid
HTS	high-throughput screening
IDA	indicator-displacement assay
LA	lactic acid
LCST	lower critical solution temperature
Leu	leucine
Lys	lysine
MA	mandelic acid
MBA	α-methylbenzylamine
Met	methionine
ML	4-methylesculetin
MNBA	α-methyl-4-nitrobenzylamine hydrochloride
MOF	metal–organic framework
NALC	L-N-acetyl-cysteine
NEA	1-(1-naphthyl)ethylammonium perchlorate
NCs	semiconductor nanocrystals
NMR	nuclear magnetic resonance
PA	phenylalaninol
PB	2-phenylbutyrate
PET	photoinduced electron transfer
Phe	phenylalanine
Phg	phenylglycine
PKU	phenylketonuria
PL	phenyllactic acid
Pro	proline
PCT	photoinduced charge transfer
PV	pyrocatechol violet
QDs	quantum dots
RAMEB-CD	random methylated β-cyclodextrin
Ser	serine
TA	tartaric acid
TMSCN	trimethylsilyl cyanide
UV-vis	ultraviolet–visible
Val	valine

REFERENCES

- (1) Bentley, R. *Chem. Soc. Rev.* **2005**, *34*, 609.
- (2) Weiss-López, B. E.; Azocar, M.; Montecinos, R.; Cassels, B. K.; Araya-Maturana, R. *Langmuir* **2001**, *17*, 6910.
- (3) Beckett, A. H. *Biochem. Soc. Trans.* **1991**, *19*, 443.
- (4) Mohan, S. J.; Mohan, E. C.; Yamsani, M. R. *Int. J. Pharm. Sci. Nanotechnol.* **2009**, *1*, 309.
- (5) Li, B.; Haynie, D. T. *Encyclopedia of Chemistry Processing: Chiral Drug Separation*; Lee, S., Ed.; Taylor & Francis: New York, 2006; p 449.
- (6) Aboul-Enein, H. Y.; Stefan, R. *Crit. Rev. Anal. Chem.* **1998**, *28*, 259.
- (7) Wolf, C. *Chem. Soc. Rev.* **2005**, *34*, 595.
- (8) Ilisz, I.; Berkecz, R.; Peter, A. *J. Pharm. Biomed. Anal.* **2008**, *47*, 1.
- (9) Simo, C.; Barbas, C.; Cifuentes, A. *Electrophoresis* **2003**, *24*, 2431.
- (10) Prokhorova, A. F.; Shapovalova, E. N.; Shpigun, O. A. *J. Pharm. Biomed. Anal.* **2010**, *53*, 1170.
- (11) Schurig, V. *J. Chromatogr. A* **2002**, *965*, 315.
- (12) (a) Valeur, B. *Molecular Fluorescence: Principles and Applications*; Wiley-VCH Verlag GmbH: New York, 2001. (b) Lakowicz, J. R. *Principles of Fluorescence Spectroscopy*, 3rd ed.; Springer: New York, 2006.
- (13) Martínez-Máñez, R.; Sancanón, F. *Chem. Rev.* **2003**, *103*, 4419.
- (14) Duong, T. Q.; Kim, J. S. *Chem. Rev.* **2010**, *110*, 6280.
- (15) Ueno, T.; Nagano, T. *Nat. Methods* **2011**, *8*, 642.
- (16) Bicker, K.; Wiskur, S. L.; Lavigne, J. J. Colorimetric Sensor Design, In *Chemosensors: Principles, Strategies, and Applications*; Wang, B., Anslyn, E. V., Eds.; Wiley Series in Drug Discovery and Development; Wiley: New York, 2011.
- (17) Joyce, L. A.; Shabbir, S. H.; Anslyn, E. V. *Chem. Soc. Rev.* **2010**, *39*, 3621.
- (18) Pu, L. *Acc. Chem. Res.* **2012**, *45*, 150.

- (19) Accetta, A.; Corradini, R.; Marchelli, R. *Top. Curr. Chem.* **2011**, *300*, 175.
- (20) Dieng, P. S.; Sirlin, C. *Int. J. Mol. Sci.* **2010**, *11*, 3334.
- (21) Leung, D.; Kang, S. O.; Anslyn, E. V. *Chem. Soc. Rev.* **2012**, *41*, 448.
- (22) de Silva, A. P.; Gunaratne, H. Q. N.; Gunnlaugsson, T.; Huxley, A. J. M.; McCoy, C. P.; Rademacher, J. T.; Rice, T. E. *Chem. Rev.* **1997**, *97*, 1515.
- (23) Gunnlaugsson, T.; Glynn, M.; Tocci, G. M.; Kruger, P. E.; Pfeffer, F. M. *Coord. Chem. Rev.* **2006**, *250*, 3094.
- (24) Kikuchi, K. *Chem. Soc. Rev.* **2010**, *39*, 2048.
- (25) Wu, J.; Liu, W.; Ge, J.; Zhang, H.; Wang, P. *Chem. Soc. Rev.* **2011**, *40*, 3483.
- (26) Gonçalves, M. S. T. *Chem. Rev.* **2009**, *109*, 190.
- (27) Han, J.; Burgess, K. *Chem. Rev.* **2010**, *110*, 2709.
- (28) Vendrell, M.; Zhai, D.; Er, J. C.; Chang, Y. *Chem. Rev.* **2012**, *112*, 4391.
- (29) Xu, Z.; Yoon, J.; Spring, D. R. *Chem. Soc. Rev.* **2010**, *39*, 1996.
- (30) Chen, X.; Zhou, Y.; Peng, X.; Yoon, J. *Chem. Soc. Rev.* **2010**, *39*, 2120.
- (31) Zhou, Y.; Xu, Z.; Yoon, J. *Chem. Soc. Rev.* **2011**, *40*, 2222.
- (32) Zhou, Y.; Yoon, J. *Chem. Soc. Rev.* **2012**, *41*, 52.
- (33) Kim, H. N.; Ren, W. X.; Kim, J. S.; Yoon, J. *Chem. Soc. Rev.* **2012**, *41*, 3210.
- (34) Chen, X.; Pradhan, T.; Wang, F.; Kim, J. S.; Yoon, J. *Chem. Rev.* **2012**, *112*, 1910.
- (35) Zhan, X.; Wang, S.; Liu, Y.; Wu, X.; Zhu, D. *Chem. Mater.* **2003**, *15*, 1963.
- (36) He, Q.; Lin, H.; Weng, Y.; Zhang, B.; Wang, Z.; Lei, G.; Wang, L.; Qiu, Y.; Bai, F. *Adv. Funct. Mater.* **2006**, *16*, 1343.
- (37) Zhou, Y.; He, Q.; Yang, Y.; Zhong, H.; He, C.; Sang, G.; Liu, Wei.; Yang, C.; Bai, F.; Li, Y. *Adv. Funct. Mater.* **2008**, *18*, 3299.
- (38) Kawamoto, M.; Aoki, T.; Shiga, N.; Wada, T. *Chem. Mater.* **2009**, *21*, 564.
- (39) Kočovský, P.; Vyskocil, Š.; Smrcina, M. *Chem. Rev.* **2003**, *103*, 3213.
- (40) Chen, Y.; Yekta, S.; Yudin, A. K. *Chem. Rev.* **2003**, *103*, 3155.
- (41) Shibasaki, M.; Matsunaga, S. *Chem. Soc. Rev.* **2006**, *35*, 269.
- (42) Feng, L.; Liang, F.; Wang, Y.; Xua, M.; Wang, X. *Org. Biomol. Chem.* **2011**, *9*, 2938.
- (43) Wang, M.; Li, K.; Hou, J.; Wu, M.; Huang, Z.; Yu, X. *J. Org. Chem.* **2012**, *77*, 8350.
- (44) Avnir, D.; Wellner, E.; Ottolenghi, M. *J. Am. Chem. Soc.* **1989**, *111*, 2001.
- (45) Hu, Q.; Pugh, V. J.; Sabat, M.; Pu, L. *J. Org. Chem.* **1999**, *64*, 7528.
- (46) Pugh, V. J.; Hu, Q.; Pu, L. *Angew. Chem., Int. Ed.* **2000**, *39*, 3638.
- (47) Gong, L.; Hu, Q.; Pu, L. *J. Org. Chem.* **2001**, *66*, 2358.
- (48) Beer, G.; Rurack, K.; Daub, J. *Chem. Commun.* **2001**, 1138.
- (49) Parker, K. S.; Townshend, A.; Bale, S. *J. Anal. Proc. Incl. Anal. Commun.* **1995**, *32*, 329.
- (50) Pu, L. *Chem. Rev.* **2004**, *104*, 1687.
- (51) Xu, K.; Qiu, Z.; Zhao, J.; Zhao, J.; Wang, C. *Tetrahedron: Asymmetry* **2009**, *20*, 1690.
- (52) Xu, K.; Yang, L.; Wang, Y.; Zhao, J.; Wang, C. *Supramol. Chem.* **2010**, *22*, 563.
- (53) Ryu, D.; Park, E.; Kim, D.; Yan, S.; Lee, J.; Chang, B.; Ahn, K. *J. Am. Chem. Soc.* **2008**, *130*, 2394.
- (54) Lin, J.; Hu, Q.; Xu, M.; Pu, L. *J. Am. Chem. Soc.* **2002**, *124*, 2088.
- (55) Xu, M.; Lin, J.; Hu, Q.; Pu, L. *J. Am. Chem. Soc.* **2002**, *124*, 14239.
- (56) Lin, J.; Zhang, H.; Pu, L. *Org. Lett.* **2002**, *4*, 3297.
- (57) Li, Z.; Lin, J.; Zhang, H.; Sabat, M.; Hyacinth, M.; Pu, L. *J. Org. Chem.* **2004**, *69*, 6284.
- (58) Lin, J.; Li, Z.; Zhang, H.; Pu, L. *Tetrahedron Lett.* **2004**, *45*, 103.
- (59) Li, Z.; Lin, J.; Pu, L. *Angew. Chem., Int. Ed.* **2005**, *44*, 1690.
- (60) Li, Z.; Lin, J.; Sabat, M.; Hyacinth, M.; Pu, L. *J. Org. Chem.* **2007**, *72*, 4905.
- (61) Li, Z.; Lin, J.; Qin, Y.; Pu, L. *Org. Lett.* **2005**, *7*, 3441.
- (62) Lin, J.; Rajaram, A. R.; Pu, L. *Tetrahedron* **2004**, *60*, 11277.
- (63) He, X.; Cui, X.; Li, M.; Lin, L.; Liu, X.; Feng, X. *Tetrahedron Lett.* **2009**, *50*, 5853.
- (64) Yang, X.; Shen, K.; Liu, X.; Zhu, C.; Cheng, Y. *Tetrahedron Lett.* **2011**, *52*, 4611.
- (65) Liu, H.; Hou, X.; Pu, L. *Angew. Chem., Int. Ed.* **2009**, *48*, 382.
- (66) Liu, H.; Zhu, H.; Hou, X.; Pu, L. *Org. Lett.* **2010**, *12*, 4172.
- (67) Liu, H.; Zhao, Q.; Hou, X.; Pu, L. *Chem. Commun.* **2011**, *47*, 3646.
- (68) Liu, H.; Peng, Q.; Wu, Y.; Chen, D.; Hou, X.; Sabat, M.; Pu, L. *Angew. Chem., Int. Ed.* **2010**, *49*, 602.
- (69) Yu, S.; DeBerardinis, A. M.; Burlington, M.; Pu, L. *J. Org. Chem.* **2011**, *76*, 2814.
- (70) Yu, S.; Pu, L. *J. Am. Chem. Soc.* **2010**, *132*, 17698.
- (71) Yu, S.; Plunkett, W.; Kim, M.; Pu, L. *J. Am. Chem. Soc.* **2012**, *134*, 20282.
- (72) Bencini, A.; Coluccini, C.; Garau, A.; Giorgi, C.; Lippolis, V.; Messori, L.; Pasini, D.; Puccioni, S. *Chem. Commun.* **2012**, *48*, 10428.
- (73) Tumambac, E. T.; Mei, X.; Wolf, C. *Eur. J. Org. Chem.* **2004**, 3850.
- (74) Mei, X.; Wolf, C. *J. Am. Chem. Soc.* **2004**, *126*, 14736.
- (75) Mei, X.; Martin, R. M.; Wolf, C. *J. Org. Chem.* **2006**, *71*, 2854.
- (76) Wolf, C.; Liu, S.; Reinhardt, B. C. *Chem. Commun.* **2006**, 4242.
- (77) Mei, X.; Wolf, C. *Chem. Commun.* **2004**, 2078.
- (78) Mei, X.; Wolf, C. *Tetrahedron Lett.* **2006**, *47*, 7901.
- (79) Tumambac, G. E.; Wolf, C. *Org. Lett.* **2005**, *7*, 4045.
- (80) Mei, X.; Wolf, C. *J. Am. Chem. Soc.* **2006**, *128*, 13326.
- (81) Iwaniuk, D. P.; Yearick-Spangler, K.; Wolf, C. *J. Org. Chem.* **2012**, *77*, 5203.
- (82) Reetz, M. T.; Sostmann, S. *Tetrahedron* **2001**, *57*, 2515.
- (83) Dubois, M.; Grandbois, A.; Collins, S. K.; Schmitzera, A. R. *J. Mol. Recognit.* **2011**, *24*, 288.
- (84) Chung, Y. M.; Raman, B.; Ahn, K. H. *Tetrahedron* **2006**, *62*, 11645.
- (85) Kyba, E. P.; Koga, K.; Siegel, M. G.; Sousa, L. R.; Cram, D. J. *J. Am. Chem. Soc.* **1973**, *95*, 2692.
- (86) Wang, H.; Tian, X.; Yang, D.; Pan, Y.; Wu, Q.; He, C. *Tetrahedron: Asymmetry* **2011**, *22*, 381.
- (87) Cho, E. N. R.; Li, Y.; Kim, H. J.; Hyun, M. H. *Chirality* **2011**, *23*, 349.
- (88) Upadhyay, S. P.; Pisurlenkar, R. R. S.; Coutinho, E. C.; Karnik, A. V. *J. Org. Chem.* **2007**, *72*, 5709.
- (89) Kim, K. S.; Jun, E. J.; Kim, S. K.; Choi, H. J.; Yoo, J.; Lee, C.; Hyun, M. H.; Yoon, J. *Tetrahedron Lett.* **2007**, *48*, 2481.
- (90) Móczár, I.; Huszthy, P.; Maidics, Z.; Kádár, M.; Tóth, K. *Tetrahedron* **2009**, *65*, 8250.
- (91) Móczár, I.; Huszthy, P.; Mezei, A.; Kádár, M.; Nyitrai, J.; Tóth, K. *Tetrahedron* **2010**, *66*, 350.
- (92) Xu, K.; Jiao, S.; Yao, W.; Xie, E.; Tang, B.; Wang, C. *Chirality* **2012**, *24*, 646.
- (93) Wei, L.; He, Y.; Xu, K.; Liu, S.; Meng, L. *Chin. J. Chem.* **2005**, *23*, 757.
- (94) Huang, X.; He, Y.; Chen, Z.; Hu, C.; Qing, G. *Can. J. Chem.* **2008**, *86*, 170.
- (95) Huang, X.; He, Y.; Hu, C.; Chen, Z. *J. Fluoresc.* **2009**, *19*, 97.
- (96) Hu, C.; He, Y.; Chen, Z.; Huang, X. *Tetrahedron: Asymmetry* **2009**, *20*, 104.
- (97) Qing, G.; Sun, T.; Chen, Z.; Yang, X.; Wu, X.; He, Y. *Chirality* **2009**, *21*, 363.
- (98) Qing, G.; Sun, T.; He, Y.; Wang, F.; Chen, Z. *Tetrahedron: Asymmetry* **2009**, *20*, 575.
- (99) Kim, Y. K.; Lee, H. N.; Singh, N. J.; Choi, H. J.; Xue, J.; Kim, K. S.; Yoon, J.; Hyun, M. H. *J. Org. Chem.* **2008**, *73*, 301.
- (100) Choi, M. K.; Kim, H. N.; Choi, H. J.; Yoon, J.; Hyun, M. H. *Tetrahedron Lett.* **2008**, *49*, 4522.
- (101) Liu, S.; Law, K. Y.; He, Y.; Chan, W. H. *Tetrahedron Lett.* **2006**, *47*, 7857.
- (102) Wang, H.; Chan, W. H.; Lee, A. W. M. *Org. Biomol. Chem.* **2008**, *6*, 929.
- (103) Costero, A. M.; Colera, M.; Gavíñia, P.; Gil, S.; Kubinyi, M.; Pál, K.; Kállay, M. *Tetrahedron* **2008**, *64*, 3217.

- (104) Costero, A. M.; Lloosa, U.; Gil, S.; Parra, M.; Colera, M. *Tetrahedron: Asymmetry* **2009**, *20*, 1468.
- (105) Zhou, X.; Yip, Y.; Chan, W.; Lee, A. W. M. *Beilstein J. Org. Chem.* **2011**, *7*, 75.
- (106) Xing, Z.; Fu, Y.; Zhou, J.; Zhu, C.; Cheng, Y. *Org. Biomol. Chem.* **2012**, *10*, 4024.
- (107) Tang, L.; Wei, G.; Nandakumar, R.; Guo, Z. *Bull. Korean Chem. Soc.* **2011**, *32*, 3367.
- (108) Pal, A.; Besenius, P.; Sijbesma, R. P. *J. Am. Chem. Soc.* **2011**, *133*, 12987.
- (109) Dhara, K.; Sarkar, K.; Roy, P.; Nandi, M.; Bhaumik, A.; Banerjee, P. *Tetrahedron* **2008**, *64*, 3153.
- (110) Tanaka, K.; Tsutsumi, T.; Fukuda, N.; Masumoto, A.; Arakawa, R. *Tetrahedron: Asymmetry* **2012**, *23*, 205.
- (111) Chen, X.; Du, D.; Hua, W. *Tetrahedron: Asymmetry* **2003**, *14*, 999.
- (112) Xu, K.; Wu, X.; He, Y.; Liu, S.; Qing, G.; Meng, L. *Tetrahedron: Asymmetry* **2005**, *16*, 833.
- (113) Xu, K.; He, Y.; Qin, H.; Qing, G.; Liu, S. *Tetrahedron: Asymmetry* **2005**, *16*, 3042.
- (114) Heinrichs, G.; Schellenträger, M.; Kubik, S. *Eur. J. Org. Chem.* **2006**, *4177*.
- (115) Alfonso, I.; Burguete, M. I.; Galindo, F.; Luis, S. V.; Vigara, L. J. *Org. Chem.* **2009**, *74*, 6130.
- (116) Burguete, M. I.; Galindo, F.; Luis, S. V.; Vigara, L. *J. Photochem. Photobiol. A: Chem.* **2010**, *209*, 61.
- (117) Xu, K.; Cheng, P.; Zhao, J.; Wang, C. *J. Fluoresc.* **2011**, *21*, 991.
- (118) Xu, Z.; Kim, S. K.; Yoon, J. *Chem. Soc. Rev.* **2010**, *39*, 1457.
- (119) Guo, Z.; Song, N. R.; Moon, J. H.; Kim, M.; Jun, E. J.; Choi, J.; Lee, J. Y.; Bielawski, C. W.; Sessler, J. L.; Yoon, J. *J. Am. Chem. Soc.* **2012**, *134*, 17846.
- (120) Lu, Q.; Dong, L.; Zhang, J.; Li, J.; Jiang, L.; Huang, Y.; Qin, S.; Hu, C.; Yu, X. *Org. Lett.* **2009**, *11*, 669.
- (121) Swamy, K. M. K.; Singh, N. J.; Yoo, J.; Kwon, S. K.; Chung, S.; Lee, C.; Yoon, J. *J. Incl. Phenom. Macrocycl. Chem.* **2010**, *66*, 107.
- (122) Yang, L.; Qin, S.; Su, X.; Yang, F.; You, J.; Hu, C.; Xie, R.; Lan, J. *Org. Biomol. Chem.* **2010**, *8*, 339.
- (123) Su, X.; Luo, K.; Xiang, Q.; Lan, J.; Xie, R. *Chirality* **2009**, *21*, 539.
- (124) Yoon, J.; Czarnik, A. W. *J. Am. Chem. Soc.* **1992**, *114*, 5847.
- (125) Fujita, N.; Shinkai, S.; James, T. D. *Chem. Asian J.* **2008**, *3*, 1076.
- (126) Mader, H. S.; Wolfbeis, O. S. *Microchim. Acta* **2008**, *162*, 1.
- (127) Guo, Z.; Shin, I.; Yoon, J. *Chem. Commun.* **2012**, *48*, 5956.
- (128) James, T. D. *Top. Curr. Chem.* **2007**, *277*, 107.
- (129) Zhang, X.; Chi, L.; Ji, S.; Wu, Y.; Song, P.; Han, K.; Guo, H.; James, T. D.; Zhao, J. *J. Am. Chem. Soc.* **2009**, *131*, 17452.
- (130) Zhang, X.; Wu, Y.; Ji, S.; Guo, H.; Song, P.; Han, K.; Wu, W.; Wu, W.; James, T. D.; Zhao, J. *J. Org. Chem.* **2010**, *75*, 2578.
- (131) James, T. D.; Samankumara Sandanayake, K. R. A.; Shinkai, S. *Nature* **1995**, *374*, 345.
- (132) Zhao, J.; Fyles, T. M.; James, T. D. *Angew. Chem., Int. Ed.* **2004**, *43*, 3461.
- (133) Liang, X.; James, T. D.; Zhao, J. *Tetrahedron* **2008**, *64*, 1309.
- (134) Li, Q.; Guo, H.; Wu, Y.; Zhang, X.; Liu, Y.; Zhao, J. *J. Fluoresc.* **2011**, *21*, 2077.
- (135) Zhao, J.; Davidson, M. G.; Mahon, M. F.; Kociok-Kohn, G.; James, T. D. *J. Am. Chem. Soc.* **2004**, *126*, 16179.
- (136) Zhao, J.; James, T. D. *J. Mater. Chem.* **2005**, *15*, 2896.
- (137) Zhao, J.; James, T. D. *Chem. Commun.* **2005**, 1889.
- (138) Chi, L.; Zhao, J.; James, T. D. *J. Org. Chem.* **2008**, *73*, 4684.
- (139) Han, F.; Chi, L.; Liang, X.; Ji, S.; Liu, S.; Zhou, F.; Wu, Y.; Han, K.; Zhao, J.; James, T. D. *J. Org. Chem.* **2009**, *74*, 1333.
- (140) Wu, Y.; Guo, H.; James, T. D.; Zhao, J. *J. Org. Chem.* **2011**, *76*, 5685.
- (141) Liu, Y.; Zhang, X.; Guo, H.; Wu, Y.; Li, Q.; Liu, L.; Zhao, J. *J. Fluoresc.* **2011**, *21*, 1979.
- (142) Wu, Y.; H. Guo, H.; Zhang, X.; James, T. D.; Zhao, J. *Chem. Eur. J.* **2011**, *17*, 7632.
- (143) Zhu, L.; Anslyn, E. V. *J. Am. Chem. Soc.* **2004**, *126*, 3676.
- (144) Zhu, L.; Zhong, Z.; Anslyn, E. V. *J. Am. Chem. Soc.* **2005**, *127*, 4260.
- (145) Zheng, Y.; Hu, Y. *J. Org. Chem.* **2009**, *74*, 5660.
- (146) Li, D.; Zheng, Y. *Chem. Commun.* **2011**, *47*, 10139.
- (147) Li, D.; Wang, H.; Zheng, Y. *Chem. Commun.* **2012**, *48*, 3176.
- (148) Mutihac, L.; Lee, J. H.; Kim, J. S.; Vicens, J. *Chem. Soc. Rev.* **2011**, *40*, 2777.
- (149) Zheng, Y.; Luo, J. *J. Incl. Phenom. Macrocycl. Chem.* **2011**, *71*, 35.
- (150) Liu, S.; He, Y.; Qing, G.; Xu, K.; Qin, H. *Tetrahedron: Asymmetry* **2005**, *16*, 1527.
- (151) Qing, G.; He, Y.; Chen, Z.; Wu, X.; Meng, L. *Tetrahedron: Asymmetry* **2006**, *17*, 3144.
- (152) Qing, G.; He, Y.; Zhao, Y.; Hu, C.; Liu, S.; Yang, X. *Eur. J. Org. Chem.* **2006**, 1574.
- (153) Durmaz, M.; Alpaydin, S.; Sirit, A.; Yilmaz, M. *Tetrahedron: Asymmetry* **2006**, *17*, 2322.
- (154) Durmaz, M.; Yilmaz, M.; Sirit, A. *Org. Biomol. Chem.* **2011**, *9*, 571.
- (155) Luo, J.; Zheng, Q.; Chen, C.; Huang, Z. *Tetrahedron* **2005**, *61*, 8517.
- (156) Lynam, C.; Diamond, D. *J. Mater. Chem.* **2005**, *15*, 307.
- (157) Miyaji, H.; Hong, S.; Jeong, S.; Yoon, D.; Na, H.; Hong, J.; Ham, S.; Sessler, J. L.; Lee, C. *Angew. Chem., Int. Ed.* **2007**, *46*, 2508.
- (158) Zhang, Y.; Noh, H.; Choi, S.; Ryoo, J. J.; Lee, K.; Ohta, K.; Fujimoto, C.; Jin, J.; Takeuchi, T. *Bull. Korean Chem. Soc.* **2004**, *25*, 377.
- (159) Shahgaldian, P.; Pieles, U. *Sensors* **2006**, *6*, 593.
- (160) Gingter, S.; Bezduzhna, E.; Ritter, H. *Macromolecules* **2010**, *43*, 3128.
- (161) Riela, S.; D'Anna, F.; Meo, P. L.; Gruttaduria, M.; Giacalone, R.; Noto, R. *Tetrahedron* **2006**, *62*, 4323.
- (162) Ikeda, H.; Li, Q.; Ueno, A. *Bioorg. Med. Chem. Lett.* **2006**, *16*, 5420.
- (163) Pagliari, S.; Corradini, R.; Galaverna, G.; Sforza, S.; Dossena, A.; Montalti, M.; Prodi, L.; Zaccheroni, N.; Marchelli, R. *Chem.—Eur. J.* **2004**, *10*, 2749.
- (164) Corradini, R.; Paganuzzi, C.; Marchelli, R.; Pagliari, S.; Sforza, S.; Dossena, A.; Galaverna, G.; Duchateau, A. *J. Mater. Chem.* **2005**, *15*, 2741.
- (165) Folmer-Andersen, J. F.; Lynch, V. M.; Anslyn, E. V. *J. Am. Chem. Soc.* **2005**, *127*, 7986.
- (166) Leung, D.; Folmer-Andersen, J. F.; Lynch, V. M.; Anslyn, E. V. *J. Am. Chem. Soc.* **2008**, *130*, 12318.
- (167) Chen, Z.; He, Y.; Hu, C.; Huang, X. *Tetrahedron: Asymmetry* **2008**, *19*, 2051.
- (168) Chen, X.; Huang, Z.; Chen, S.; Li, K.; Yu, X.; Pu, L. *J. Am. Chem. Soc.* **2010**, *132*, 7297.
- (169) Kwong, H.; Wonga, W.; Lee, C.; Yeung, C.; Ten, P. *Inorg. Chem. Commun.* **2009**, *12*, 815.
- (170) Jintoku, H.; Takafuji, M.; Odac, R.; Ihara, H. *Chem. Commun.* **2012**, *48*, 4881.
- (171) He, X.; Zhang, Q.; Wang, W.; Lin, L.; Liu, X.; Feng, X. *Org. Lett.* **2011**, *13*, 804.
- (172) He, X.; Zhang, Q.; Liu, X.; Lin, L.; Feng, X. *Chem. Commun.* **2011**, *47*, 11641.
- (173) Wanderley, M. M.; Wang, C.; Wu, C.; Lin, W. *J. Am. Chem. Soc.* **2012**, *134*, 9050.
- (174) Shinoda, S.; Okazaki, T.; Player, T. N.; Misaki, H.; Hori, K.; Tsukube, H. *J. Org. Chem.* **2005**, *70*, 1835.
- (175) Montgomery, C. P.; New, E. J.; Parker, D.; Peacock, R. D. *Chem. Commun.* **2008**, 4261.
- (176) Xu, S.; Hu, B.; Flower, S. E.; Jiang, Y.; Fossey, J. S.; Deng, W.; James, T. D. *Chem. Commun.* **2013**, *49*, 8314.
- (177) Kim, H. N.; Guo, Z.; Zhu, W.; Yoon, J.; Tian, H. *Chem. Soc. Rev.* **2011**, *40*, 79.
- (178) Xu, Y.; Zheng, L.; Huang, X.; Cheng, Y.; Zhu, C. *Polymer* **2010**, *51*, 994.
- (179) Song, F.; Wei, G.; Wang, L.; Jiao, J.; Cheng, Y.; Zhu, C. *J. Org. Chem.* **2012**, *77*, 4759.

- (180) Meng, J.; Wei, G.; Huang, X.; Dong, Yu.; Cheng, Y.; Zhu, C. *Polymer* **2011**, *52*, 363.
- (181) Fukuhara, G.; Inoue, Y. *Chem. Commun.* **2012**, *48*, 1641.
- (182) Capek, I. *Adv. Colloid Interface Sci.* **2009**, *150*, 63.
- (183) Shen, J.; Sun, L.; Yan, C. *Dalton Trans.* **2008**, 5687.
- (184) Wang, Z.; Lu, Y. *J. Mater. Chem.* **2009**, *19*, 1788.
- (185) Su, S.; Wu, W.; Gao, J.; Lu, J.; Fan, C. *J. Mater. Chem.* **2012**, *22*, 18101.
- (186) Hatchett, D. W.; Josowicz, M. *Chem. Rev.* **2008**, *108*, 746.
- (187) Carrillo-Carrión, C.; Cárdenas, S.; Simonet, B. M.; Valcárcel, M. *Anal. Chem.* **2009**, *81*, 4730.
- (188) Freeman, R.; Finder, T.; Bahshi, L.; Willner, I. *Nano Lett.* **2009**, *9*, 2073.
- (189) Zhang, M.; Ye, B. *Anal. Chem.* **2011**, *83*, 1504.
- (190) Su, H.; Zheng, Q.; Li, H. *J. Mater. Chem.* **2012**, *22*, 6546.
- (191) Oh, W.; Jeong, Y. S.; Lee, K. J.; Jang, J. *Anal. Methods* **2012**, *4*, 913.